APPLYING DECLINE CURVE ANALYSIS IN THE LIQUID-RICH SHALES:

EAGLE FORD SHALE STUDY

A Thesis

by

PURVI INDRAS

Submitted to the Office of Graduate and Professional Studies of
Texas A&M University
in partial fulfillment of the requirements for the degree of

MASTER OF SCIENCE

Chair of Committee,	W. John Lee
Committee Members,	Walter B. Ayers
	Yuefeng Sun
Head of Department,	A. Daniel Hill

May 2014

Major Subject: Petroleum Engineering

ABSTRACT

With the emergence of liquid rich shale (LRS) plays like Eagle Ford and Northern Barnett, the petroleum industry needs a simple, easily applied technique that provides reliable estimates of future production rates in this kind of reservoir. There is no guarantee that methodology that has proved to work in gas reservoirs will necessarily be appropriate in LRS reservoirs. In this work, we found that without corrections of early data, the Stretched Exponential Production Decline (SEPD) model, designed for transient flow, usually produces pessimistic forecasts of future production. The Duong method, another transient model, may be reasonable during long term transient linear flow, but notably optimistic after boundary-dominated flow (BDF) appears. For wells in BDF, the Arps model provides reasonable forecasts, but the Arps model may not be accurate when applied to transient data. A hybrid of early transient and later BDF models proves to be a reasonable solution to the forecasting problem in LRS.

In addition, use of diagnostic plots (like log-log rate-time and log-log rate-material balance time plots) improves confidence in flow regime identification and production forecasting. In some LRS's, BDF is observed within 12 months. In any case, it is essential to identify or to estimate the time to reach BDF and to discontinue use of transient flow models after BDF appears or is expected.

We validated our methodology using “hindcast analysis”; that is, matching the first half of production history to determine model parameters, then forecasting the second half of history and comparing to observed production data.

We also found that application of pressure-corrected rates in decline curve analysis (DCA) may substantially improve the interpretation of data from unconventional oil wells flowing under unstable operating conditions. Fetkovich (hydraulically fractured well) type curve analysis can be added to improve confidence in flow regime identification from diagnostic plots and to estimate the Arps hyperbolic exponent b from the matching b stem on the type curve, which can then be extrapolated to determine estimated ultimate recovery.

DEDICATION

I want to dedicate this to my guru Dr. John Lee and my parents for their constant support and guidance. I want to express them my sincere gratitude for believing in me and for helping me to achieve my academic goals.

ACKNOWLEDGEMENTS

I want to thank my committee members, Dr. Ayers and Dr. Sun for their support and recommendations. I want to thank Fekete for providing their software support for my research.

I want thank Government of India for sponsoring my education. I am thankful to Dr. Datta-Gupta for giving me this opportunity. I am also thankful to my Aggie friends for making my stay memorable at TAMU.

Special thanks to my parents, sister and my brother-in-law for their motivation and encouragement. I also want thank my best friend, Tejal for supporting me and cheering me up when I needed the most.

Finally, heartfelt gratitude to Texas A&M University for giving me the most memorable experience of my life.

Thanks and Gig'em

TABLE OF CONTENTS

LIST OF FIGURES

Page

LIST OF TABLES

Page

1. INTRODUCTION

The three key issues faced by the industry today are (1) uncertain gas prices, (2) steep production decline rates in shale reservoirs, and (3) lack of knowledge about the new shale plays which adds to uncertainties about recovery.

First, natural gas prices have remained relatively low since 2009 because of the shale boom in the US oil and gas industry. Due to the success of multi-fractured horizontal wells in shale reservoirs, there has been an increase in the supply of gas with demand remaining relatively the same. This led to a decline in natural gas prices. The impact observed due to the decline in natural gas prices is a shift to liquids-rich shale regions. Second, high production decline rates in shale reservoirs are observed. These plays show high peak production rates and flow in transient linear flow regime for a few years during which the early decline rate is quite high. Last, the lack of knowledge about these plays is a big issue as they are fairly young and still developing. Due to heterogeneity in these reservoirs, finding analogs and correlations in these plays is difficult; at the same time, application of knowledge from these plays to the other plays is essential but due to insufficient understanding of developing or undeveloped plays, it still remains a big challenge.

Field examples from the Eagle Ford shale were studied to help us understand liquid production in low permeability shale reservoirs that have multi-fractured horizontal wells. Learning from the study of publicly available production data of 360

wells from the northern Barnett shale can be extrapolated to the Eagle Ford due to long production history and similar decline behavior.

In this study, utility of hybrid forecasting models was assessed in developing a technique that is simple, easy to apply and provides a reliable estimate of future production rates. Barnett Shale play located in the Fort Worth basin was discovered in 1980, but the first multi-fractured horizontal well was drilled in 2004. In this study, northern parts of Barnett shale located in the oil window that consists of parts of Montague, Cooke and Wise counties were analyzed. The average gas to oil ratio, GOR, of the northern Barnett shale is 10 Mscf/bbl and peak production rates vary from 1to100 bbl/month (Gong et al. 2011).

In the Eagle Ford shale play located in south-west Texas the fluid type varies from black oil to volatile oil, gas condensate and finally dry gas. The research study area mainly includes oil wells in Karnes, Gonzales, McMullen, Atascosa, La Salle, and Dimmitt counties. The peak production rates in Karnes and Gonzales counties recently exceeded 16,000/bbl/month/well (Tian et al. 2013).

1.1 Research Objectives

The objective of this research was to determine appropriate decline models and methodology for liquid-rich shale wells.

Field examples from the northern Barnett shale and the Eagle Ford shale were studied to identify dominant flow regimes and to determine the applicability of different production decline models.

We performed hindcasting to estimate the error in cumulative production due to inaccurate prediction of BDF onset.

We studied the applicability the following decline models:

- Arps hyperbolic with 5% minimum decline
- Duong model
- Stretched exponential production decline method (SEPD)
- Stretched exponential production decline method with Arps hyperbolic tail for BDF
- Duong model with Arps hyperbolic tail for BDF
- YM-SEPD model

The time and annual decline rate of boundary-dominated flow onset was estimated for Eagle Ford and northern Barnett shale.

In addition, we evaluated pressure correction of rates in shale oil wells and we forecasted 30-year production profiles in the Eagle Ford shale using different diagnostic plots and decline models.

2. DECLINE CURVE ANALYSIS IN UNCONVENTIONALS

2.1 Introduction to DCA

Decline curve analysis is the most common technique for predicting future production performance due to its simplicity and the fact that it requires no prior knowledge of fluid flow physics in the reservoir. The traditional Arps decline model (Arps 1945) is based on the assumptions of boundary dominated flow (BDF) regime and unchanged operating conditions and reservoir properties. These assumptions are rarely met by unconventional wells in ultra-low permeability reservoirs. To overcome the BDF limitation of the Arps model, several new empirical models for DCA have been developed, including SEPD (Valkó and Lee 2010) and Duong models (Duong 2011) which are applicable for the wells exhibiting long-term transient flow, and dual models (Joshi and Lee 2013) that can switch from the transient flow regime to the BDF regime at a specified decline rate.

An important limitation of DCA models is that they are based only on production rates, relying on the assumption of stable flowing pressures. Since pressure stabilization is not reached rapidly in most cases, the applicability of these methods and the reliability of their solutions may be compromised.

Therefore, ignoring flowing pressure changes and using only conventional rate-time techniques to interpret decline data may cause misinterpretations and erroneous reserve estimations (Anderson et al. 2012, Anderson and Mattar 2003). As pointed out

by Anderson and Mattar (2003), there is a possibility of over-predicting EUR if pressures are steeply declining, even if a conservative exponential decline model is applied.

2.2 Decline Analysis Models

Decline curve analysis is one of the oldest techniques to predict oil and gas production. A major perceived advantage of this technique is that no prior knowledge of the physical properties of the reservoir or fluid flow physics is required. This technique is simple, easy to apply and is perceived to provide reliable results for forecasting production in shale gas and oil wells. The following models are among the techniques available for production forecasting in shale reservoirs:

2.2.1 Modified Hyperbolic (Terminal Decline)

In this method, a switch from an initial Arps hyperbolic decline model—usually with a b exponent greater than 1—to an Arps BDF model is made either at a specific time (end of linear flow (t_{elf})) or when a predetermined terminal decline rate, D_{min}, is reached. This is a practical way to constrain the EUR by fitting early-time transient data with traditional hyperbolic equations and the resulting *b* parameter higher than 1 (Ilk et al. 2011).

For example, the hyperbolic decline Arps model can be followed by an Arps exponential decline model that begins when the annual production decline rate falls to 5%.

Hyperbolic decline flow rate:

$$q(t) = q_i/(1 + bD_i t)^{\frac{1}{b}} \quad \text{..... (1)}$$

Exponential decline flow rate, 5% decline:

$$q = q_i * \exp[-a * t] \quad \text{..... (2)}$$

Imposing a minimum decline rate will constrain the tendency of Arps curve to over-predict the EUR.

2.2.2 Stretched Exponential Production Decline method (SEPD)

SEPD, proposed by Valkó and Lee (2010), is a different form of hyperbolic modeling, effectively with a b exponent varying over time. According to Valkó and Lee (2010), the SEPD model offers an important benefit over the traditional Arps hyperbolic decline model: that is, more realistic forecasts for low-permeability wells with long-duration transient flow. The following equations describe production rate (Eq. 4), and cumulative production (Eq. 5) in the SEPD model:

$$dq/dt = -n\,(t/\tau)^{n} * (q/t) \quad \text{..... (3)}$$

$$q = q_o * \exp\left[-(t/\tau)^{n}\right] \quad \text{..... (4)}$$

$$N_p = (q_o * \tau/n) * (\Gamma[1/n] - \Gamma\left[1/n, (t/\tau)^{n}\right]) \quad \text{..... (5)}$$

2.2.3 Duong Method

Duong's model is based on a plot of inverse material balance time (q/Q) vs. time, which forms a straight line when plotted on a log-log coordinates. The production trend may deviate from the log-log straight line when BDF is reached (Kanfar and Wattenbarger 2012). In Eq. 6, *m* represents the slope and *a* is the intercept of this straight line. Although the slope is always negative, the *m* value is always positive and greater than unity for unconventional reservoirs.

$$q/Q = at^{-m} \quad \text{.....(6)}$$

Duong's equations for rate (Eq. 7) and cumulative production (Eq. 8):

$$q = q_1 t(a, m) \quad \text{.....(7)}$$

$$N_p = q_1 t(a, m)/at^{-m} \quad \text{.....(8)}$$

$$t(a, m) = t^{-m} \exp\left[\frac{a}{1-m} * (t^{1-m} - 1)\right] \quad \text{.....(9)}$$

$$EUR = \frac{q1}{a} * \exp\left(\frac{a}{1-m} * (t^{1-m} - 1)\right) \quad \text{.....(10)}$$

a = intercept from a linear plot of log q/N_p versus log time

m = slope from a linear plot of log q/N_p versus log time

q_1 = flow rate at t = 1

With short production history, Duong's model works well in shale wells (Joshi and Lee 2013). However, since it essentially assumes life-of-well linear flow it tends to over-estimate recovery for wells exhibiting a BDF regime (Mangha et al. 2012).

2.2.4 Dual Models

Dual models are a combination of two models—e.g., Duong, SEPD, Arps Hyperbolic or Exponential—where each of these models has the advantage of more accurate production forecasting during a specific flow regime. For unconventional reservoirs, the best dual-model configurations are those with the ability to model transient linear flow during early times and later switch to a BDF model at an appropriate time—that is, at a specified time or at a specified minimum decline rate. The Arps equations can model production data in BDF and are the best simple BDF decline models available. Two appropriate Arps BDF models are the hyperbolic model with the b exponent between 0.3 and 0.4 (0.4 for gas wells or 0.3 for solution-gas-drive oil wells) and the exponential model, b = 0 (for single phase liquid production. high pressure gas, tubing-restricted gas production).

DCA methods assume constant operating conditions and recovery mechanisms. Analysis of production data above bubble point (b=0) with data below the bubble point (0.1>b>0.4) may violate this assumption and results obtained from the analysis will no longer be valid (Fekete 2013).

2.2.4.1 Modified Duong

Joshi and Lee (2013) proposed modifications to Duong's model to account for BDF in wells with long-duration transient flow. One modification uses a dual model to switch from Duong to Arps at a specified time or specified decline rate—ideally at the onset of BDF. In their study, a switch point at 5% of decline rate (D_{switch} @ 5%) was used, but the optimal D_{switch} and b values for the BDF Arps model should be selected through a rigorous study of each case.

2.2.4.2 Modified Stretched Exponential

(1) MSE

This model switches from SEPD to a terminal Arp's BDF model when a limiting condition is reached, similar to the modified Duong and the modified hyperbolic methods.

(2) YM-SEPD

Yu and Miocevic (2013) introduced a specialized logarithmic plot of Ln (q_o/q) versus time to define parameters for SEPD model n and τ, by manually matching production data from the second year and beyond.

In this study, I evaluated the implications of excluding the entire first year of production history and also including the first year of production history but keeping only those data points that lie on the straight line of the specialized plot. The slope and intercept of the specialized plot can be used to determine the *n* and τ parameters for the SEPD model (**Fig. 1**). *n* is read from the slope and τ is calculated using the intercept, Int, and eq.11.

$$\tau = \exp(-Ln\,(Int)/n) \quad \text{..... (11)}$$

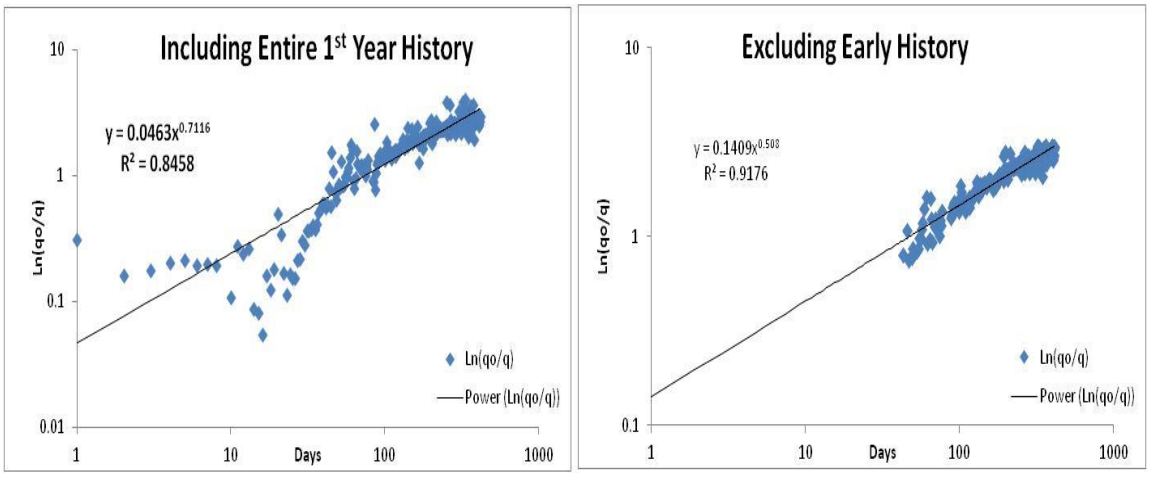

Fig. 1—Specialized plots for YM-SEPD model

Table 1 gives the parameters calculated from the specialized plot for forecasting 30 year production rates using original SEPD model Eq.4 (**Fig. 2**).

Table 1—Estimation of n and τ from a specialized plot (Fig.1)

	n	Int	τ, days	q_1, bbl/D
Excluding history	0.508	0.1409	47.35568	902.2
Including history	0.7116	0.0463	75.03044	902.2

Fig.2, a cumulative plot, shows that either excluding and or including first-year production history does not have a significant impact on 30 year EUR, but that the rate forecasts differ substantially.

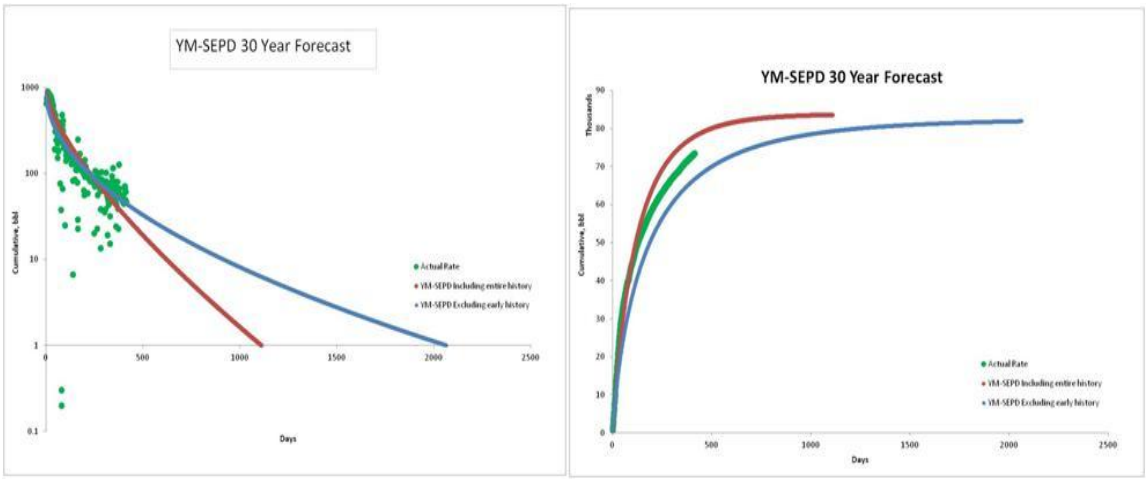

Fig. 2—30-year production forecast for YM-SEPD model

2.3 Identification of Flow Regimes in Multi-Fractured Horizontal Wells

Identification of flow regimes is a critical step prior to performing DCA in multi-fractured horizontal wells (MFHW). Inaccurate identification of flow regimes can affect the final recovery estimates, as the dominant and the final flow regime will determine the shape of the decline curve and hence, the EUR. MFHW can exhibit a combination of flow regimes. In the Eagle Ford and the northern Barnett, two flow regimes are commonly identified, linear flow usually followed by boundary dominated flow. In the early production life of the well, these flow regimes are affected by the fracture network in the stimulated reservoir volume, SRV (Mayerhofer et al. 2008), and in the later life of the well, by the flow boundaries and heterogeneities of the reservoir (Clarkson 2013).

Linear flow (LF) appears early in the life of the MFHW, when the flow is perpendicular to the hydraulic fractures. Sometimes, a late or compound linear flow is observed when flow from the unstimulated matrix into the SRV occurs. This new linear flow pattern is perpendicular to the wellbore length. Boundary dominated flow may occur at the end of LF mainly due to fracture interference.

2.3.1 Normalization and Corrections for Bottom-Hole Pressures

In most cases, pressure history is not available for analysis. Rate normalization is an essential feature if bottom-hole pressures are available or can be calculated from casing or tubing head pressures. The rates are divided by the corresponding delta-pressure function (i.e., $\Delta p=p_i - p_{wf}$) (Anderson et al. 2012), that accounts for the operating (flowing pressure) conditions.

Duong (2010) proposed a new decline analysis model for well exhibiting transient flow regimes. As part of his workflow, he included pressure corrected rates (PCR) in diagnostic plots to account for the early choke-back effect and to improve identification of the linear flow regime, but not to improve the forecasting capacity of the model.

For oil wells, two methods suggested for rate normalization are presented in Table 2.

Table 2—Rate normalization methods for oil wells

Pressure Normalized Rate (PNR)	$\mathrm{PNR} = \frac{q_o}{\Delta p} = \frac{q_o}{p_i - p_{wf}}$
Pressure Corrected Rate (PCR)	$\mathrm{PCR} = q_{obs} * \left[\frac{p_i - pwf_{stb}}{p_i - pwf_{obs}}\right]$

Once the data is corrected and normalized for unstable flowing conditions, it can then be analyzed for the presence of various flow signatures.

2.3.2 Diagnostic Plots

Diagnostic plots allow us to identify flow regimes with confidence. A combination of the following plots can be used when pressure data is also available to increase our confidence that the flow regimes have been identified correctly.

- Logarithmic plot of rate vs. time
- Logarithmic plot of rate/ ΔP vs. time
- Logarithmic plot of pressure-corrected-rate vs. time
- Logarithmic plot of rate vs. material-balance time
- Logarithmic plot of rate/ ΔP vs. material-balance time

- Logarithmic plot of pressure-corrected-rate vs. material-balance time
- YM-SEPD logarithmic plot of $\ln(q_o/q)$ vs. time

When pressure history is unavailable, a log-log plots of rate vs. time and log-log plots of rate vs. material balance time may be used as of the best available method to identify flow regimes, but data from the first several months to one year should be excluded from the analysis because they are likely to lie off the true decline trend.

These plots are particularly useful when the data points are scattered and the well is flowing under unstable conditions. Use of material balance time is recommended as it is particularly useful when BDF is suspected, in which case the plot will have a distinct negative unit slope (Clarkson 2013).

The YM-SEPD specialized plot is useful for wells under transient flow conditions. Any deviation from the straight line may be attributed to the presence of BDF. Table 3 summarizes the various diagnostic plots and their utility.

Table 3—Identification of flow regimes using diagnostic plots

Diagnostic Plots	Flow Regimes	Description
Log q - Log t	Linear and BDF	Logarithmic plot of production rate vs. real time
Log q - Log MBT	Linear and BDF	Logarithmic plot of production rate vs. MBT
Log q/ΔP - Log MBT	Linear and BDF	Logarithmic plot of PNR vs. MBT
Log PC- q - Log t	Linear and BDF	Logarithmic plot of PC-rate vs. real time (Duong 2011)
Log (Ln(q_o/q))- Log t	Linear and BDF	Logarithmic plot of ln(q_o/q) vs. real time (Yu and Miocevic 2013)

The slope represented by the data points is a convenient method for visualizing the sequence of flow regimes exhibited by the well during its production history. The slopes for the representative flow regimes are:

- Bilinear Flow: -1/4 slope
- Linear Flow: -1/2 slope
- BDF: -1 slope

In this study, we found that the dominant flow regimes are linear flow and BDF. Bilinear and radial flows were not observed and are not included in the discussion about

the various flow regimes exhibited by MFHW. The main purpose of flow regime identification (FRI) is to understand the flow behavior and to forecast future production rates with confidence which depends on the final dominant flow regime exhibited by the well. Thus, the final shape of the forecasted rate curve is determined by final flow regime and inaccurate FRI can cause misleading results.

2.3.3 Fetkovich Type Curves

In 1980, Fetkovich presented type curves for decline curve analysis. He combined analytical transient radial flow equations and boundary-dominated flow equations (Arps 1945) .

Fig. 3 is the Fetkovich type curve: the left side is the analytical solution for transient radial flow, while the right side is the Arps equations for BDF. At the end of transient flow, all analytical solutions converge into a single curve. Thus, the one type curve is capable of representing the entire production history of a well from early transient radial flow to late time BDF (Fekete 2013).

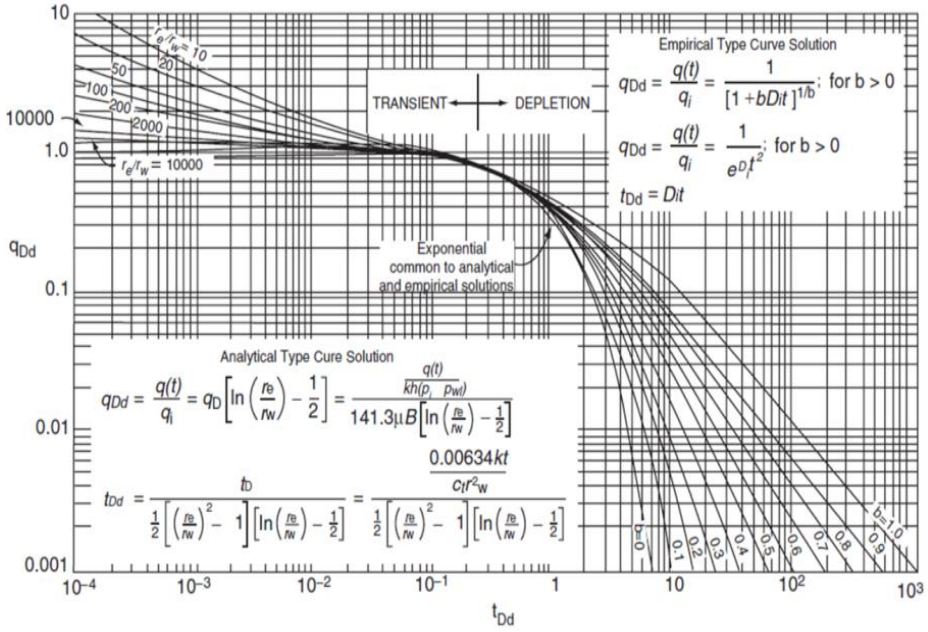

Fig. 3— Fetkovich type curves: composite of analytical and empirical solution (Fetkovich, 1980)

2.4 Workflow for Production Data Analysis

I followed a systematic workflow for production data analysis in LRS, summarized in **Fig. 4**. Each step is explained in detail in the following sections.

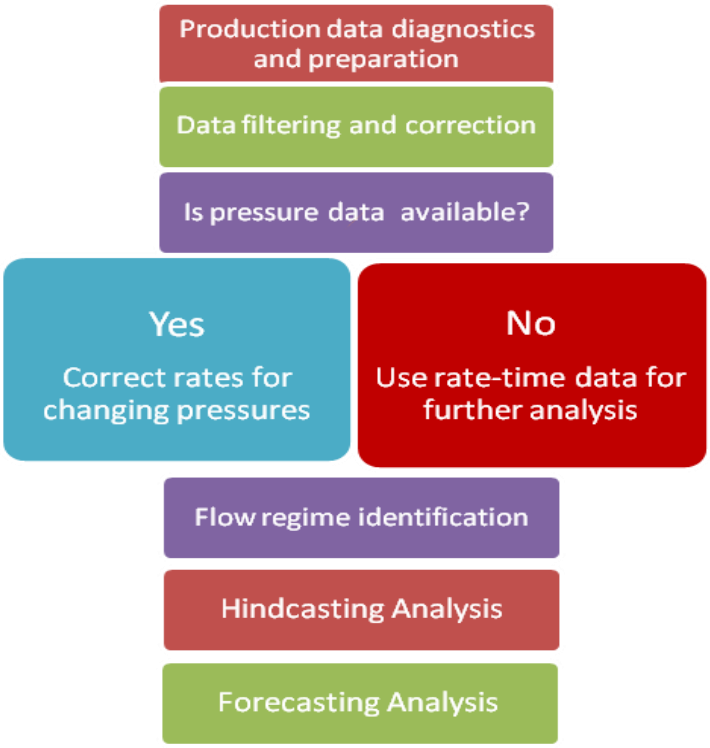

Fig. 4 —Workflow for forecasting production rates

2.4.1 Production Data Diagnosis and Preparation

The first step before performing any analysis is to prepare raw data using diagnostic process to make it into a high quality data. This process involves identification of anomalous events like change in flowing conditions (for example installation of artificial lift system, choke management, etc.) that can help in taking account the assumptions made in DCA.

2.4.2 Data Filtering and Correction

The second step is to identify inconsistent production behavior and filter the anomalies to avoid misleading results. (1) Sometimes, the initial data when the well is cleaning up, a decreasing WOR may be attributed to fracture fluid clean up. In this case, it is suggested to remove first few months of data till the time when WOR is stable. (2) Liquid loading is another phenomenon that occurs due well's inability to lift liquids to the surface, leading to abnormally low flow rates. These low flow rates can lead to misleading interpretation of flow regimes. This phenomenon is discussed in more detail in the following section of flow regime identification. In any case, it is necessary to remove any outliers and inconsistent data points to get reliable results.

2.4.3 Flow Regime Identification

The third step is to identify dominant flow regime as discussed in section 2.3.To assess techniques for estimating future production in the Eagle Ford Shale (EFS), I analyzed publically available production data from 2043 wells in six oil-rich counties. The fluid types in the EFS evolve basin-ward from black oil, volatile oil, gas condensate, and dry gas (Tian et al. 2013). The production history available varies from 12 to 36 months. Due to the limited-duration of production data available for the Eagle Ford shale, I also analyzed 360 oil wells in the northern Barnett to further assess forecasting techniques in liquid-rich shale reservoirs.

The production data in the northern Barnett range from March 2003 to August 2013. With such long production histories, it is easier to identify long term behavior of hydraulically fractured horizontal wells (HFHW). Two dominant flow regimes were identified in liquid-rich counties: linear flow and boundary dominated (BDF) flow.

In field examples, no bilinear flow signatures were observed. Some believe that the presence of bilinear may be more perceived than real, and may be a result of the latter stages of fracture fluid cleanup and, especially, decreasing bottom-hole pressure with time. True bilinear flow is caused by transient flow within finite-conductivity fractures with appreciable pressure drop within the fractures (Anderson et al. 2010).

Linear flow regime is much more common and is virtually always observed in low permeability wells with hydraulic fractures; this implies that negligible pressure drop in the fractures is common. Boundary-dominated flow regime appears when the

area between adjacent hydraulic fractures is being drained (fracture interference) or when the entire drainage area associated with the well contributes to production. Ultimate reserves for a well can be estimated with confidence only if BDF is reached (Anderson and Mattar 2003).

The boundary dominated flow regime can be identified with confidence using a diagnostic plot based on material balance time (MBT), if the variation in flow rate and pressure is smooth (Anderson and Mattar 2003). On a log-log diagnostic plot of MBT and flow rate, q, bilinear flow is identified with a line of negative quarter slope: linear flow with negative half slope, and boundary dominated flow with negative unit slope. In addition, as insurance, I also used log-log rate vs. time plots to identify flow regimes; both the plots should agree. The rate-time plot does not have unit slope during BDF, but the points should deviate downward noticeably from the linear flow (half-slope line trend) to confirm the conclusions from the MBT-rate plot. The material balance plot has a serious weakness that off-trend low rates produce abnormally large MBT values and possibly define the final trend in the data that can confuse identification of BDF. We must have the final rates (in actual time sequence) to also be the final rates in material balance time sequence on our diagnostic plots.

Bilinear flow is uncommon in practice, and when we have pressure data to accompany rate data so that we can calculate and plot pressure-corrected rate data, most apparent bilinear flow disappears. Another problem is not amenable to correction by simple methods: fracture fluid cleanup (Wang et al. 2009). Water rates are the best indicator of fracture fluid cleanup. As long as water production is decreasing toward

zero, the hydraulic fractures in the wells are cleaning up (which, in turn, means decreasing skin and therefore data that should not be included in performance analysis (constant skin absolutely required)). Fracture cleanup frequently requires 3-6 months and sometimes longer (e.g. 12 months in the Barnett Shale oil well area). Therefore, it is advisable to use only data collected after water production has dropped to a low and relatively unchanging level for production analysis. Rates from wells with changing pressures should be corrected when pressure data are available, and then flow regimes should be identified. We eliminated outliers in our data -- any data point that is more than one standard deviation off a good trend line through the rate-time profile should be eliminated from further processing.

Fig. 5 illustrates an oil well from Wise County in the Barnett shale, exhibiting linear flow followed by BDF. BDF becomes more evident when we prepare a MBT and rate diagnostic plot. Water oil ratio (WOR) decreases for the initial 12 months of production, while GOR (gas-oil ratio) is fairly constant (**Fig. 6**). WOR increases late in the well's life (after 60 months), but both oil and water rates have diminished considerably (**Fig. 6**).

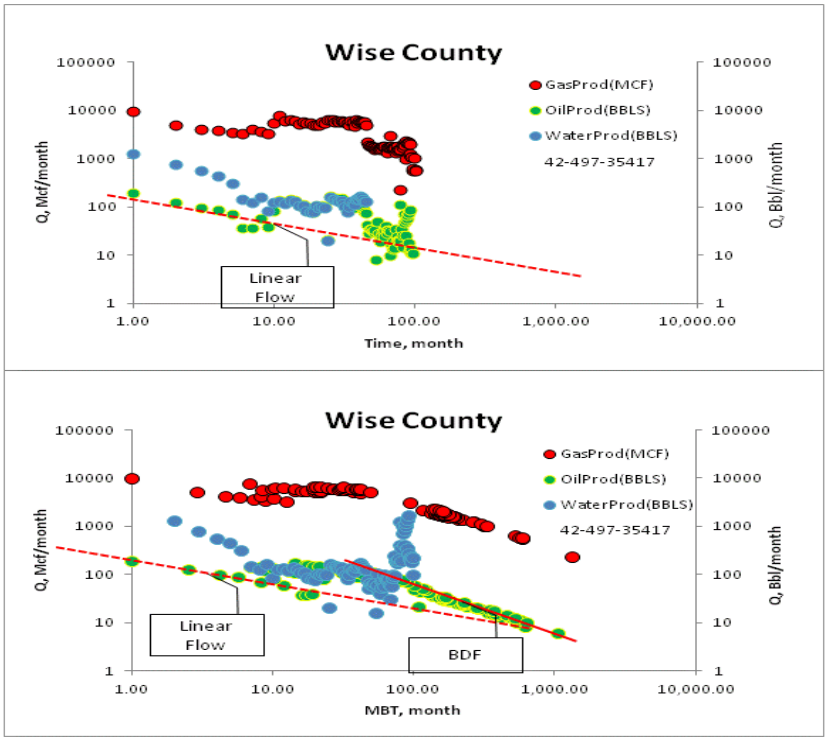

Fig. 5— Identification of flow regimes from a Barnett shale oil well exhibiting BDF

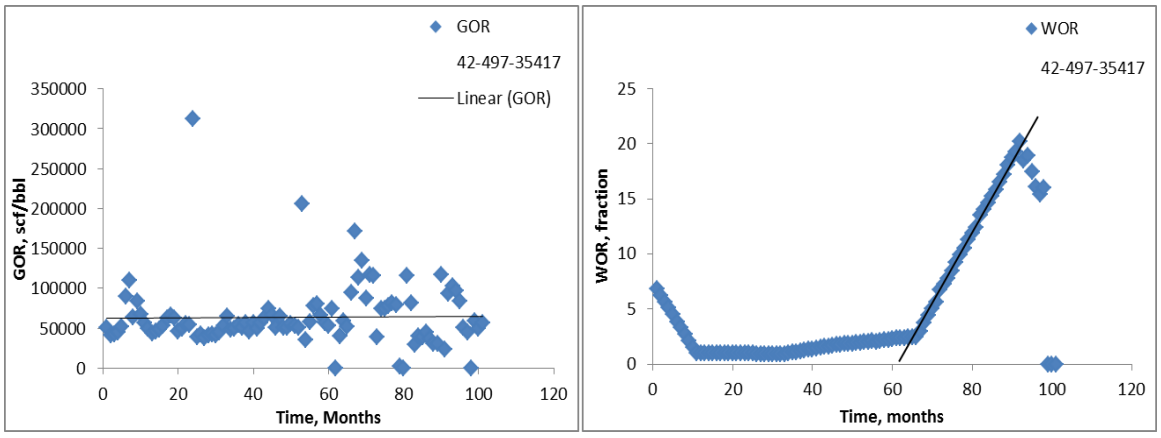

Fig. 6— GOR and WOR for Barnett shale oil well from Wise County, TX.

2.4.3.1 Linear Flow Analysis

Fig. 7 shows an example of an oil well in Wise County. From the diagnostic plots, negative half slope line depicts the linear flow as a dominant flow regime. The Fetkovich type curve confirms that the well is in the linear flow regime. Sometimes linear flow is affected by skin due to flow convergence in horizontal wells and/ or finite conductivity in hydraulic fractures. This skin effect can cause distortions for linear flow to appear like transient radial flow with boundaries (Nobakht and Mattar 2010). In this case, we clearly see presence of linear flow on the half-slope line on Fetkovich fractured-well type curve.

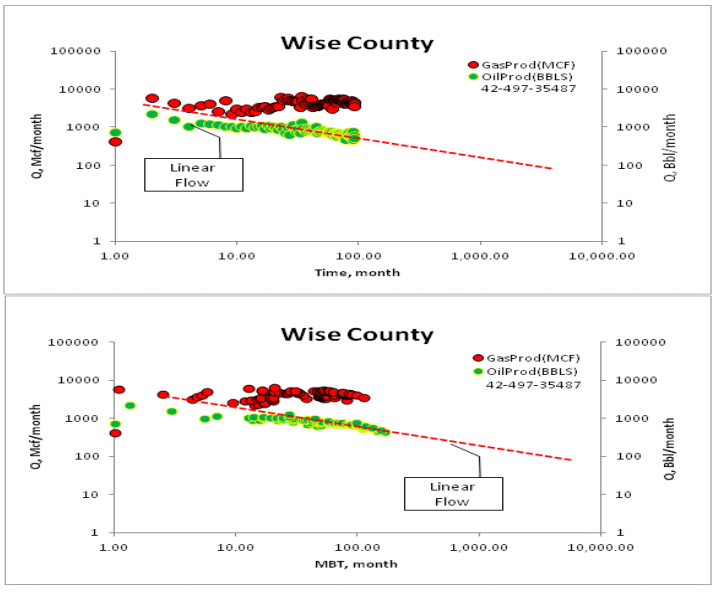

(a)

Fig. 7—Example of an oil well in Wise County in linear flow regime

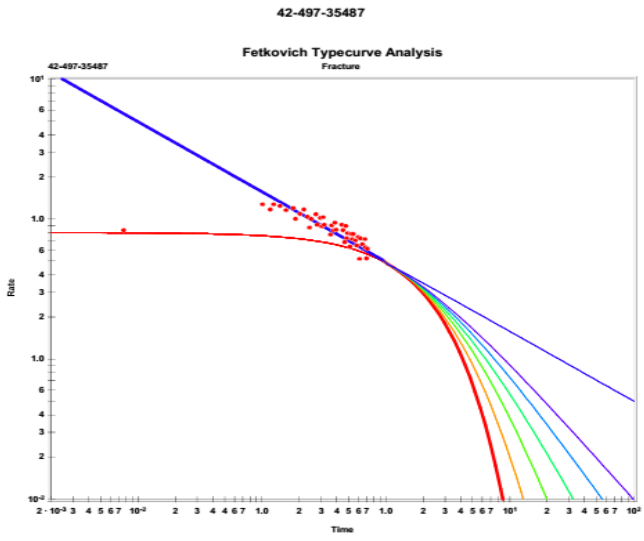

(b)

Fig. 7—Continued

2.4.3.2 End of Linear Flow Analysis

Fig. 8 is an example of a well showing deviation from linear flow, but the deviation does not form a negative unit slope line on a logarithmic plot of rate-time. A logarithmic plot of rate vs. MBT gives a better representation of flow regimes.

Unlike a rate vs. linear superposition time, a rate-MBT plot gives a straight line with a negative half slope in transient linear flow and negative unit slope during BDF and it keeps the characteristic shapes of both the flow regimes (Liang et al. 2011). Hence, it is the preferred superposition time function when variable rates in linear flow are analyzed. The deviation from the straight line can be interpreted as the end of linear

flow. This deviation is attributed to the possibility of fracture interference or variation from initial pressure in the area between fractures (Reese et al. 2013).

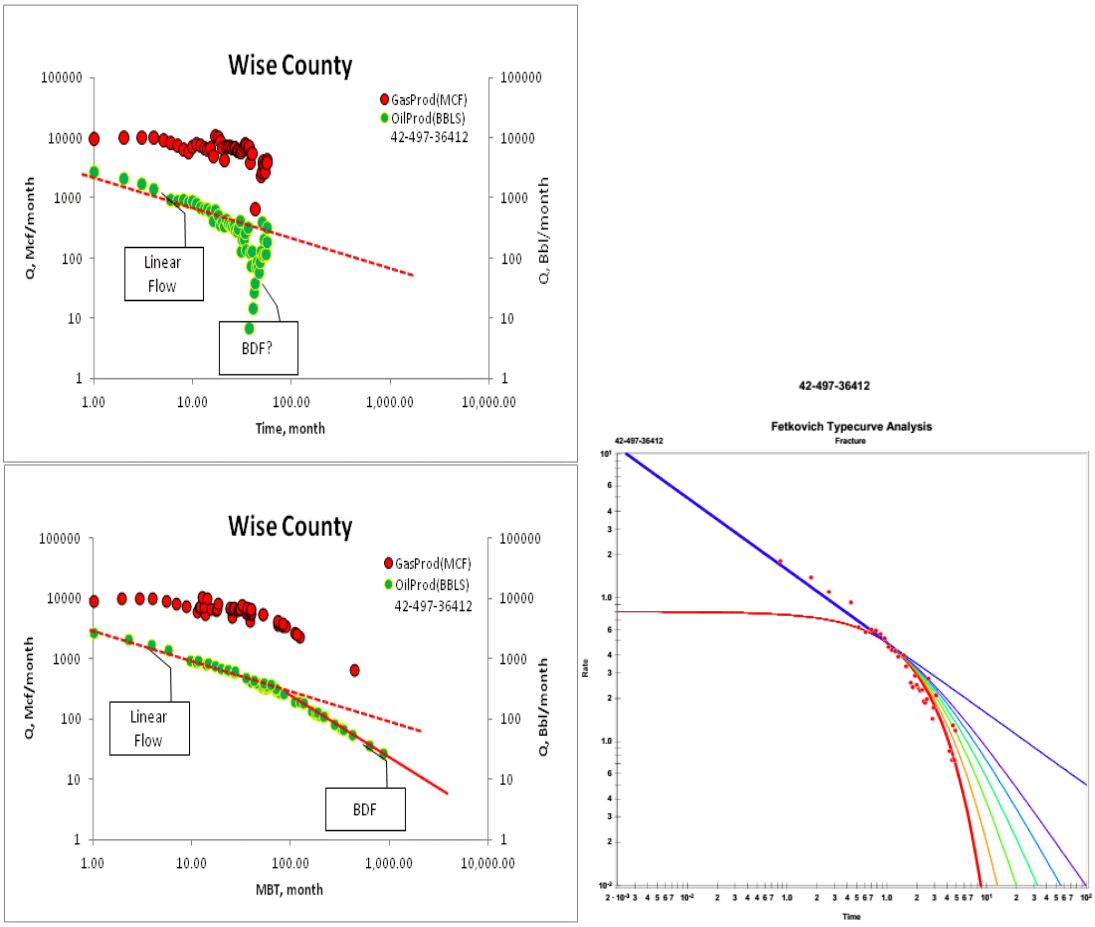

Fig. 8— Example of oil well in Wise County, TX in linear flow regime followed by BDF regime

2.4.4 Hindcasting

Hindcasting is performed by matching a portion of the known production history and comparing the other portion of known production history to the forecast. To investigate the decline behavior of the DCA models, I performed hindcasting of Barnett shale oil wells in Montague County and results are discussed in detail in sections 3.1.2 and 3.1.3.

2.4.5 Forecasting

This step involves the application of decline curve analysis techniques to forecast future production performance using various decline models as discussed in section 2.2.

The process of FRI followed by forecasting is explained in more detail using a field example of an oil well from Eagle Ford shale for which historical daily rate and pressure data are available.

The raw data available for analysis is shown below in **Fig. 9** and **Fig. 10.** It is difficult to analyze this data without removing the outliers and anomalous data points, as their inclusion may cause misleading interpretations. Furthermore, due to variable bottom-hole pressures, it is necessary to correct rates before analyzing further.

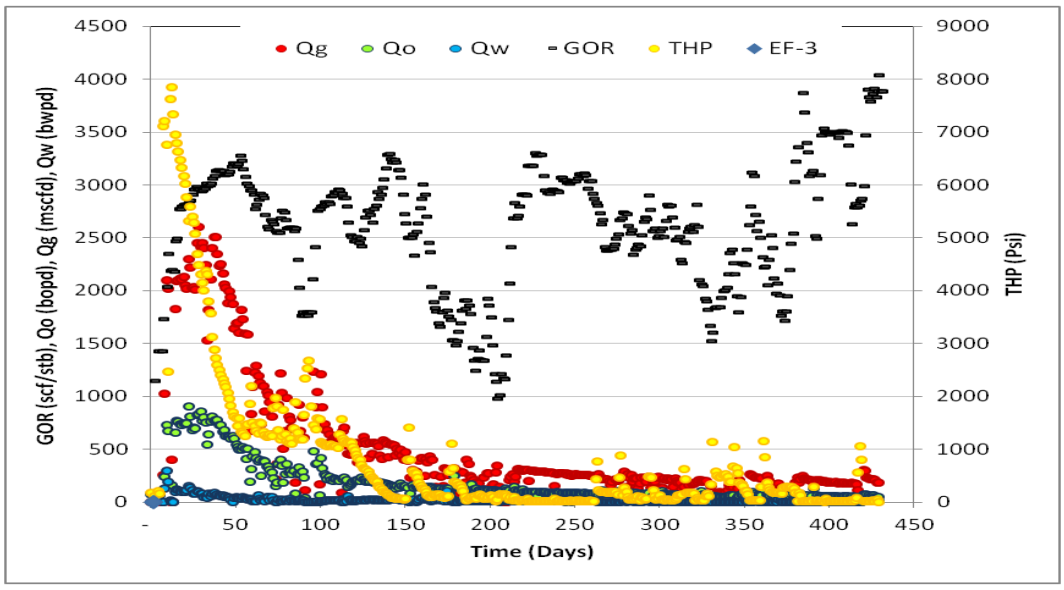

Fig. 9— Flow rates for an oil well in Eagle Ford shale showing unstable flowing conditions (well#3)

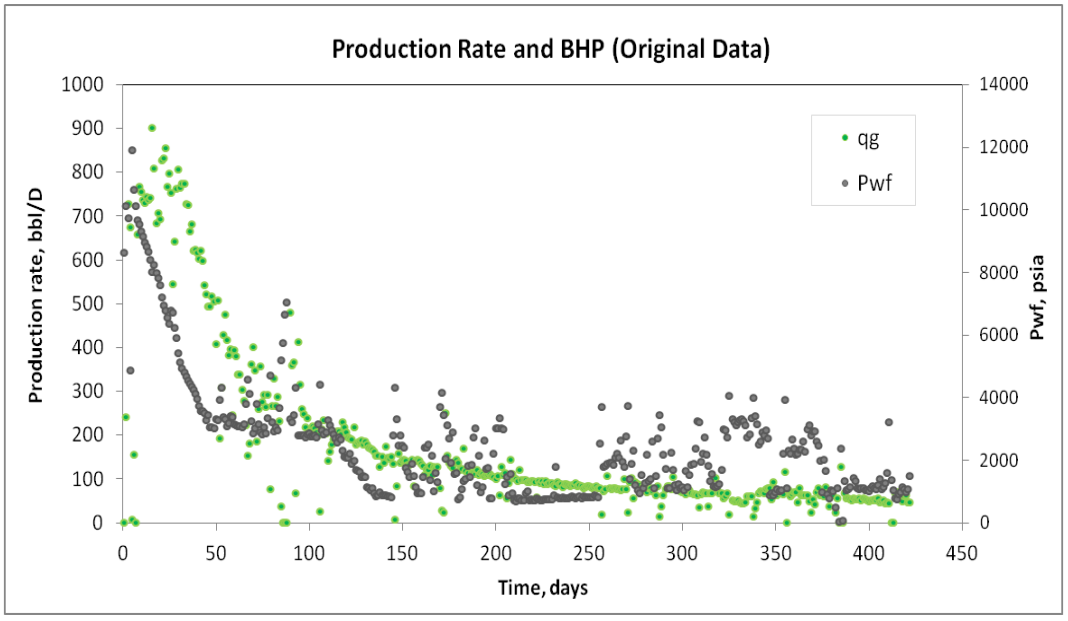

Fig. 10— Example of an oil well from Eagle Ford shale producing under variable operating conditions (well#3)

Once the outliers are removed, next step is to perform FRI. Various diagnostic plots are used to confirm the presence of BDF, and the time of onset of BDF can be determined accurately (**Fig. 11**).

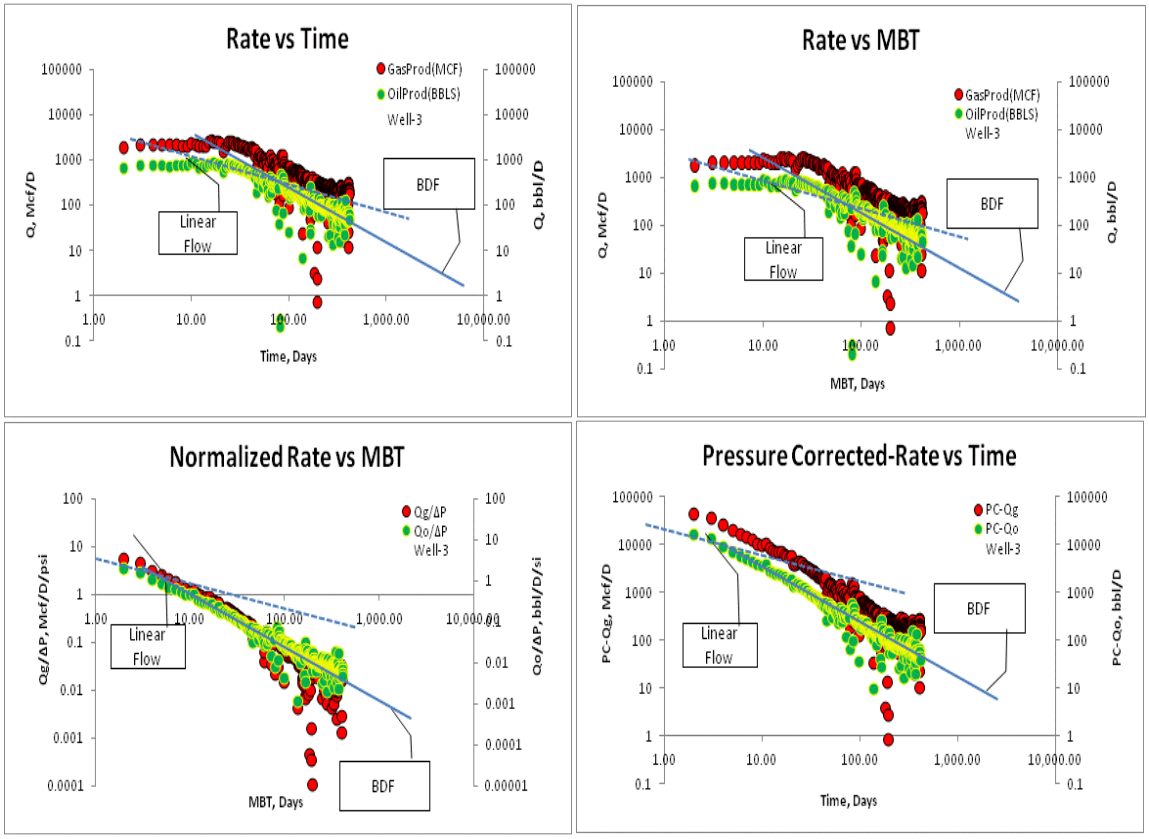

Fig. 11 —Identification of flow regimes using diagnostic plots

The Fetkovich type curve was used to further confirm the presence of BDF and to estimate the Arps decline parameters that were used to constrain the empirical models for BDF effects (**Fig. 12**).

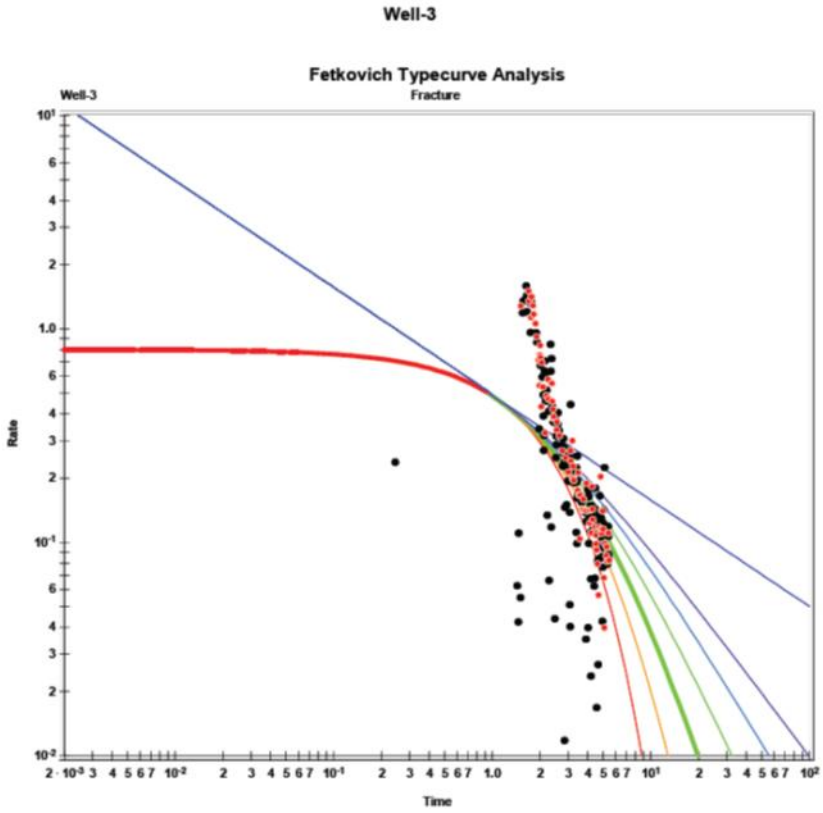

Fig. 12— Fetkovich type curve analysis for an oil well in the Eagle Ford shale. Black dots represent the outliers, whereas red dots are the oil rates included in the analysis. Data points lying outside the type curve represent transient flow.

After identifying the dominant flow regimes and determining the Arps decline parameters, the next step is to forecast production rates. All the models described in

section 2.2 (Duong, SEPD, Arps Hyperbolic, Duong/Arps, SEPD/Arps, YM-SEPD) are applied to forecast production rates (**Fig. 13** and **Fig. 14**). The Duong model is the most optimistic when BDF is present; in comparison, all other models are conservative. Duong/Arps gave the least EUR as expected due to the BDF constraint applied.

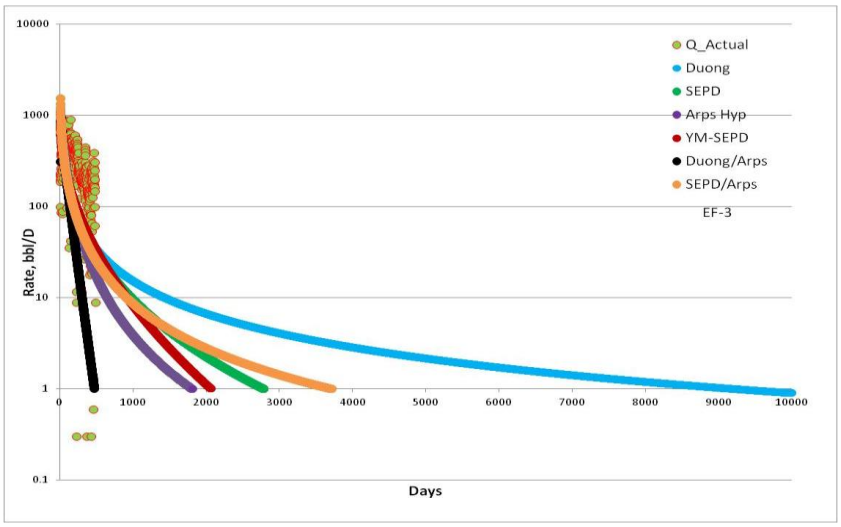

Fig. 13 — Production forecasting using various rate decline models for an oil well in the Eagle Ford shale

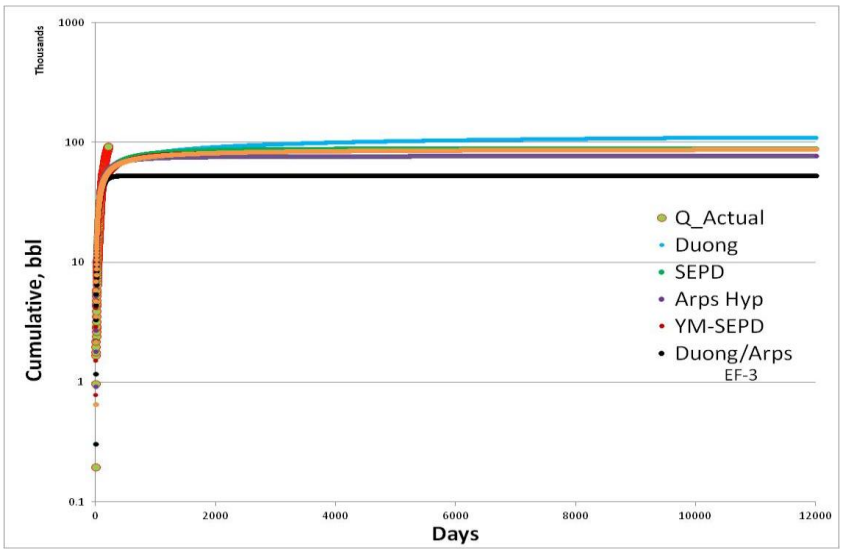

Fig. 14—Cumulative production profile for an oil well in Eagle Ford. Duong model is optimistic, while SEPD and Arps Hyperbolic are conservative.

3. NORTHERN BARNETT SHALE STUDY

Liquid-rich counties in the northern Barnett shale (Montague, Cooke and Wise counties) have more than 600 wells producing liquids. Production data are available from 2003 to August 2013. With such long production histories, it is easier to identify long term behavior of hydraulically fractured horizontal wells (HFHW). I used publically available data from drillinginfo.com . 801 wells were studied to identify the decline trends of liquid hydrocarbon in Barnett shale. I identified two types of flow regimes in these counties: (1) linear flow only and (2) linear flow followed by BDF.

In this study we did not encounter any cases of bilinear flow. The occurrence of bilinear flow is attributed mainly to fractures with significant pressure drop within the fracture.

Linear flow regime is observed mainly in low permeability reservoirs, particularly wells with long fractures. There is widespread misunderstanding of the long term performance of shale gas and oil wells. Due to ultra-low permeability of shale reservoirs, long durations of transient flow effects are observed which makes production forecasting uncertain. Usually bilinear and radial flow regimes observed during transient flow for short durations of production in hydraulically fractured wells (HFW) are affected by stimulated reservoir volume (SRV) and, in the long term, by heterogeneities in the reservoir and flow boundaries (Clarkson, 2012). In this section, I analyzed production performance of the northern Barnett by first identifying the

dominant flow regimes. Material balance times versus flow rate diagnostic plots were used to identify flow regimes.

The following section illustrates the distribution of various flow regimes identified in the three counties of the northern Barnett shale (**Fig. 15**). Two dominant flow patterns were identified: (1) linear flow and (2) linear flow followed by BDF. In many cases, due to noisy and scattered production data, no flow regime could be identified and in some cases constant production rates were observed.

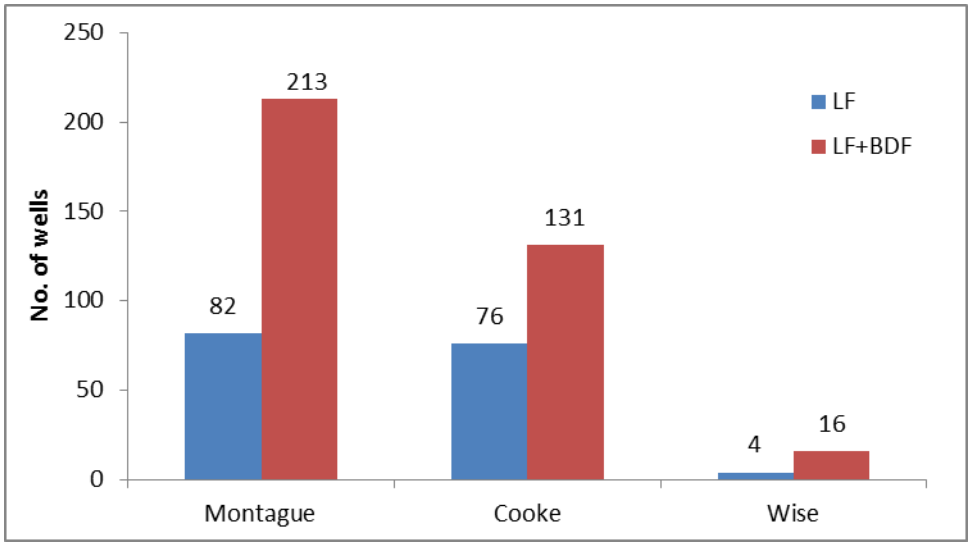

Fig. 15— Flow regimes identified in the three counties of the northern Barnett shale

3.1 Flow Regime Identification: Montague County

213 wells were identified to be in BDF in Montague County. Diagnostic plots mentioned in previous section were used for FRI. The following section discusses the implications on cumulative production at the end of production history for causing inaccurate estimates of time for end of linear flow and the onset of BDF. The location of wells studied is shown in **Fig. 16** with yellow dots.

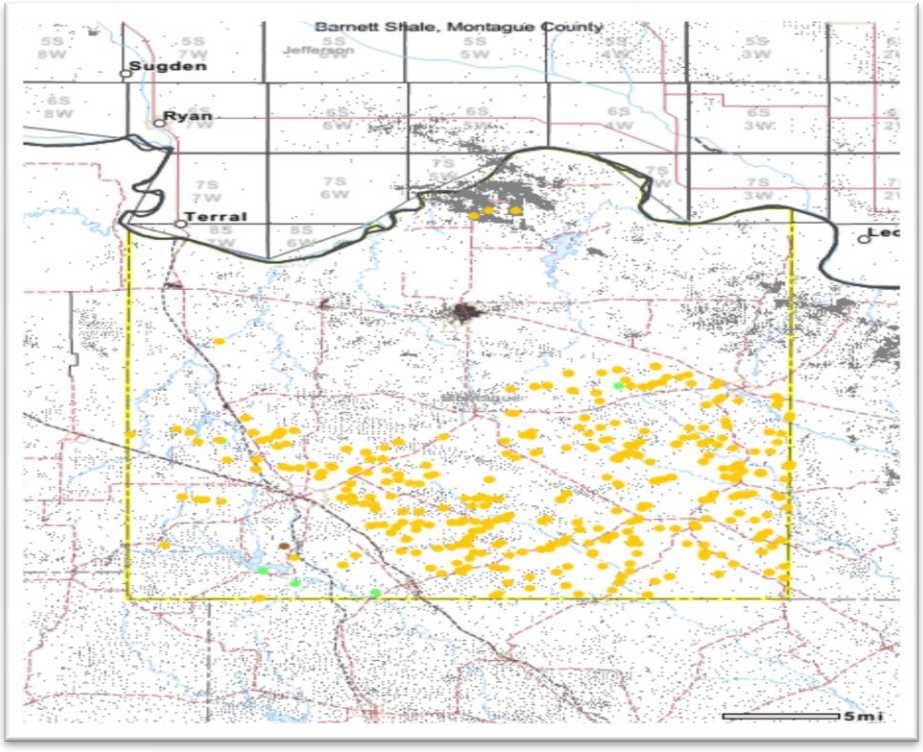

Fig. 16—Location of oil wells studied (marked with yellow dots) in Barnett shale, Montague County, TX

3.1.1 Inaccurate Estimation of BDF

Two examples of hindcasting from Montague County illustrate the percentage error at the end of production history. Rate-time plot in **Fig. 17** shows the decline profile of the well with 9.2 years of production history.

Fig. 18 shows that the well entered into BDF at around 24 months of production. BDF is confirmed from rate versus material-balance-time (MBT) plot, shows the BDF onset at 90 MBT.

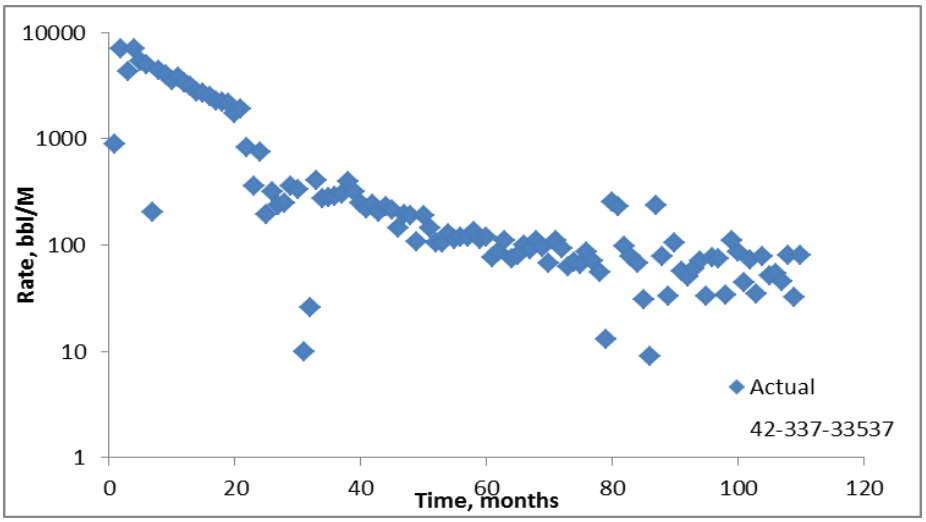

Fig. 17—Production profile for oil well API# 33537

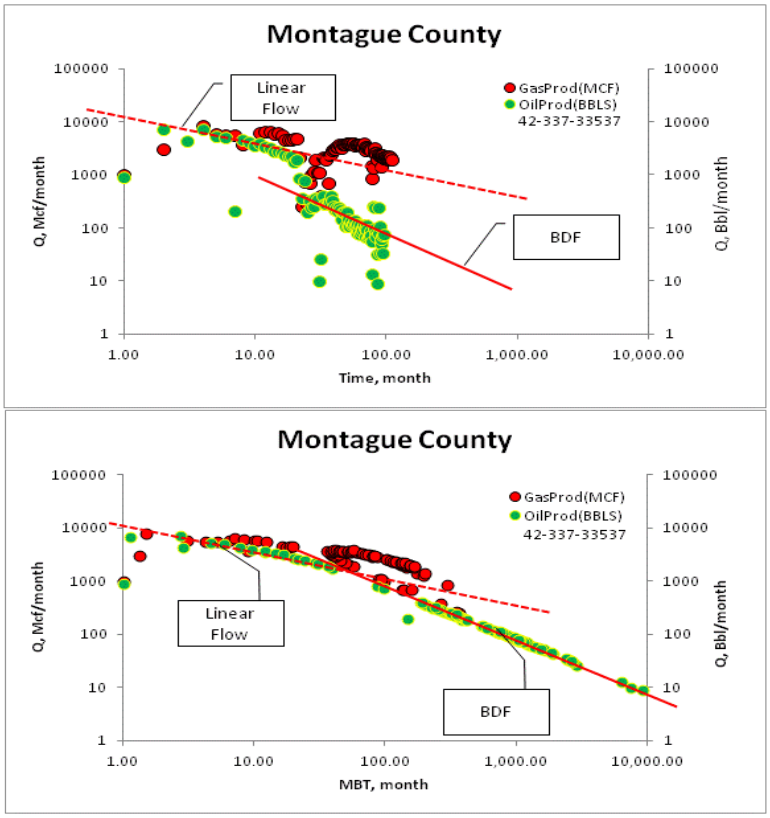

(a)

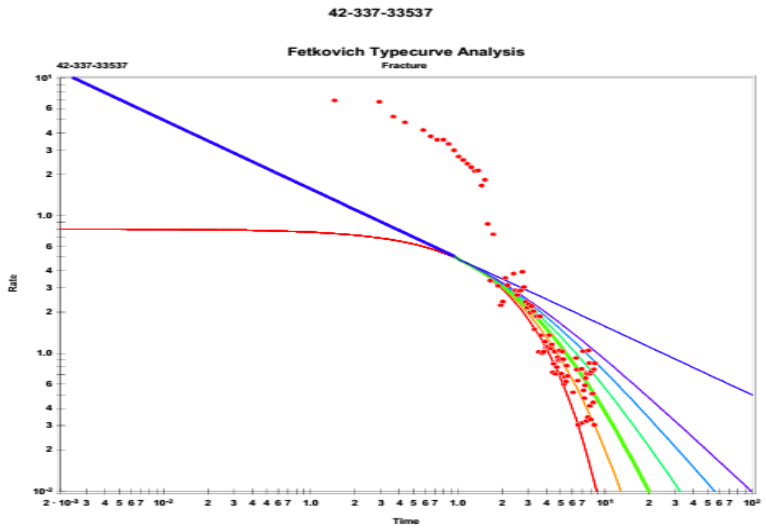

(b)

Fig. 18— (a) Flow regime identification of oil well in Montague County; (b) Fetkovich type curve confirms the presence of BDF

3.1.2 Hindcast Analysis for Montague County Wells

I performed hindcast analysis to determine whether the onset of BDF was ignored while forecasting production rates that could lead to significant errors in EUR. For well API# 33537, linear flow ends at 35 months and half of the production history (60 months) provided the basis to forecast the final 60 months of production rates. The forecast is then compared to the actual production during these final months.

In **Fig. 19**, deviation from linear flow is well captured by the green curve that takes into account effect of BDF on the production forecast, whereas the unconstraint model is unable to correct for BDF effects and overestimates the production rates.

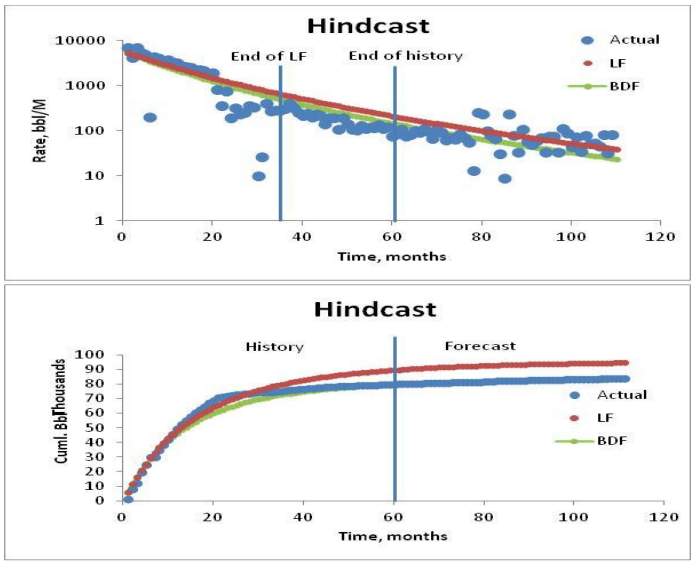

Fig. 19—Hindcast of well API# 33537 in Montague County, TX to analyze the error due to misinterpretation of BDF onset time

A similar analysis of BDF interpretation is done for well API# 33624 (**Fig. 20, Fig. 21 and Fig. 22**) and the error in the cumulative production at the end of production history is summarized in Table 4.

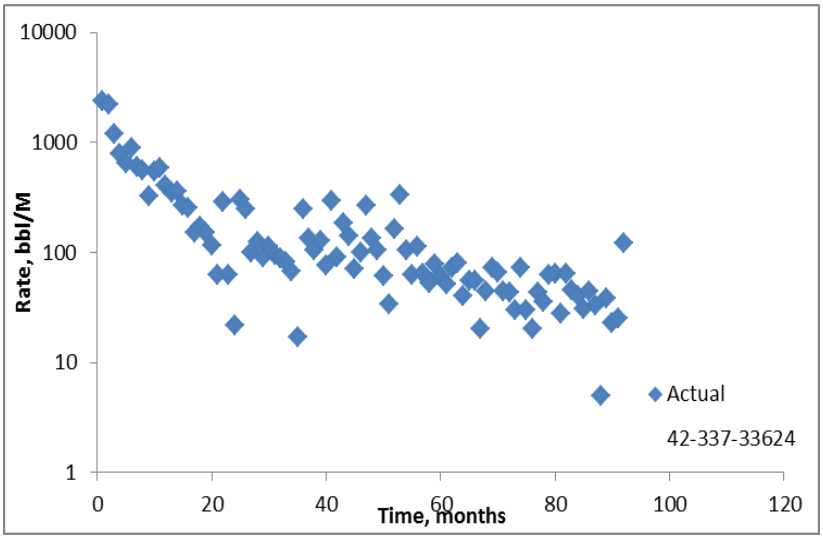

Fig. 20— Actual production data of well API# 33624 in Montague County, TX

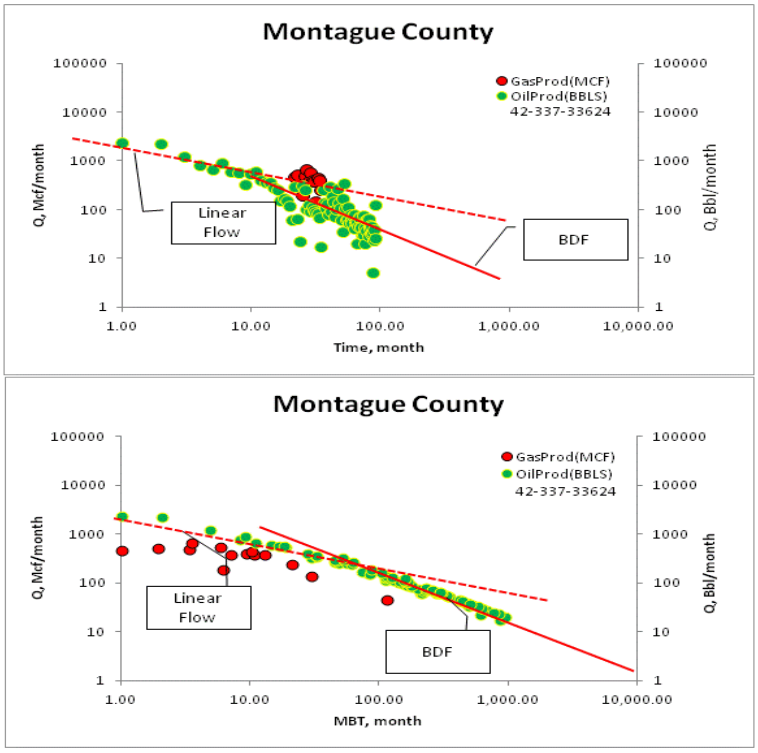

(a)

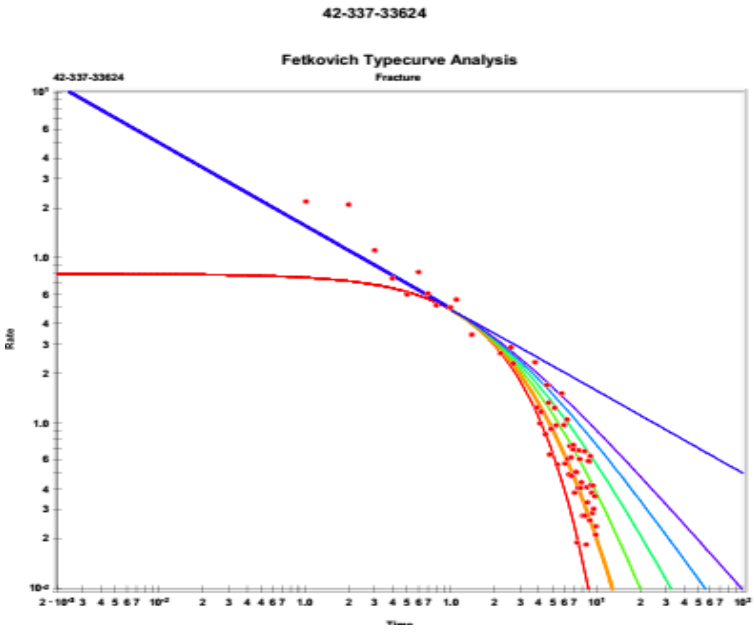

(b)

Fig. 21—(a) Flow regime identification of Barnett shale oil well, Montague County, TX; (b) Fetkovich type curve confirms the presence of BDF regime

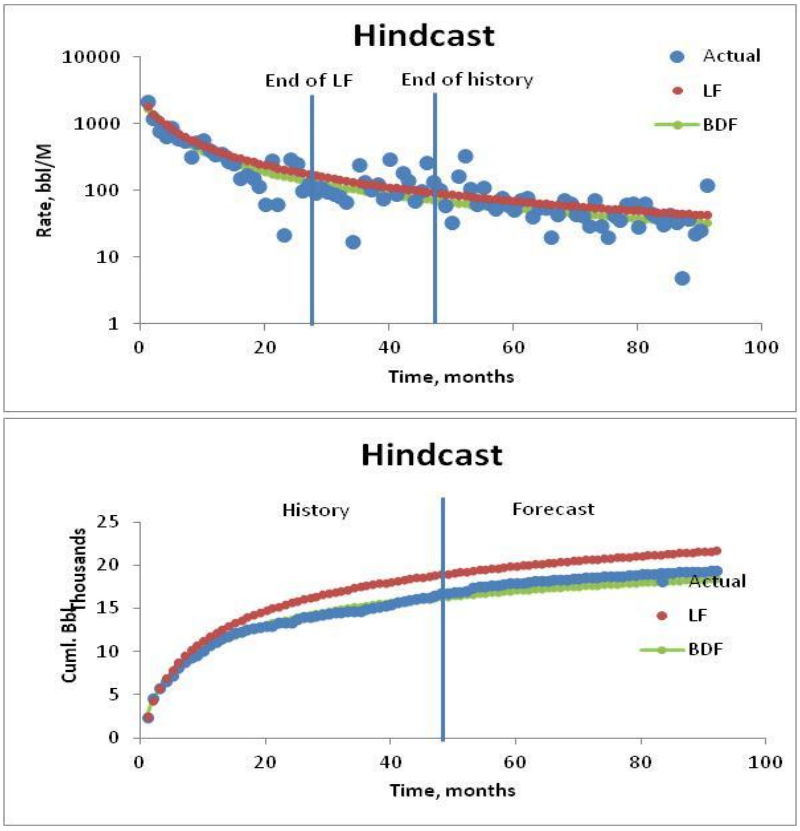

Fig. 22— Hindcast of well API# 33624; misinterpretation of BDF onset time causes significant error in the error

In summary, identification of flow regimes and estimation of expected or observed time of BDF onset is a crucial step. Otherwise, errors in cumulative production will likely appear and may grow throughout the remaining well life.

Table 4— Accurate estimation of time of onset of BDF from diagnostic plots leads to smaller hindcast error in the EUR at the end of production history

Well API#	Onset of BDF accurately estimated and accounted in forecast	Onset of BDF not accounted in forecast
33537	0.83%	-12.93%
33624	5.06%	-11.53%

3.1.3 Hindcasting for Montague Country Wells in BDF Regime Using Various Decline Models

Error in cumulative production was calculated from various hybrid models to analyze the effect of flow regimes on the decline behavior predicted by each models. The FRI for well API# 33537 and 33624 were discussed in previous section and **Fig. 23** and **Fig. 24** show the hindcast analysis of these well.

Additional examples of wells in BDF are presented in Appendix A. These wells are representative of wells in BDF in Montague County and the decline trend observed is attached in Appendix A. It is observed that in all the cases presented below, the Duong model is optimistic if BDF has been observed, whereas SEPD is always conservative. Table 5 provides a summary of the hindcast analysis for these wells.

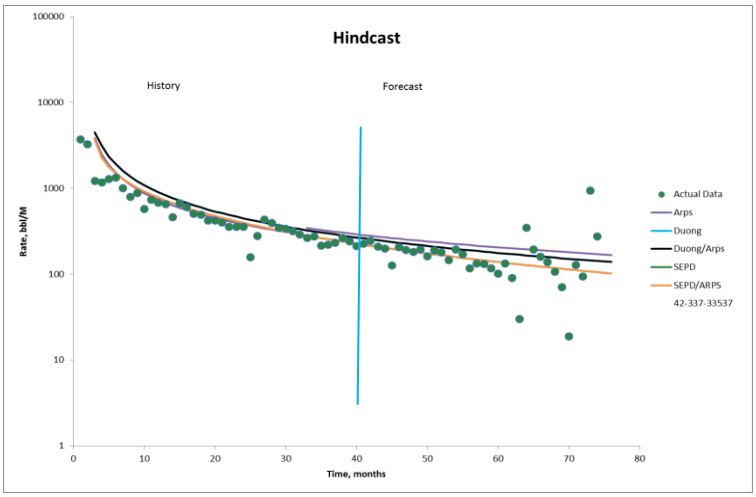

Fig. 23—Hindcasting of well API# 33537 to analyze error in cumulative production at the end of production history. Vertical line at 40 months represents production history used to determine model parameters used for forecasting step.

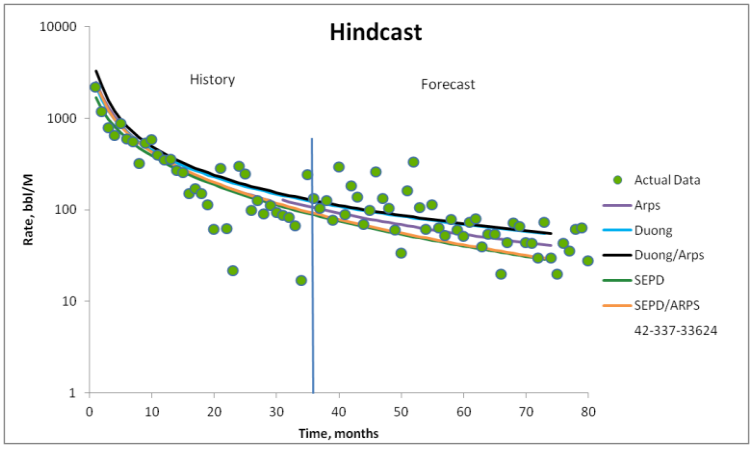

Fig. 24—Hindcasting for wells API# 33624 to analyze error in cumulative production at the end of production history. Vertical line at 35 months represents production history used to determine model parameters used for forecasting step.

Diagnostic plots (rate vs. time and rate vs. MBT) confirm the onset of BDF and the time for the end of linear flow and onset of BDF. In most cases, these times may be same, while in some cases it is observed that there is a transition period between the end of linear flow and onset of BDF. The general production decline trend of Montague county wells is linear flow followed by BDF. Furthermore, once a well enters BDF, it is observed to remain in BDF till the end of its economic life.

Table 5—Montague County percentage error in cumulative production at the end of production history

Well API#	Arps Hyp	Duong	Duong/Arps	SEPD	SEPD/ARPS
42-337-33624	6.26%	-15.15%	-15.15%	11.97%	11.97%
42-337-33614	-4.77%	-23.69%	-23.69%	-1.02%	-1.02%
42-337-33537	-1.47%	19.73%	19.73%	16.01%	16.01%
42-337-33675	-7.00%	-16.96%	-16.96%	-14.26%	-14.26%
42-337-33683	7.28%	-43.88%	-43.88%	3.89%	3.89%
42-337-33688	22.72%	-2.74%	-2.74%	21.22%	21.22%

The percentage error calculated from the hindcast analysis of Montague County representative wells is summarized in Table 5. Models with lowest percentage error in the EUR at the end of production history are highlighted with yellow color. For wells with BDF as the final flow regime, the Arps hyperbolic model gives the minimum error in cumulative production at the end of production history. For two cases (API# 33614

and 33683) SEPD with a switch to Arps tail was more accurate method while for one case (API# 33688), the Duong model with a switch to Arps model gave more accurate estimate of production rates.

3.2 Flow Regime Identification: Cooke County

Cooke County is another of the liquid producing counties in the Barnett shale. In this study, I analyzed publically available monthly production data of more than 350 wells (concentrated in western Cooke County). Wells that have reported zero production for more than three months and inactive wells were excluded from this study. I found 131 wells exhibiting BDF. The average time to end of linear flow was 12 months. The following map shows the location of wells analyzed in Cooke County for this study (**Fig. 25**).

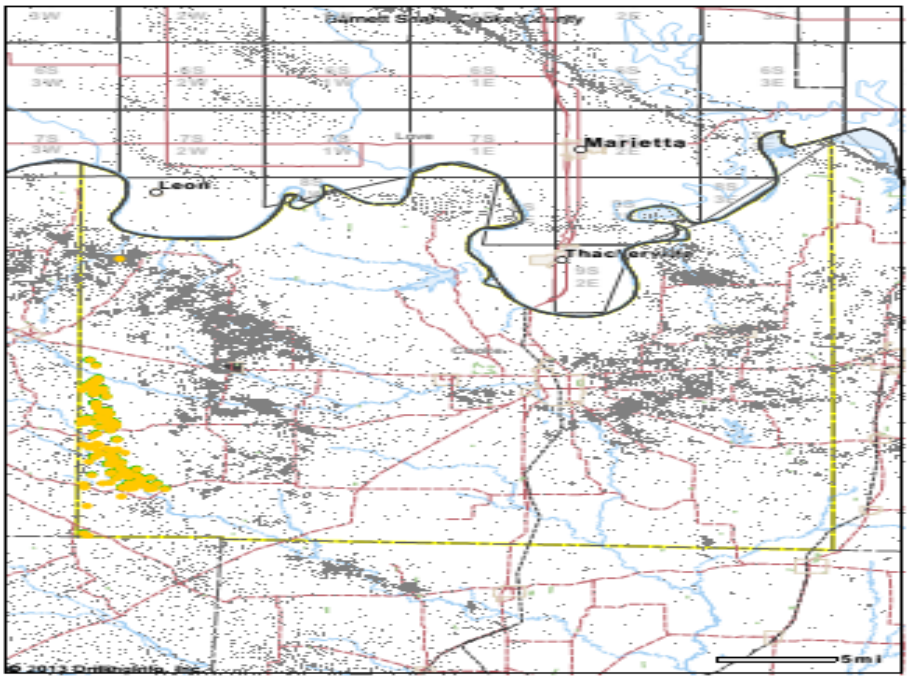

Fig. 25—Yellow dots represent the location of oil wells in Cooke County, TX

Fig. 26, **Fig. 27 and Fig. 28** are examples of diagnostic plots for horizontal oil wells in Cooke County in the Barnett shale.

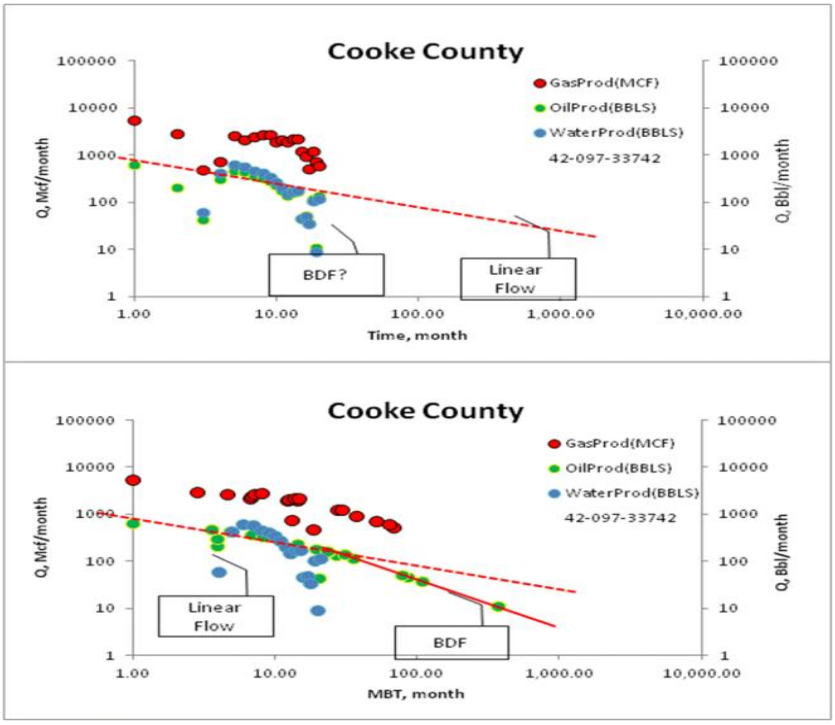

Fig. 26— Flow regime identification of an oil well API# 33742 in Barnett shale, Cooke County, TX

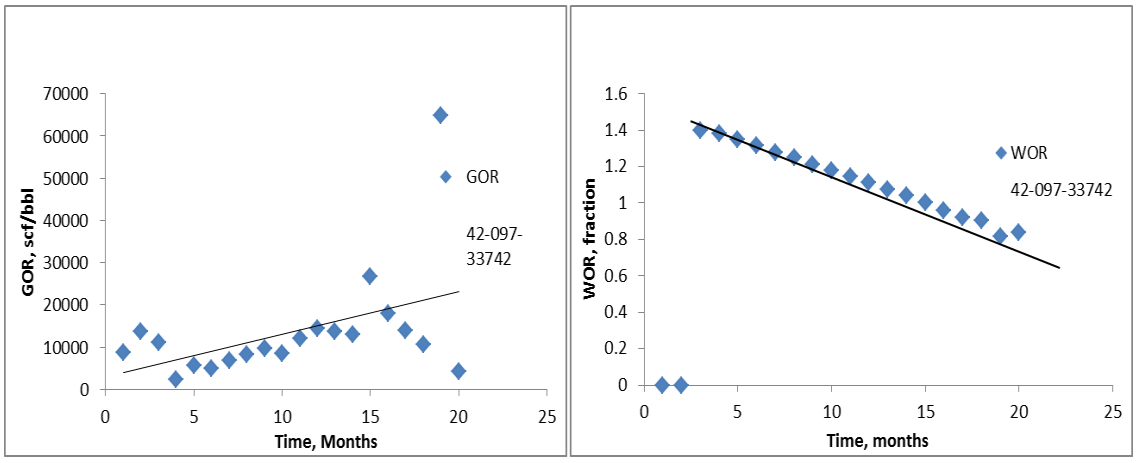

Fig. 27— GOR increases while WOR decreases for well API# 33742

The data points on straight line with a negative half slope represent the linear flow. Deviation from this straight line after linear flow ends can be attributed to fracture interference. The initial offset of data points from the straight line in the beginning of production could be due to fracture fluid clean up or constraints in production, etc.

In **Fig. 28**, low rates deviating from straight line of negative half slope could also be due to liquid loading. GOR is increasing while WOR is decreasing **(Fig. 29**).

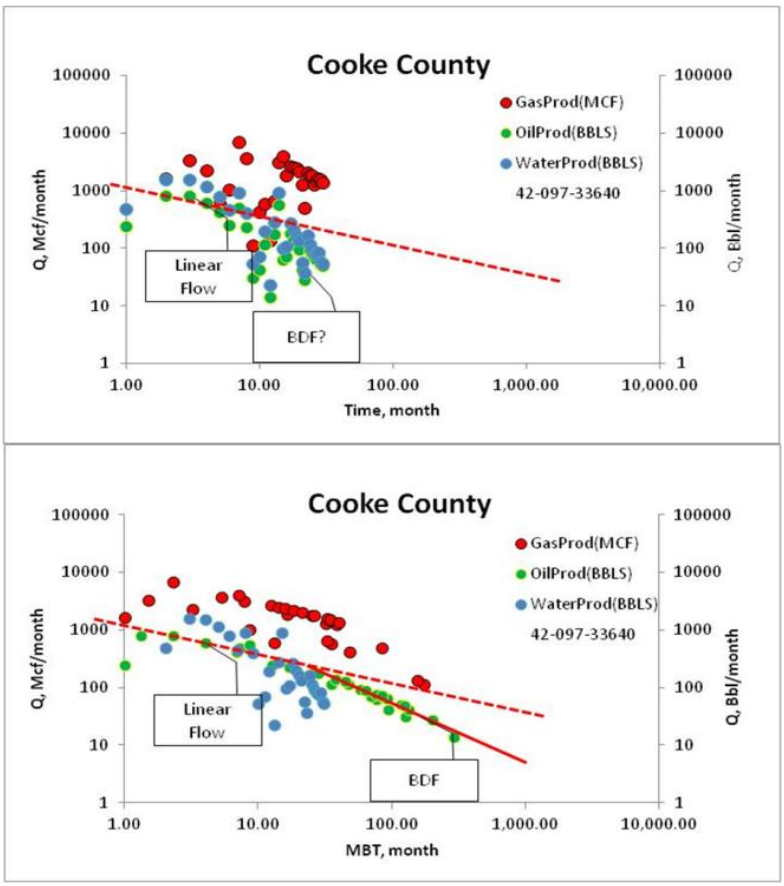

Fig. 28—Flow regime identification of an oil well API# 33640 in Barnett shale, Cooke County, TX

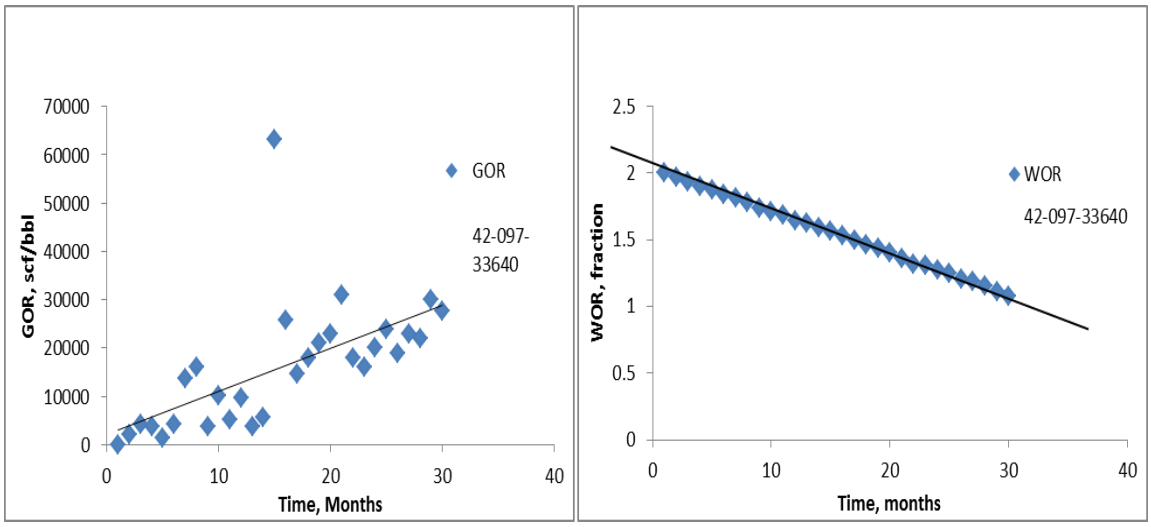

Fig. 29— GOR increases while WOR decreases for well API# 33640

3.3 Flow Regime Identification: Wise County

Wise County is located in the oil window of the Barnett shale. In this study, I analyzed publically available monthly production data for 20 wells (**Fig. 30**). Wells that reported zero production for more than three months and inactive wells were excluded from this study. I found 16 wells exhibiting BDF.

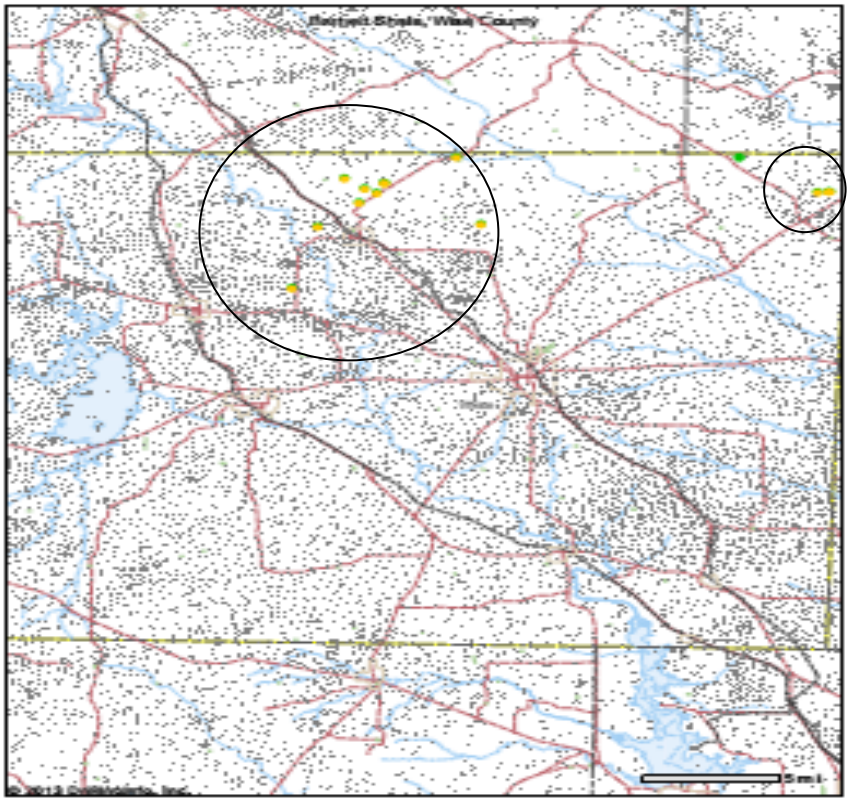

Fig. 30—Yellow dots in the circles represent the location of oil wells analyzed in Wise County, TX

4. EAGLE FORD SHALE STUDY

Eagle Ford Shale (South Texas, USA) is unique due to the variations in geology and fluid type across the play. It is also known as a stacked play as it is sandwiched between Buda Lime and Austin Chalk and it has been the source rock for these two formations. The play-wide analysis of fluid types and GOR variation, peak monthly oil production and other geological characteristics are discussed by Tian et al. (2013). In this study, 2043 oil/condensate wells from liquid-rich counties including Dimmit, Atascosa, La Salle, Karnes, Gonzales and McMullen were evaluated (**Fig. 31**). The main objective was to identify a technique that is easy to apply and that gives confidence in production forecasting. Hindcast analysis was performed to validate the methodology. Distribution of the flow regimes is shown in **Fig. 32**.

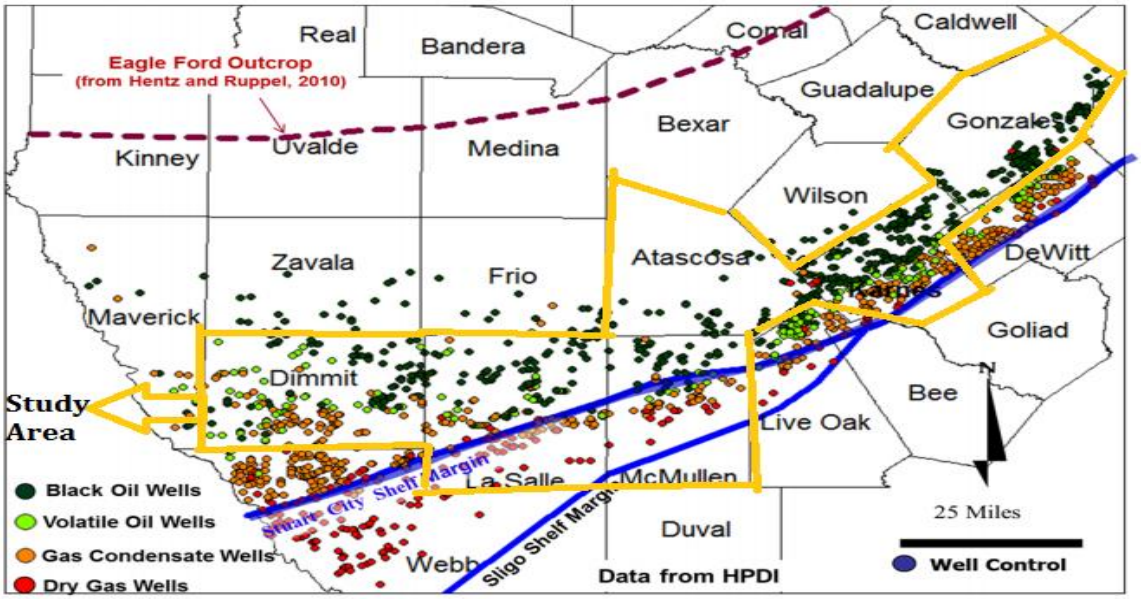

Fig. 31—Location of wells studied in the Eagle Ford shale. (modified from Tian et al. (2013))

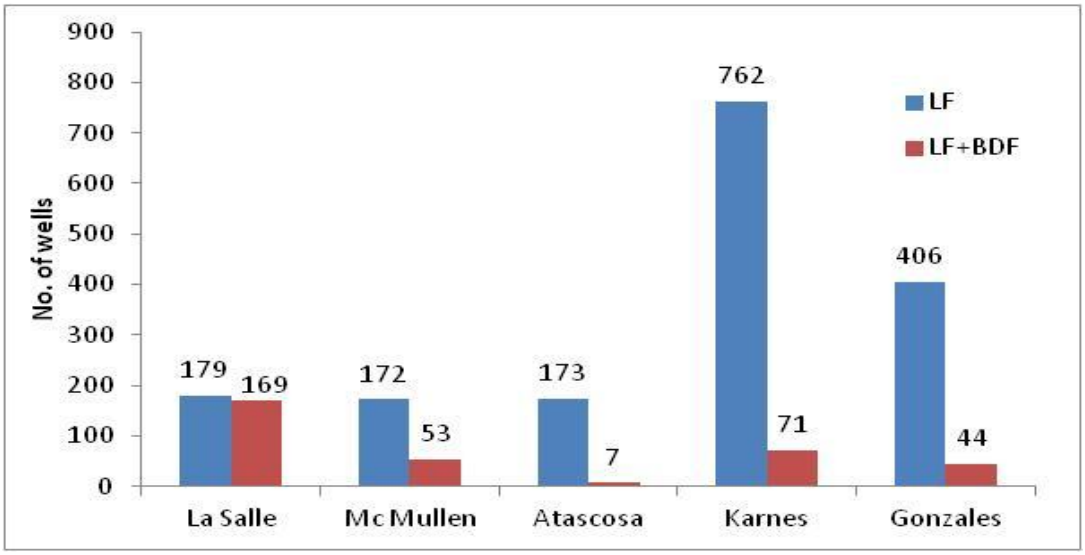

Fig. 32—Flow regime distribution in the Eagle Ford shale; with short production history available, linear flow seems to be the dominant flow regime.

4.1 Atascosa County

Atascosa County is located in the oil window of the Eagle Ford shale. In this study, I analyzed publically available monthly production data from 180 wells. Wells that have reported zero production for more than three months and inactive wells were excluded from this study. I found seven wells exhibiting BDF and the average b was 0.45 for BDF regime. The location of wells analyzed with yellow dots (**Fig. 33**).

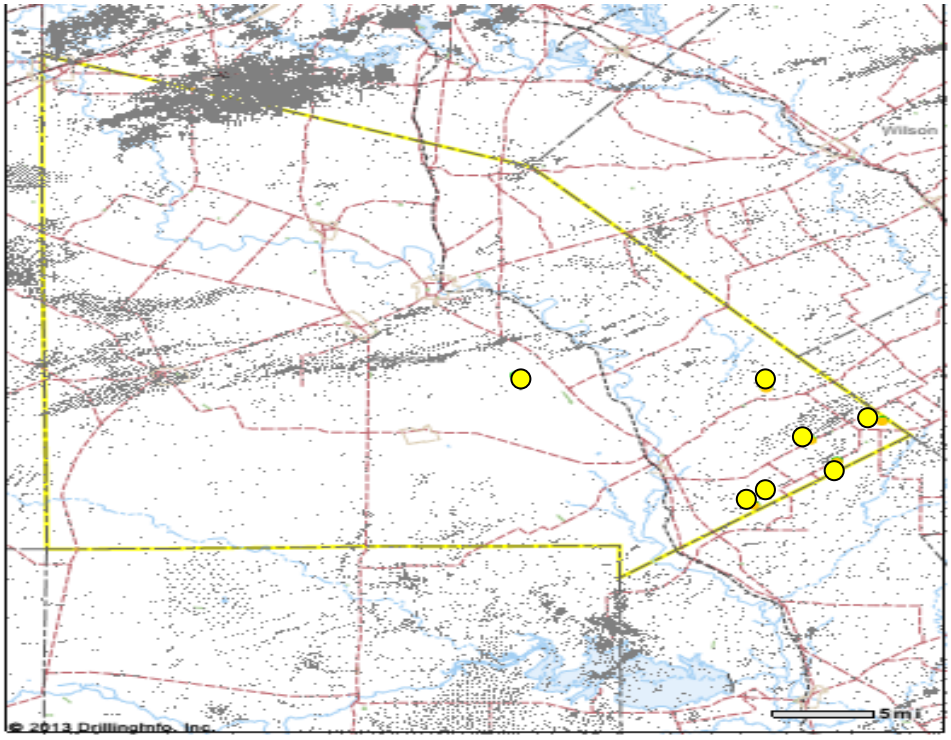

Fig. 33—Location of wells analyzed in the Eagle Ford shale, Atascosa County, TX is shown with yellow dots

4.1.1 Flow Regime Identification: Atascosa County

Fig. 34 is an example diagnostic plot for an oil well from Atascosa County in the Eagle Ford shale. A log-log plot of rate vs. time shows the presence of BDF in the first six months of production. A log-log plot of rate vs. MBT shows that the initial flow regime is linear flow. Thus, using only a rate vs. time plot can lead to misleading results. To gain more confidence, it is advisable to correct or normalize rates for changes in pressure. For cases which do not have pressure history available, constant bottom-hole pressure is implicitly assumed. GOR increases for 20 months then decreases.

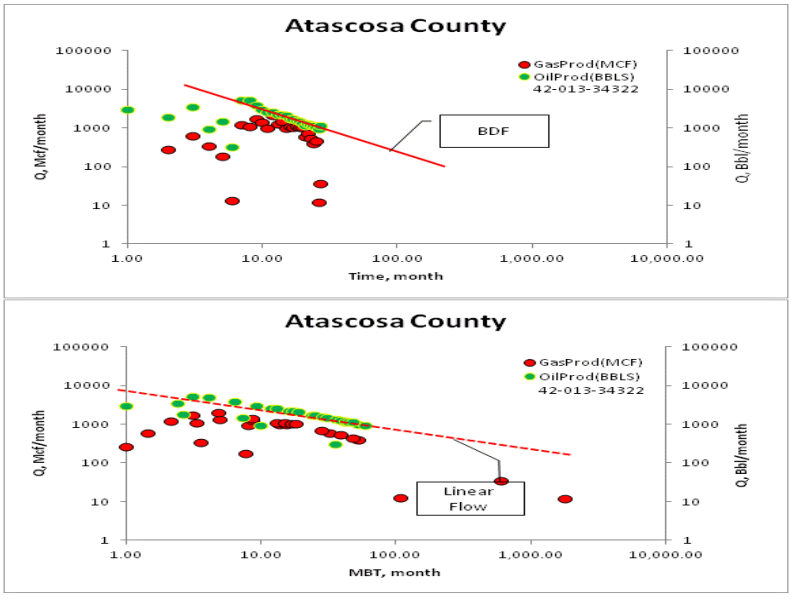

(a)

Fig. 34—(a) Example oil well API# 34322 exhibiting linear flow regime and (b) GOR increases initially the decreases after 20 months of production

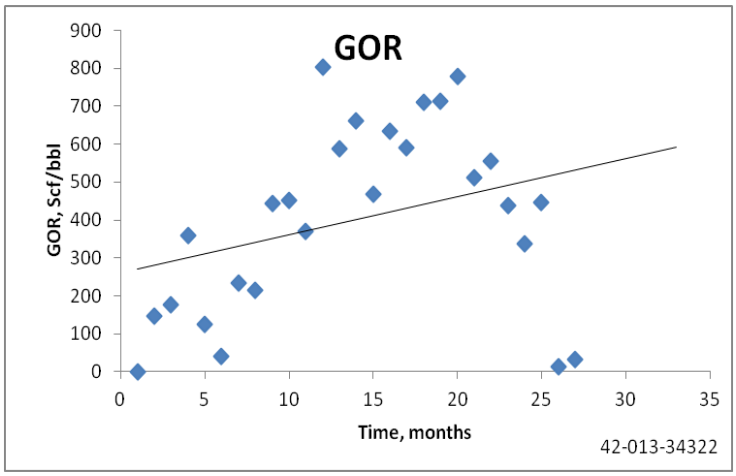

(b)

Fig. 34—Continued

4.1.2 Hindcasting

A summary of hindcast results is given in Table 6. It is observed that the Arps hyperbolic decline model is more accurate more often than other methods (**Fig. 35**).

4.1.3 Forecasting

Production forecasts from various decline models were obtained to evaluate the decline trend. To constraint the models for BDF effects, a D_{switch} of 5%/year and an Arps tail with a b value of 0.3 was imposed (**Fig. 35**).

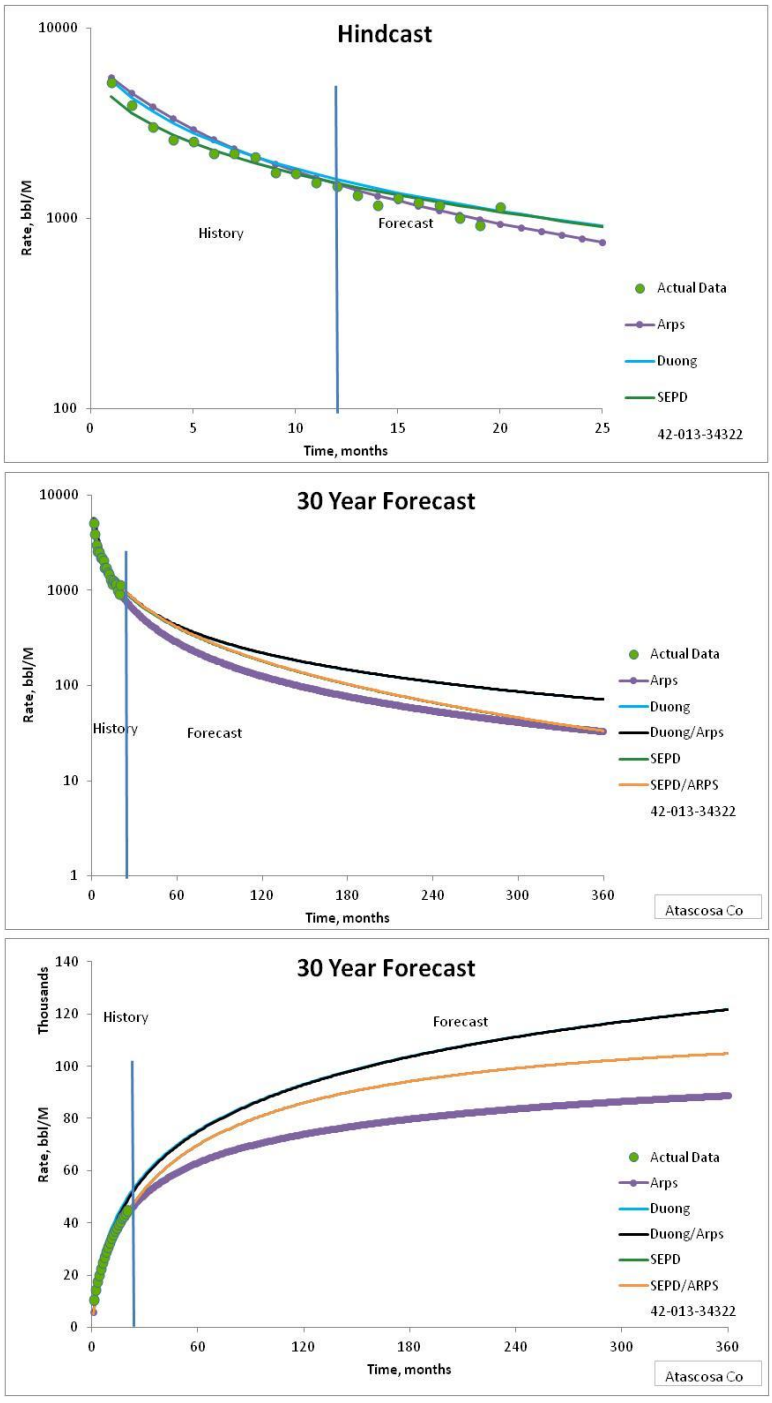

Fig. 35—Hindcast and forecast for well API# 34322 in the Eagle Ford shale Atascosa County, TX

4.2 Gonzales County

Gonzales County is located in the oil window of the Eagle Ford shale. In this study, I analyzed publically available monthly production data of more than 450 horizontal oil wells (**Fig. 36**). Wells that have reported zero production for more than three months and currently inactive wells are excluded from this study. I found 44 wells exhibiting BDF regime. The average time of end of linear flow is 12 months.

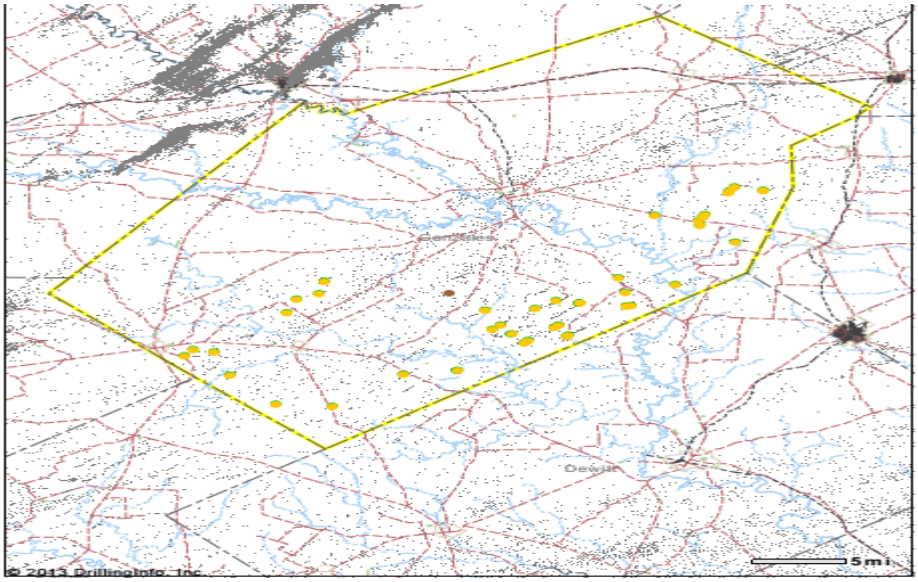

Fig. 36—Yellow dots represent the location of oil wells studied in Gonzales County

4.2.1 Flow Regime Identification

From this example of oil well from Gonzales County (**Fig. 37** and **Fig. 38**), BDF is observed from the two diagnostic plots, but log-log rate vs. time fails to capture the correct duration of linear flow. MBT plot demonstrates the characteristics of both the flow regimes and is more accurate in cases when linear flow is not clearly identified by log-log plot of rate-time. Fetkovich type curve shows the onset of BDF and b value can be read from the type curve for performing production forecasting for Arps model. GOR is fairly unstable during the life of the well.

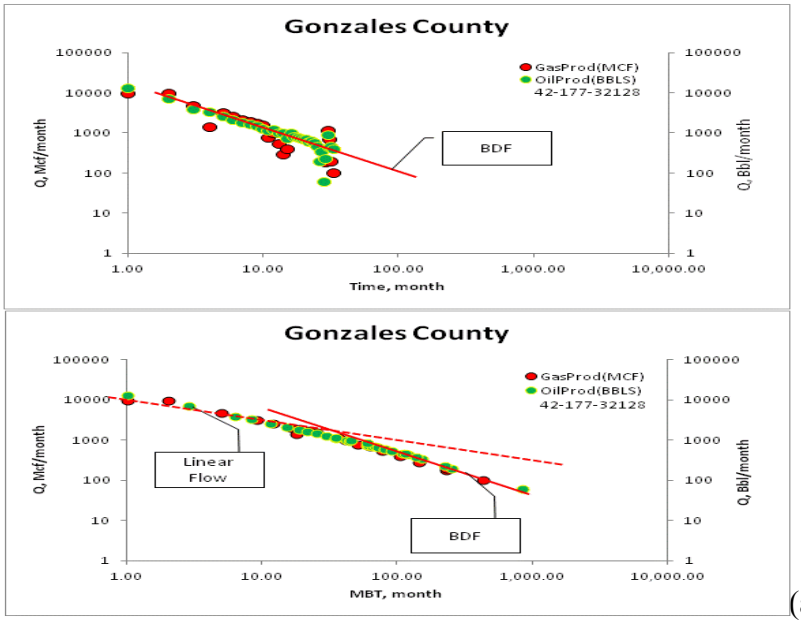

(a)

Fig. 37 —(a) Flow regime identification for an oil well API# 32128 in Gonzales County, TX; (b) from Fetkovich type curve b=0.2 is observed.

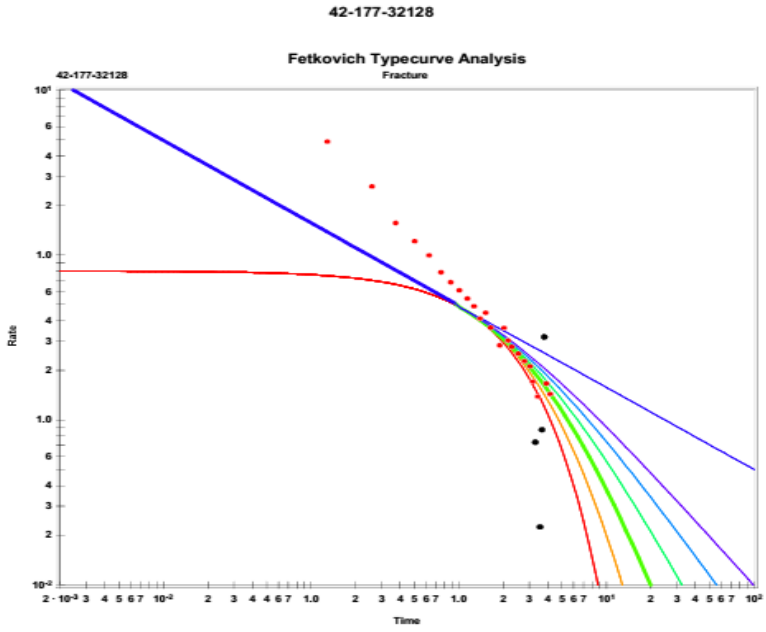

(b)

Fig. 37 —Continued

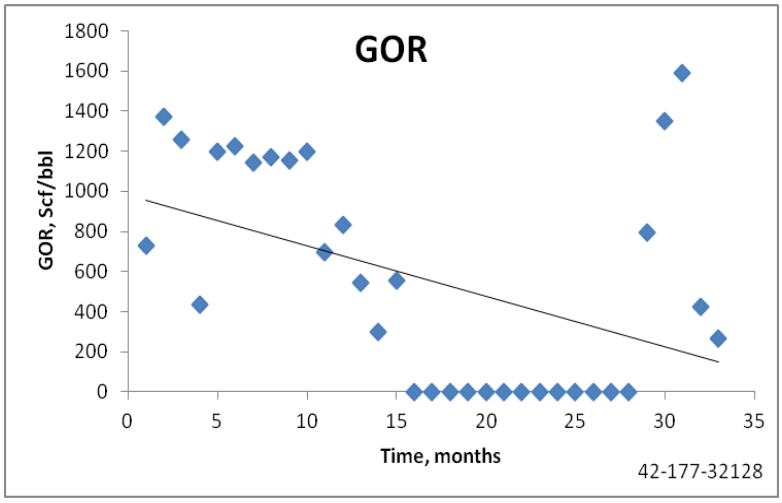

Fig. 38—GOR is unstable for most part of production

4.2.2 Hindcast and 30 Year Forecast

After identification of BDF (**Fig. 37** and **Fig. 38**), hindcasting was performed for well API# 32128. In **Fig. 39**, 15 months of production data was used to forecast next 15 months of production rates. It is observed that models give a fairly similar forecast. A minor scatter of data is observed after 24 months of production. As this well enters into BDF after 12 months, the Duong model gives an optimistic forecast as it assumes well to stay in transient flow regime for the life of the well. The Arps model gives a reasonable forecast while SEPD gives a conservative forecast.

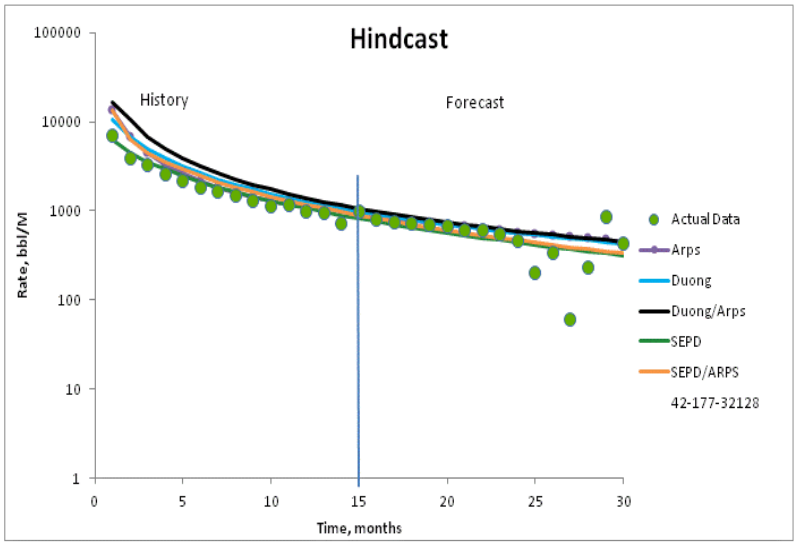

(a)

Fig. 39—(a) Hindcast and (b) forecast for well API# 32128 in Gonzales County, TX; the Duong model is most optimistic while SEPD is conservative.

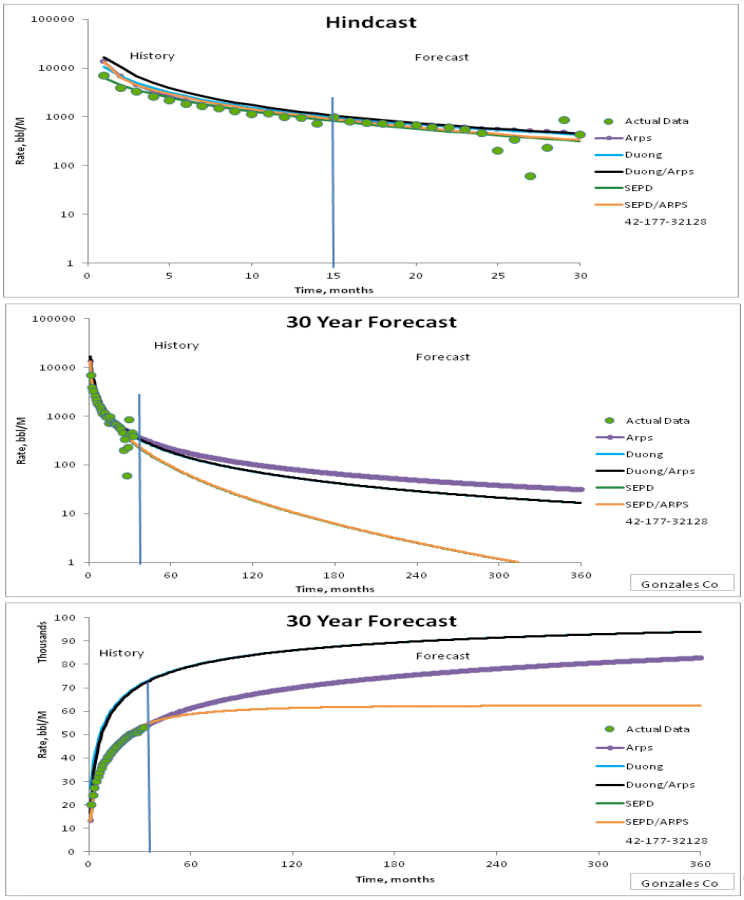

(b)

Fig. 39— Continued

4.2.3 Flow Regime Identification

Another example of a horizontal oil well in Gonzales County is shown in. From FRI it is observed to be in transient state for about 12 months then it enters into BDF. The GOR increases as expected (**Fig. 40**).

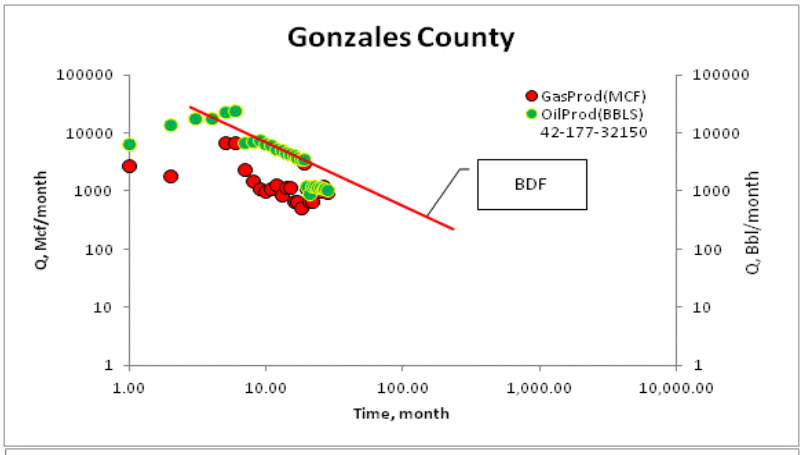

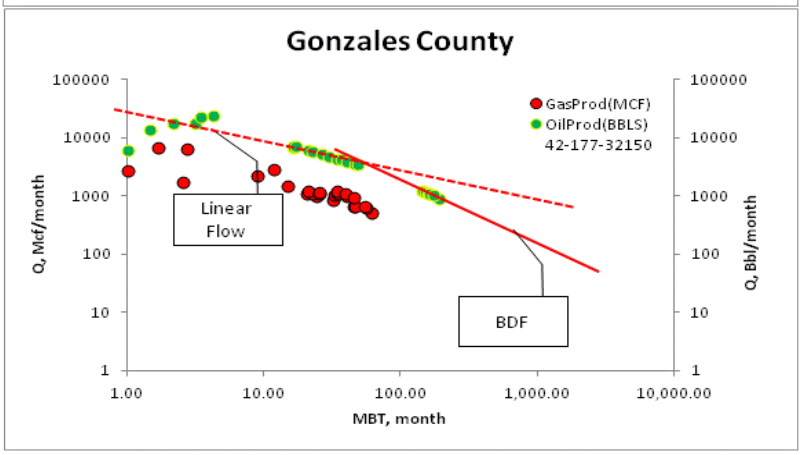

(a)

Fig. 40—(a) MBT vs. rate plot is more reliable to identify linear and BDF; (b) GOR is increasing with time regime for well API# 32150

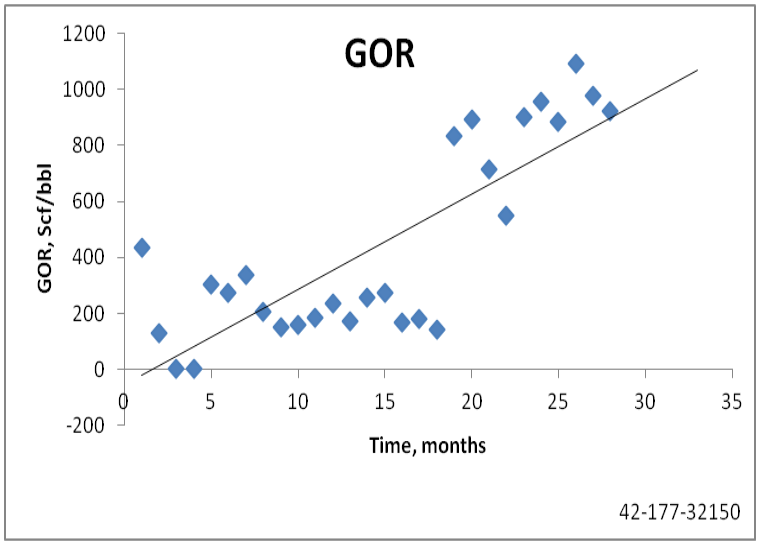

(b)

Fig.40— Continued

4.2.4 Hindcast and 30 Year Forecast

In this example, a drop in production rates is observed after 14 months of production (**Fig. 41**). This change could be caused by variable operating conditions or change in bottom-hole conditions. None of the models seem to predict the production rates accurately. With limited production history of 24 months it is difficult to predict production rates as the bottom-hole pressure may not be stabilized. From hindcasting, it is clearly visible that use of only rate-time data can lead to inaccurate forecasts. In situations like this, it is advisable to use pressure data to correct rates or normalize rates

for changes in bottom-hole pressure (BHP). FRI plots and hindcast for well API# 32167 are attached in Appendix A.

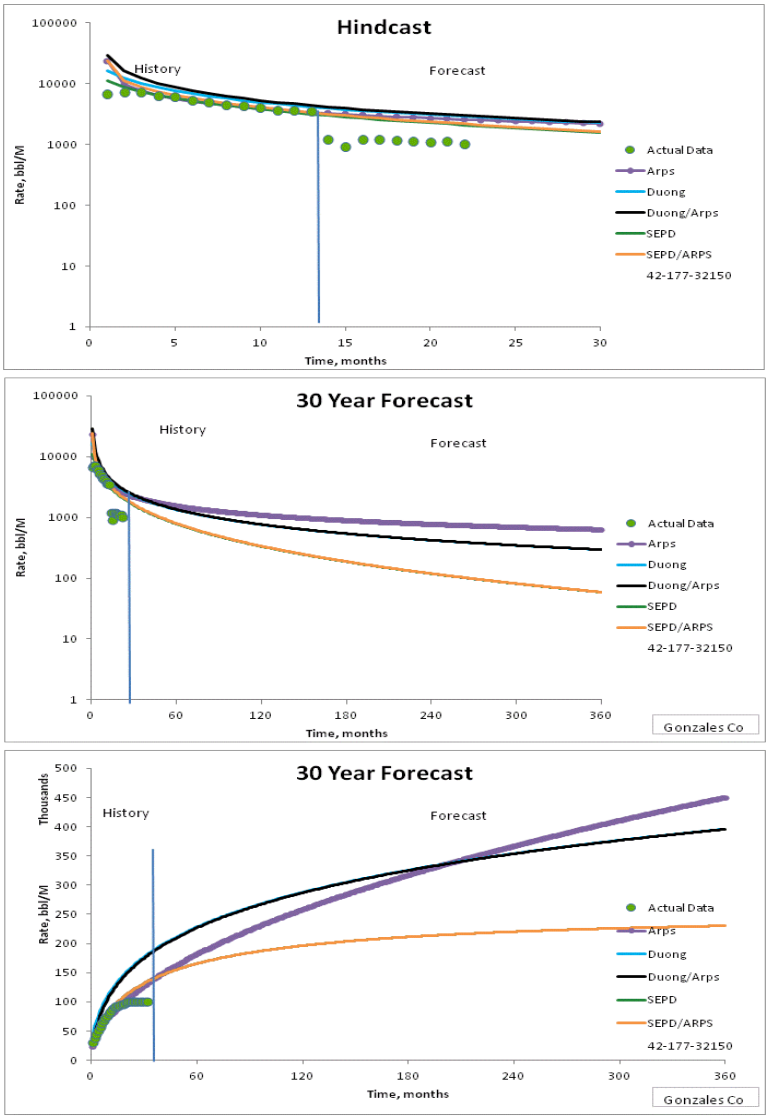

Fig. 41— Hindcast and forecast for oil well API# 32150; drop in production rate leads to inaccurate production forecasts

4.3 Karnes County

Karnes is one of the more productive liquid-rich counties in the Eagle Ford shale. The observed first-month maximum production is more than 5000 bbls (Tian et al. 2013). In this study, I analyzed publically available monthly production data of 833 wells. Wells that have reported zero production for more than three months and inactive wells are excluded from this study. I found 71 wells exhibiting BDF regime. The average time of end of linear flow is 12 months. The location of wells analyzed with yellow dots (**Fig. 42**).

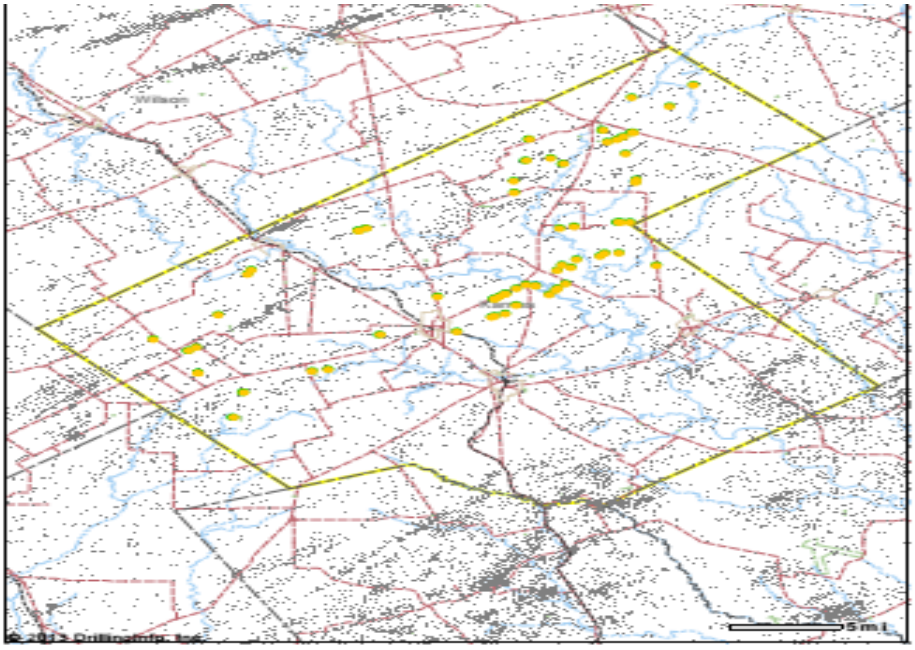

Fig. 42—Location of wells analyzed in Eagle Ford shale, Karnes County, TX

4.3.1 Flow Regime Identification In Karnes County

Fig. 43 is an example of an oil well with peak production rate more than 10,000 bbl/ month and increasing GOR. The end of linear flow at 12 months from diagnostic plots is used to forecast production rates. Unlike the logarithmic rate-time plot, the rate-MBT plot shows a clear transition from linear flow to BDF **(Fig. 43**). **Fig. 44** gives the hindcast and forecast for the same well.

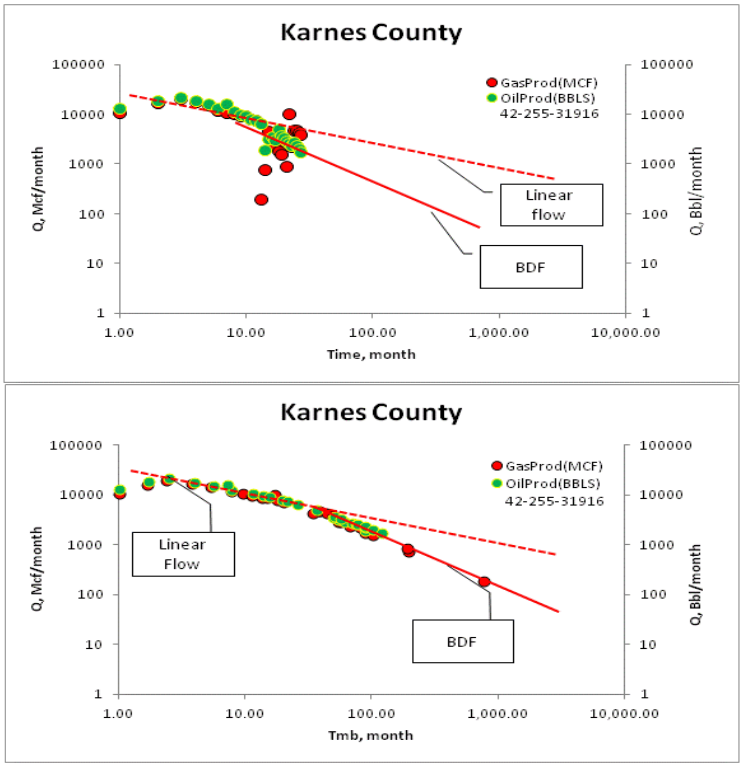

(a)

Fig. 43—(a) Example of an oil well API# 31916 in Karnes County, TX in BDF regime; (b) GOR is increasing

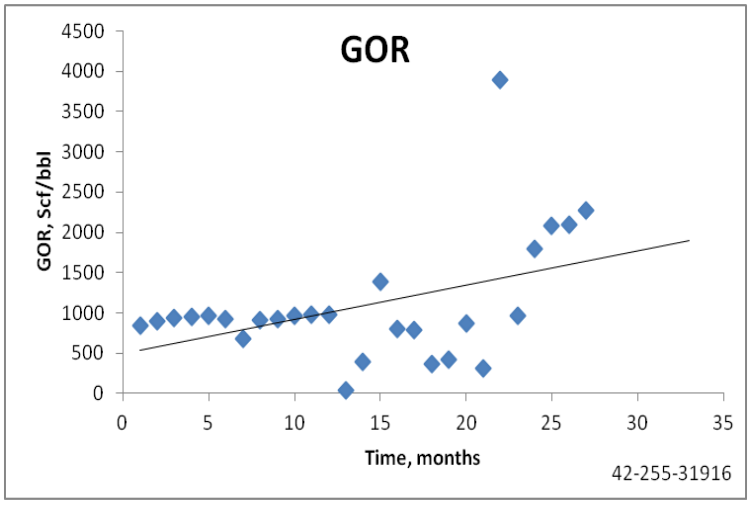

(b)

Fig. 43—Continued

4.3.1 Hindcast and 30 Year Forecast

From **Fig. 44**, after 13 months, well enters into BDF. Hindcast analysis shows that using 13 months of production history, next 13 months of production forecast is obtained using various decline models. All models give close but not exact match to the production data after 13 months.

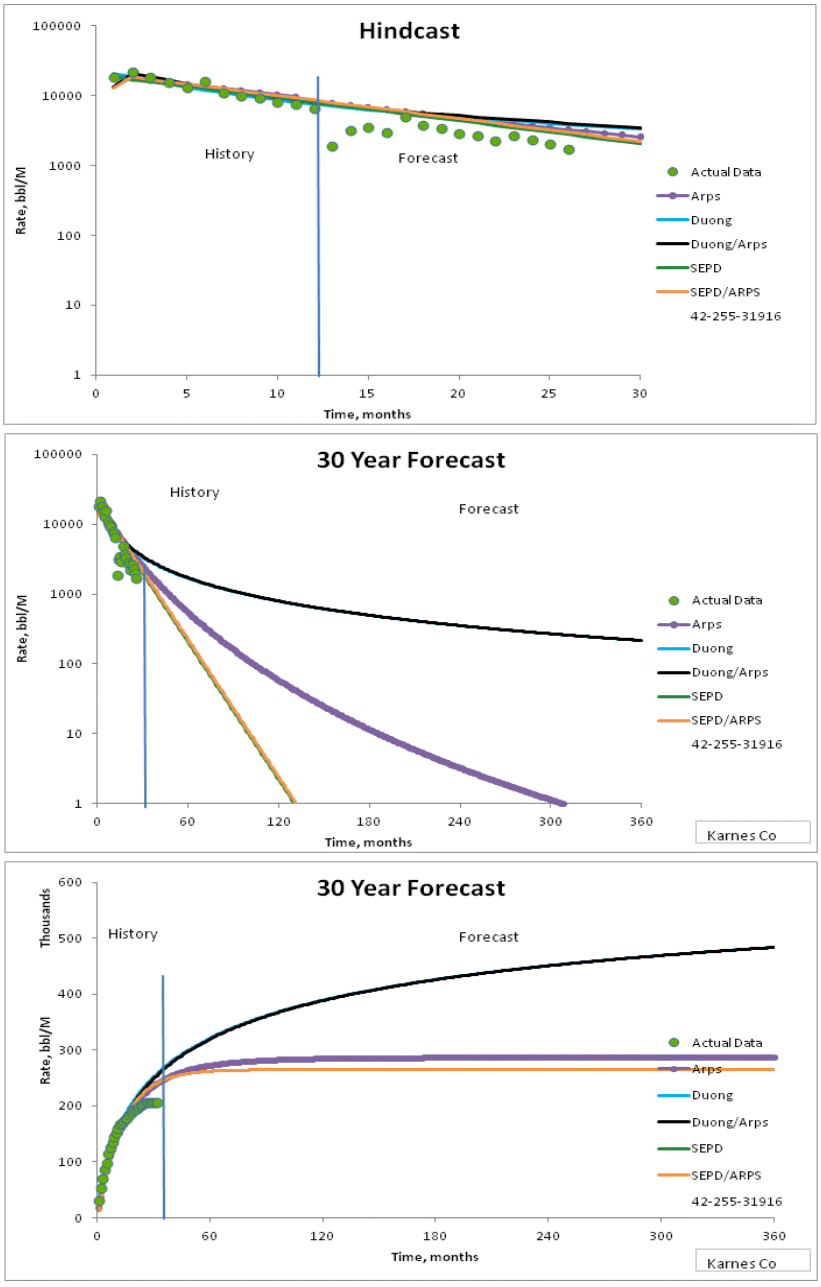

Fig. 44—Hindcast and forecast for oil well API# 31916; Duong and Duong/Arps give an optimistic forecast, while Arps Hyperbolic and SEPD give a conservative fit forecast for 30 year EUR.

4.4 La Salle County

La Salle County is located in the oil window of the Eagle Ford shale. In this study, I analyzed publically available monthly production data of more than 348 wells. Wells that have reported zero production for more than three months and inactive wells are excluded from this study. I found 169 wells exhibiting BDF. **Fig. 45** shows the location of wells analyzed with yellow dots.

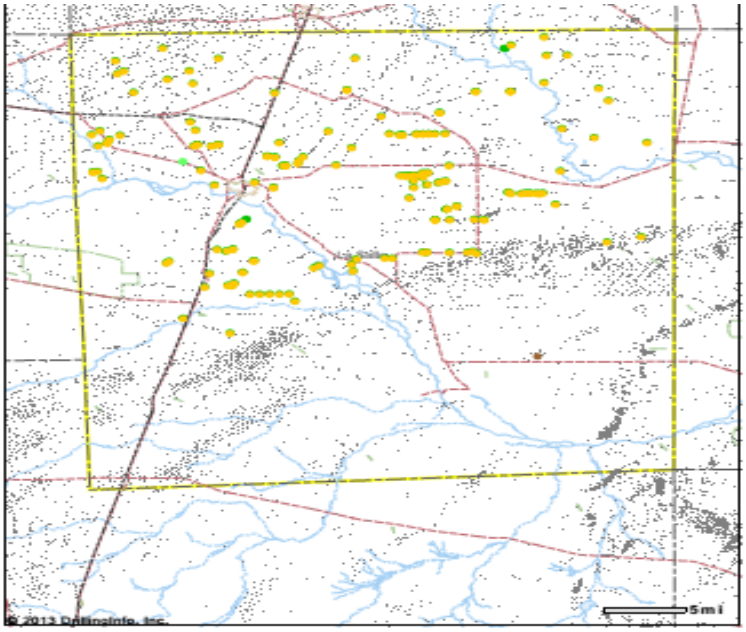

Fig. 45—Yellow dots show location of oil wells analyzed in La Salle County, TX

4.4.1 Flow Regime Identification in La Salle County

Following is an example of double linear flow observed in one of the wells in La Salle County, TX (**Fig. 46**). The first linear may represent flow from the formation to the fractures in a perpendicular direction and each fracture behaves independently. Second linear flow is also known as compound linear flow and it occurs after the drainage area has extended beyond the stimulated region. Flow is parallel in direction to fracture planes and mainly comes from the outer matrix region. Presence of compound linear flow can only be confirmed by analyzing longer production history and including pressure data.

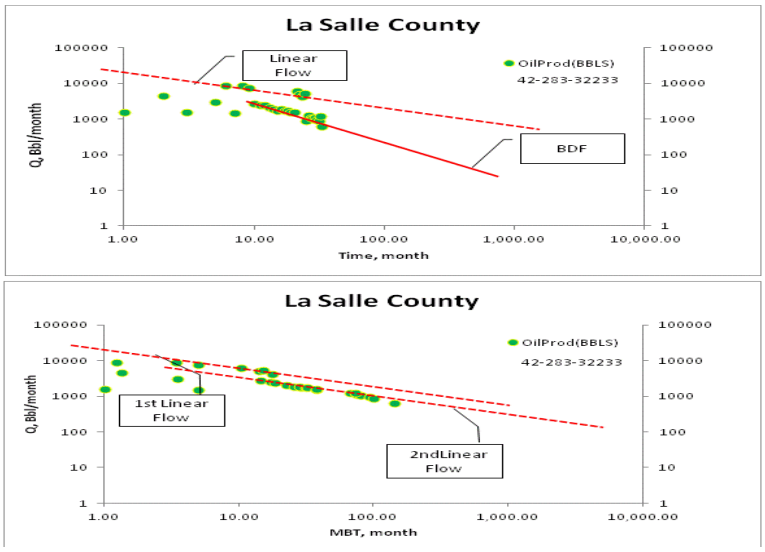

(a)

Fig. 46—(a) Double linear flow observed in well API# 32233; (b) Gas oil ratio is increasing as expected for well API# 32233 in La Salle County, TX

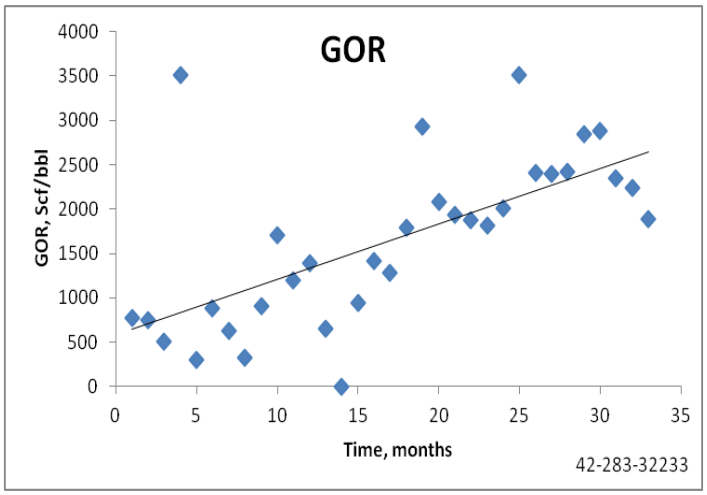

(b)

Fig. 46— Continued

4.4.2 Hindcasting

Rate-time plots below (**Fig. 47**) show data is scattered and only the Duong model gives a close approximation to actual data with a short production history. It is interesting to see the forecasts from different models based on analysis of a short production history of 10 months in transient flow regime. It is difficult to say which decline models works best here. Including pressure data with more production history would help in producing more reliable forecasts.

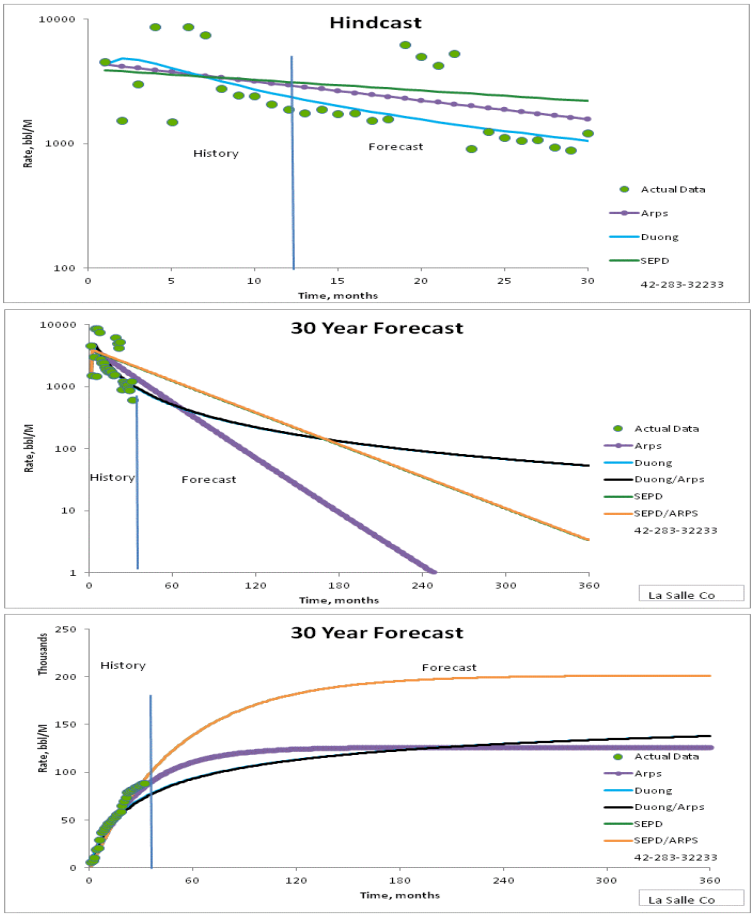

Fig. 47—Unstable flow rates give ambiguous hindcast and forecast results for well API# 3223

4.5 McMullen County

McMullen County is located in the oil window of the Eagle Ford shale. In this study, I analyzed publically available monthly production data of 225 wells. Wells that have reported zero production for more than three months and inactive wells are

excluded from this study. I found 53 wells exhibiting BDF regime. **Fig. 48** shows the location of wells analyzed with yellow dots.

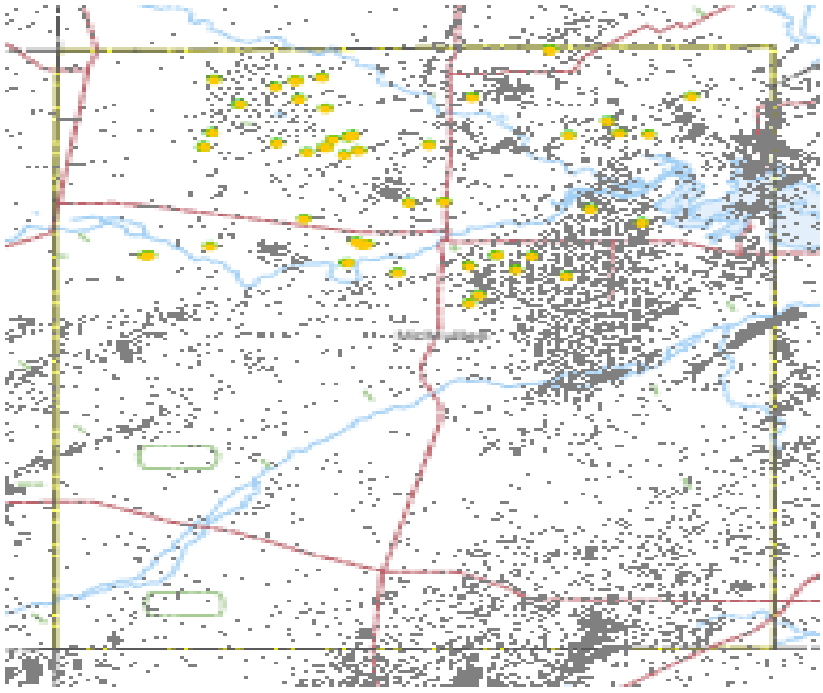

Fig. 48—Location of wells analyzed in Eagle Ford shale, McMullen County, TX are shown with yellow dots

An example of an oil well API# 34541 in McMullen County, TX is found to be linear flow regime (**Fig. 49** and **Fig. 50**). The 12 months of production history is too short to perform hindcast and forecast analysis with confidence. Examples from Dimmit county oil wells have similar production profile and are attached in Appendix A.

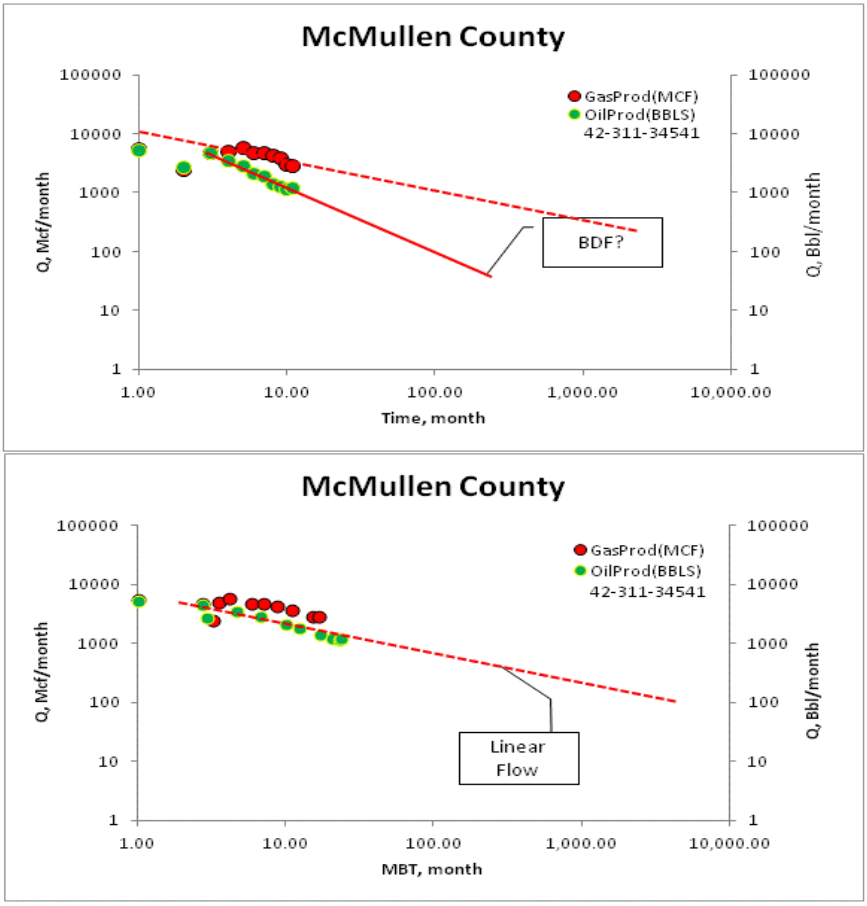

Fig. 49—Linear flow is identified as dominant flow regime in well API# 34541 in Eagle Ford shale, McMullen County, TX

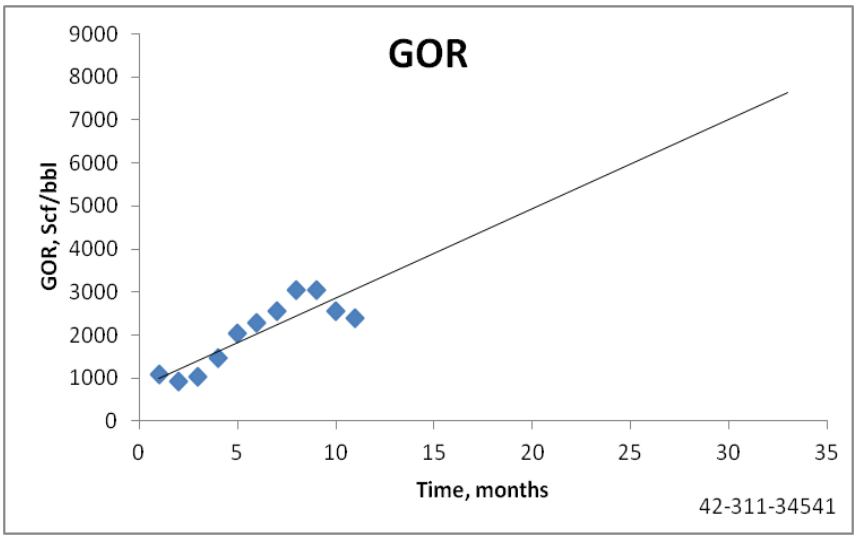

Fig. 50—GOR is increasing with time for API# 34541 in Eagle Ford shale, McMullen County, TX

5. SUMMARY OF HINDCAST RESULTS

Results from analysis of all the examples of hindcasting presented in the previous sections for Eagle Ford and northern Barnett are summarized below. It is interesting to see that, for most cases, the Arps hyperbolic model had the least error in the production at the end of known history (highlighted in yellow color). Due to the short production history varying between 12 to 36 months, not much difference is observed between Duong and Duong/Arps and SEPD and SEPD/ Arps; the error is same up to 2 decimal places.

Table 6—Hindcast Summary: percentage error in the EUR at the end of production for representative oil wells in Eagle Ford and Barnett shale

County	Well API#	Dominant Flow regime	Arps Hyp	Duong	Duong/ Arps	SEPD	SEPD/ ARPS
Gonzales	32128	BDF	1.38%	-35.35%	-35.35%	5.17%	5.17%
Gonzales	32150	BDF	-9.34%	-54.81%	-54.81%	-17.40%	-17.40%
Gonzales	32167	BDF	-2.72%	-3.93%	-3.93%	-8.77%	-8.77%
Karnes	31916	BDF	-9.56%	-14.21%	-14.21%	-10.60%	-10.60%
La Salle	32233	BDF	4.04%	17.02%	17.02%	4.97%	4.97%
Atascosa	34322	LF	1.53%	9.96%	9.96%	0.68%	0.68%
Montague	33065	LF	12.00%	2.56%	2.56%	4.72%	4.72%
Cooke	34160	BDF	-22.17%	-20.58%	-20.58%	-35.08%	-35.08%

For the Eagle Ford shale, following histograms (**Fig. 51**) summarize the Arps parameters observed at the end of linear flow. In general, the Eagle Ford shale experiences end of linear flow after 12 months of production and average b of 0.36 at the end of linear flow.

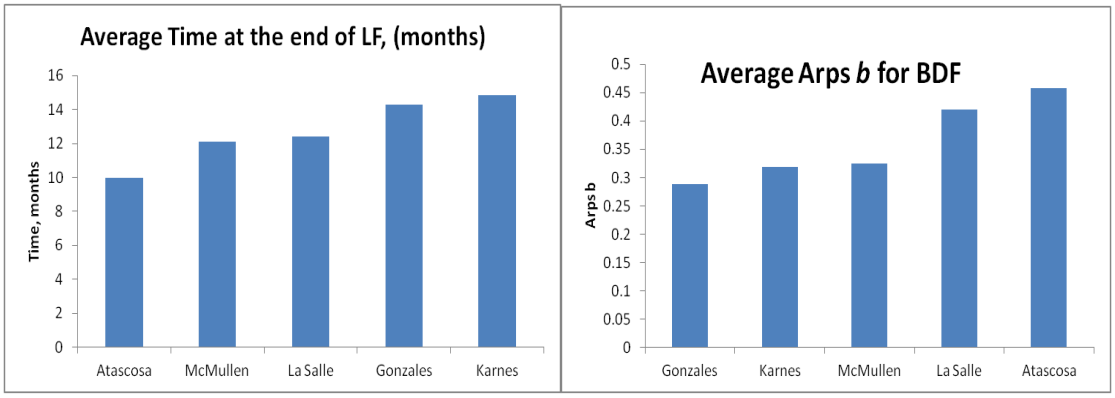

Fig. 51—Average parameters at the end of linear flow for Eagle Ford shale liquid-rich counties

6. LRS WITH PRESSURE DATA: EAGLE FORD FIELD CASES

6.1 Flow Regime Identification for Eagle Ford Wells with Pressure Data

Below is an example of an oil well (EF-8) with pressure data. The reservoir pressure is 10,000 psi and **Fig. 52** shows the variation of rate with tubing-head pressure (THP). The bottom-hole pressure was calcluated from THP using Fekete software.

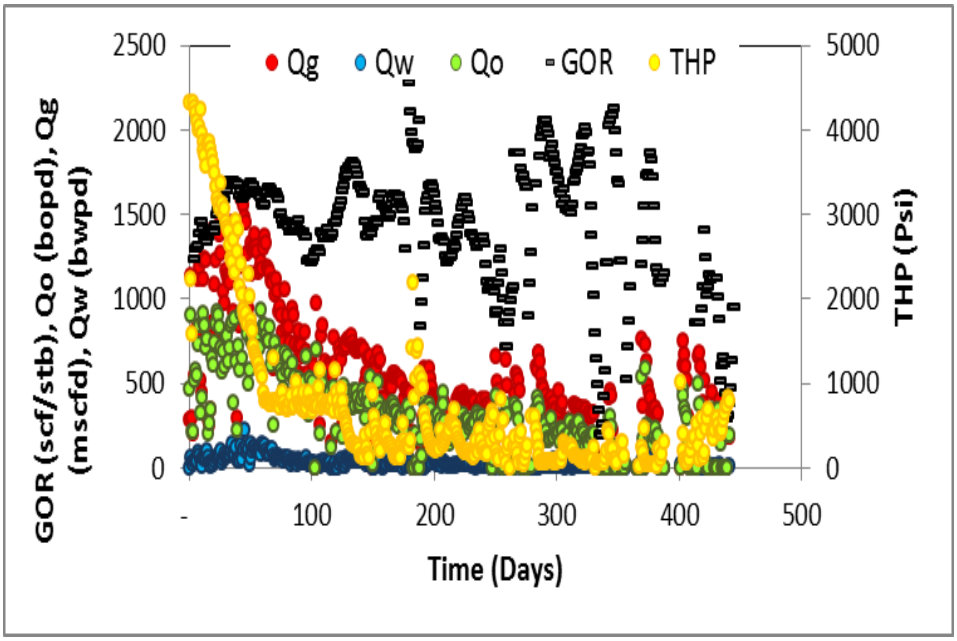

Fig. 52–Production data of an oil well in the Eagle Ford shale with pressure (EF-8)

Due to unstable operating conditions, the well did not have a smooth decline profile. It was necessary to remove outliers that are one standard deviation away from a smooth decline trend. Pressure corrections were made to account for unstable flowing conditions. The well exhibits linear flow followed by BDF (**Fig. 53**).

Use of Fetkovich plots helps in improving confidence in flow regime identification and b=0.4 is a good to match the data (**Fig. 54**).

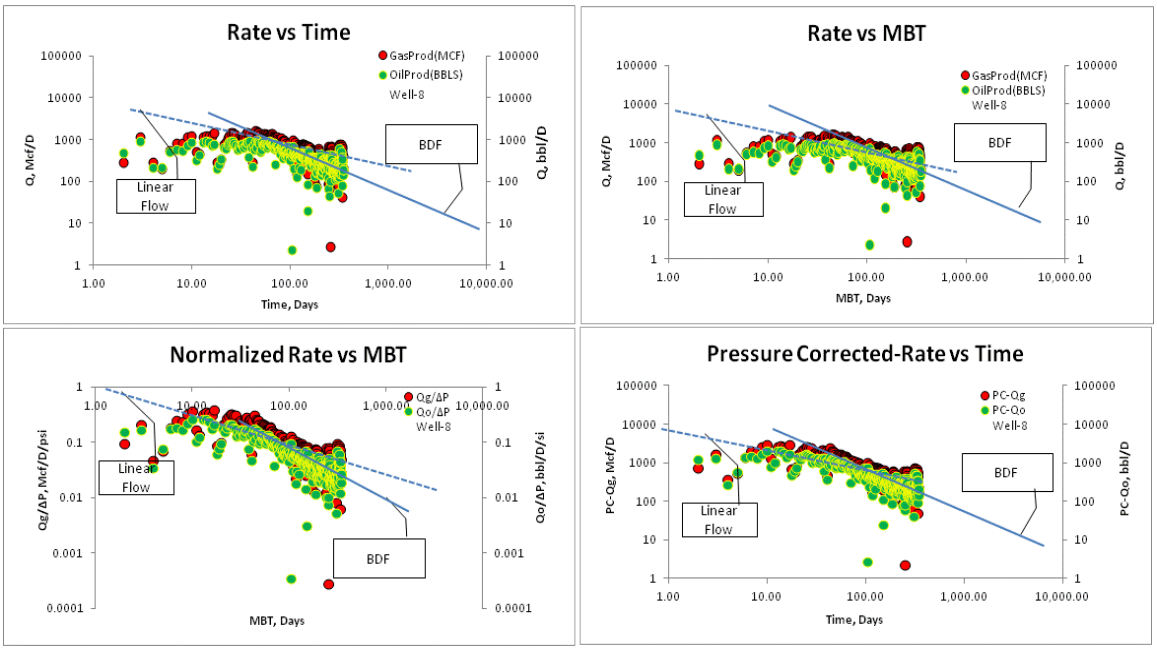

Fig. 53 —Flow regime identification of an oil well in Eagle Ford; corrections for unstable flowing conditions were made by normalizing and using Duong's PC factor (Duong 2010).

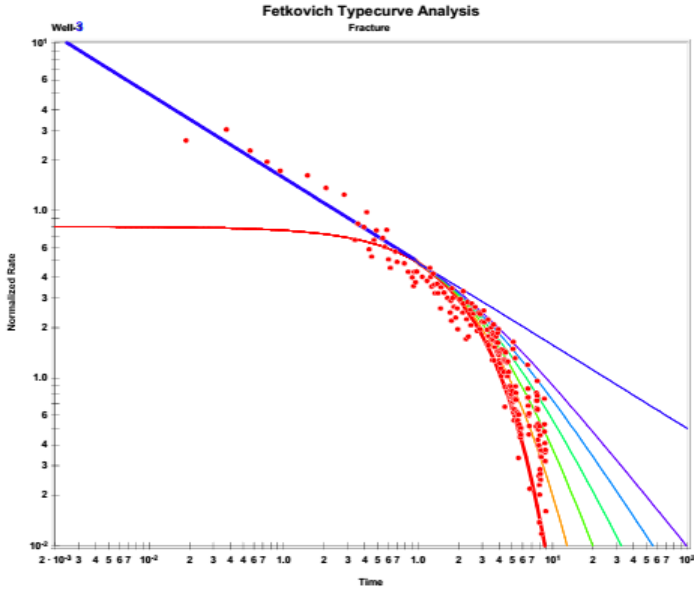

Fig. 54—Fetkovich type curve for EF-8; b=0 gives a good fit to the data (EF-8)

6.2 YM-SEPD Model Analysis

Yu and Miocevic (2013) suggested removing the first year of production history before estimating the SEPD parameters *n* and τ . The two analyses were obtained by including initial data and then excluding initial data (**Fig. 55**). We did not use any data point more than one deviation off a clear trend line. Excluding initial production history improved the correlation coefficient.

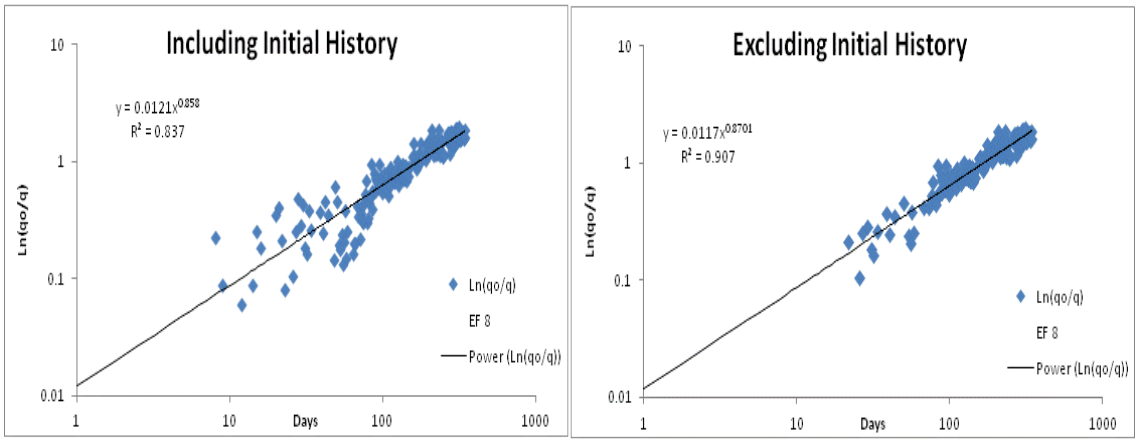

Fig. 55—Specialized plot for EF-8 to estimate the SEPD parameters n and τ

The *n* and τ obtained from the above two plots were used to forecast production rates using the SEPD model equations. The 30 year forecast from two cases was obtained. There is little difference in the two forecasts. Including initial data led to higher forecasted rates than when initial data was excluded, but the EUR is almost the same at the end of 30 years (**Fig. 56**).

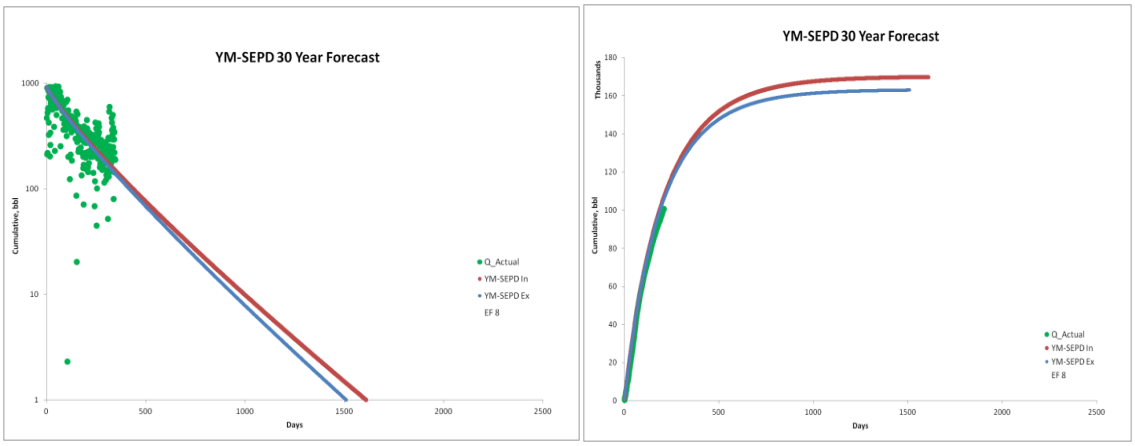

Fig. 56—30 year EUR from YM-SEPD model: initial data is included (red curve) and initial data is excluded (blue curve) (EF-8)

6.3 YM-SEPD Model Forecast Comparison with Other Models for Well EF-8

The forecasts obtained from various decline models (**Fig. 57**) shows that YM-SEPD (red curve) and original SEPD model (green curve) give very different forecasts. YM-SEPD and Duong/Arps model (black curve) give a similar and most conservative forecast, while Duong (blue curve) and SEPD give an optimistic forecast.

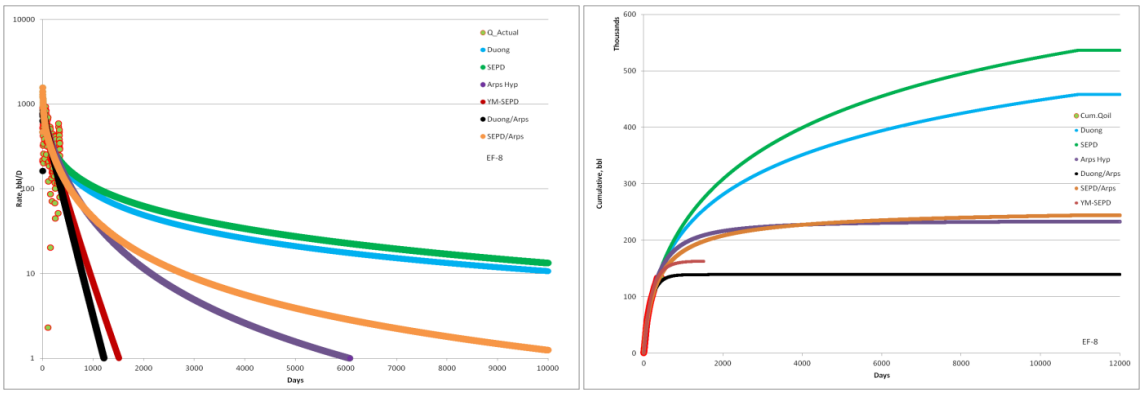

Fig. 57—Comparison various decline models with YM-SEPD; Duong/Arps and YM-SEPD give a similar forecast (EF-8)

Another example of an oil well from the Eagle Ford shale is presented below with daily rates and pressure data (**Fig. 58** and **Fig. 59**).

As described previously, FRI is performed and end of linear flow is estimated.

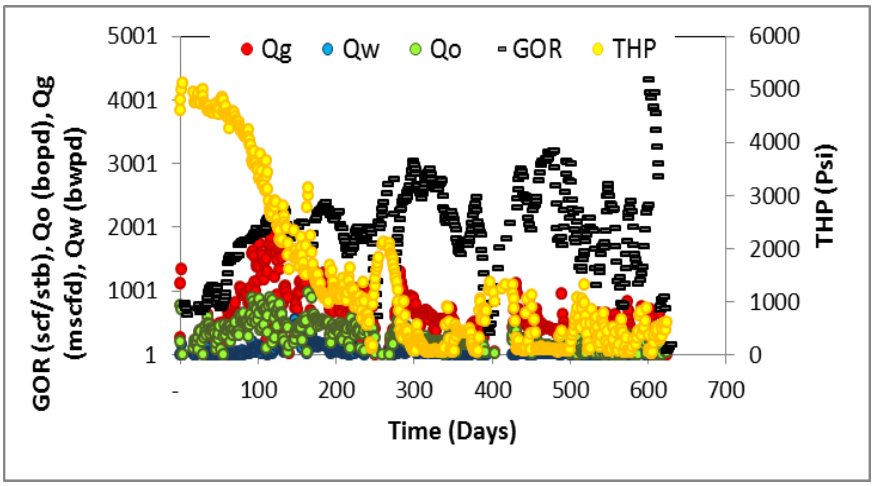

Fig. 58– Production data from Eagle Ford shale with pressure (EF-6)

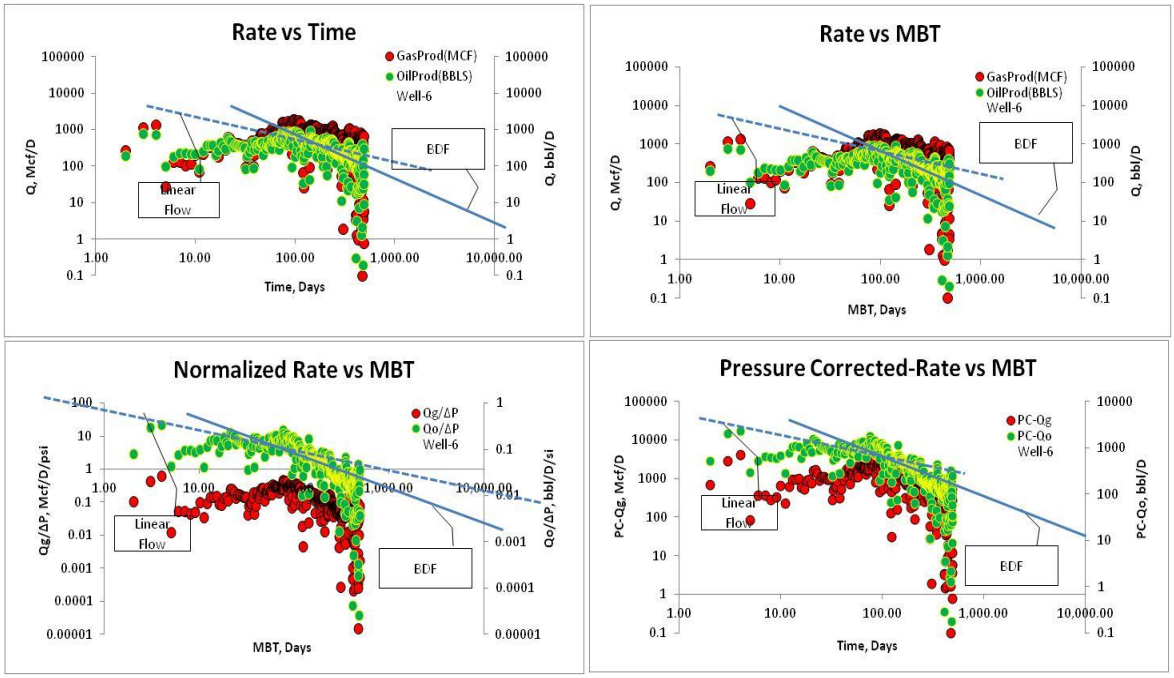

Fig. 59— Flow regime identification for oil well (EF-6) in Eagle Ford; corrections for unstable flowing conditions were made by normalizing and using Duong's PC factor (Duong 2010)

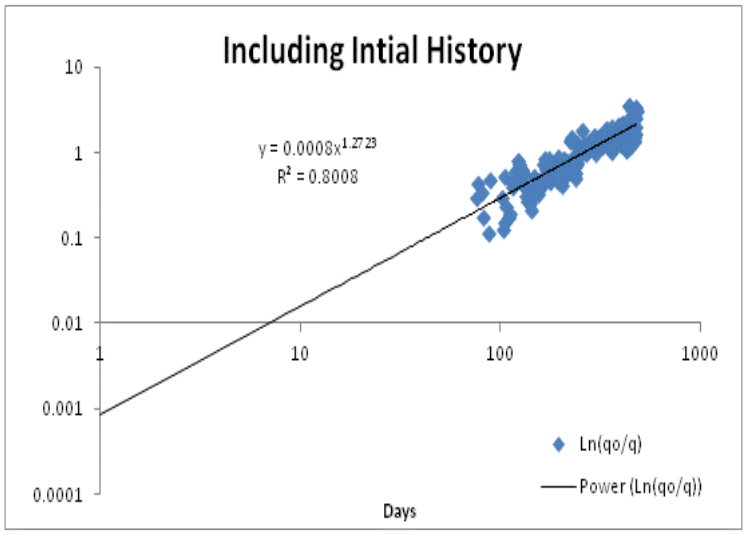

Fig. 60— YM-SEPD Specialized plot for well EF-6 to estimate the SEPD parameters n and τ

To check the applicability of the YM-SEPD model, we prepared the YM-SEPD specialized plot (**Fig. 60**) to calculate *n* and τ as described in previous sections. As less than one year of production history was available for well EF-6, early production data was removed to improve the accuracy of the analysis.

The 30-year forecast with the YM-SEPD model fit the production data well. The YM-SEPD forecast was conservative as the well reached its economic limit of 1 bbl/day in about 1,300 days of production (**Fig. 61**).

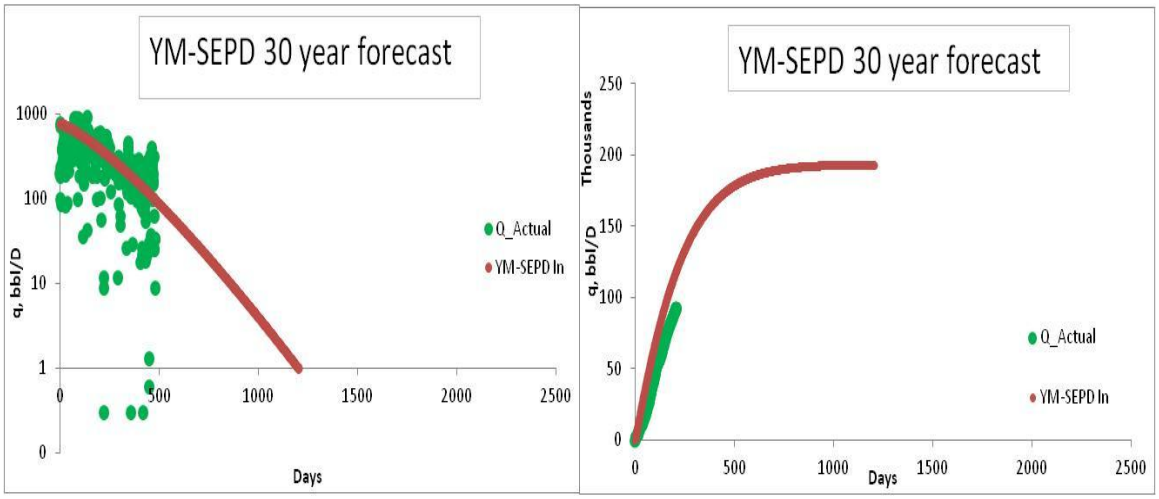

Fig. 61—30-year EUR from YM-SEPD model: initial data included (red curve) for well EF-6

6.4 YM-SEPD Model Forecast Comparison with Other Models for Well EF-6

Similar to the well EF-8 forecast, Duong/Arps (black curve) and YM-SEPD (red with blue ring curve) gave similar but conservative EUR's, while Duong (blue curve) and SEPD (green curve) gave optimistic EUR's (**Fig. 62**).

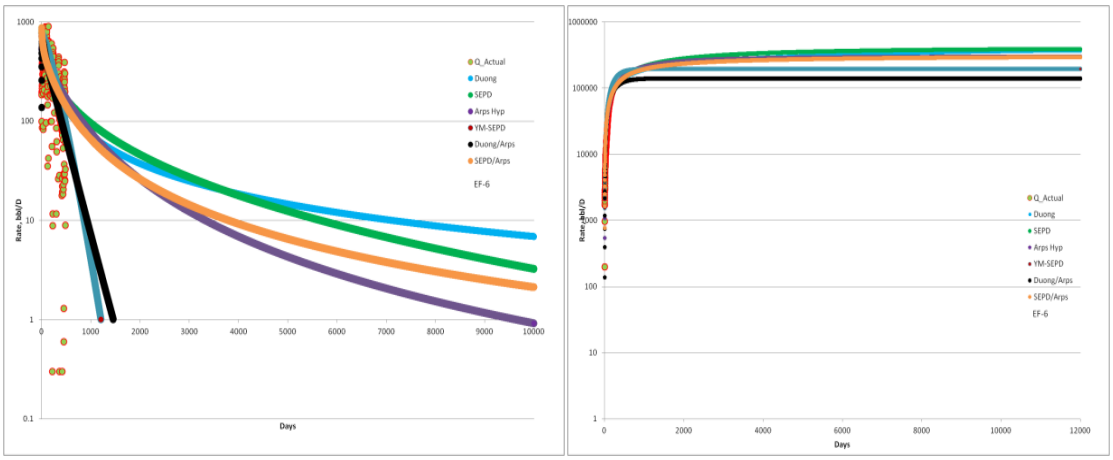

Fig. 62— Comparison of 30 year EUR from YM-SEPD model with other decline models（EF-6)

7. ANALYSIS OF LINEAR FLOW USING YM-SEPD MODEL FOR FIELD EXAMPLES FROM MONTAGUE COUNTY

Yu and Miocevic (2013) stated that the YM-SEPD method is independent of flow regimes exhibited by the well. In this section, an oil well from Montague County was analyzed to check the applicability of the YM-SEPD model for oil wells in transient linear flow for 8.5 years (**Fig. 63**).

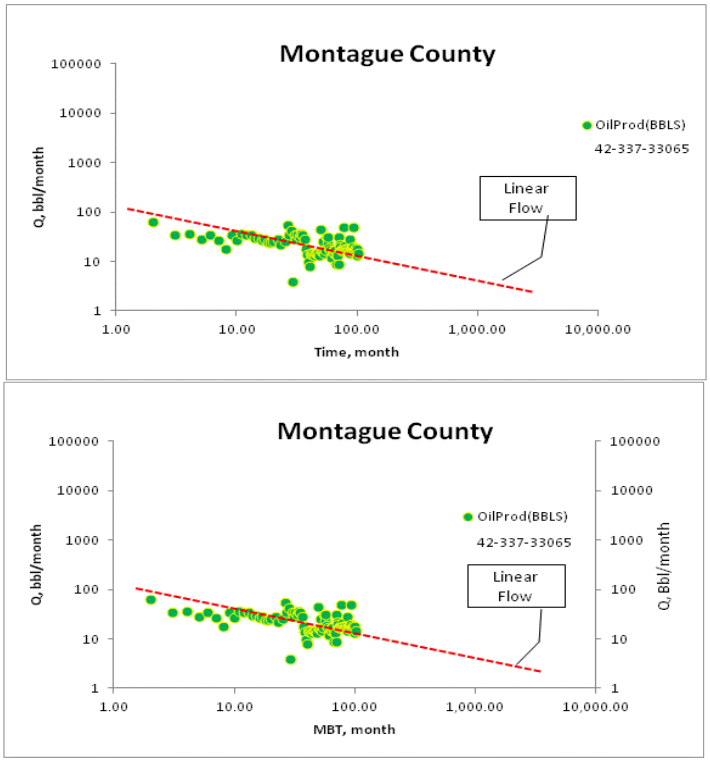

Fig. 63— Linear flow is the dominant regime for oil well API #33065 in Montague County, TX

7.1 Comparison of YM-SEPD Model is Performed for Cases When Initial Data is Included and When Initial Data is Excluded to Increase Accuracy in the Analysis

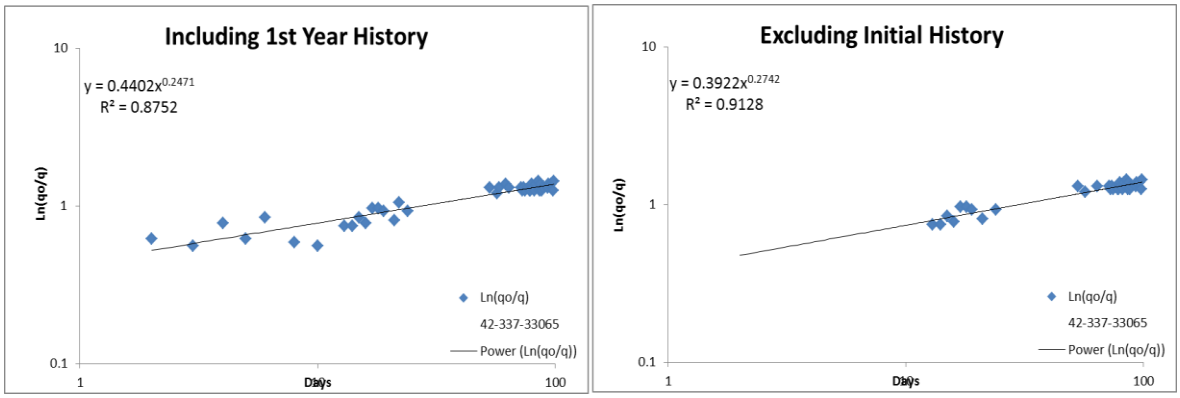

Fig. 64— Specialized plots for well API# 33065 to estimate the SEPD parameters n and τ

Table 7 summarizes the YM-SEPD model parameters obtained from specialized plot for the two cases (**Fig. 64**). The percentage error in EUR at the end of the known production history was lower when the initial production history was excluded from the specialized plot and only those data points that lie on the straight line were used.

Table 7—YM-SEPD model parameters well API #33065 from specialized plots (Fig. 65) and % error in the EUR at the end of production

Well API#	YM-SEPD	*n*	int	τ, days	q_o, Bbl/day	% Error in EUR at the end of production history
33065	Excluding initial production	0.274	0.39	30.371	63	2.99
	Including initial production	0.247	0.44	27.677	63	4.80

Fig. 65 shows the fit and forecast using the YM-SEPD model. No difference is observed visually in the curve fits to the actual production data.

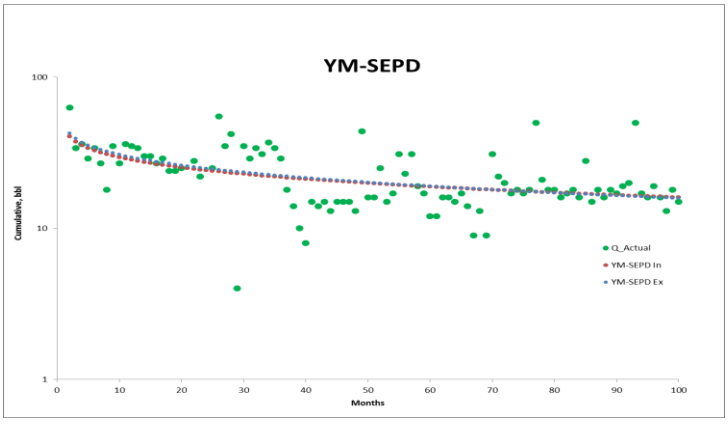

Fig. 65— YM-SEPD model gives a good fit the to the actual production data for well API #33065

The 30 year forecast of YM-SEPD model (**Fig. 66)** shows no difference was observed visually in the two curve fits. Difference in the actual production data and the model forecasts is more prominent in the cumulative production plot.

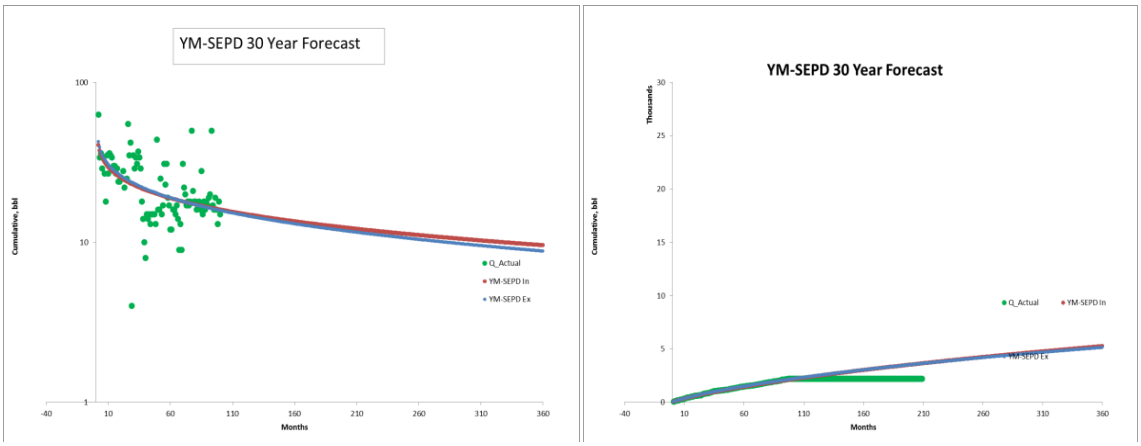

Fig. 66— 30 year EUR from YM-SEPD model: initial data included (red curve), initial data excluded (blue curve) for well API# 33065

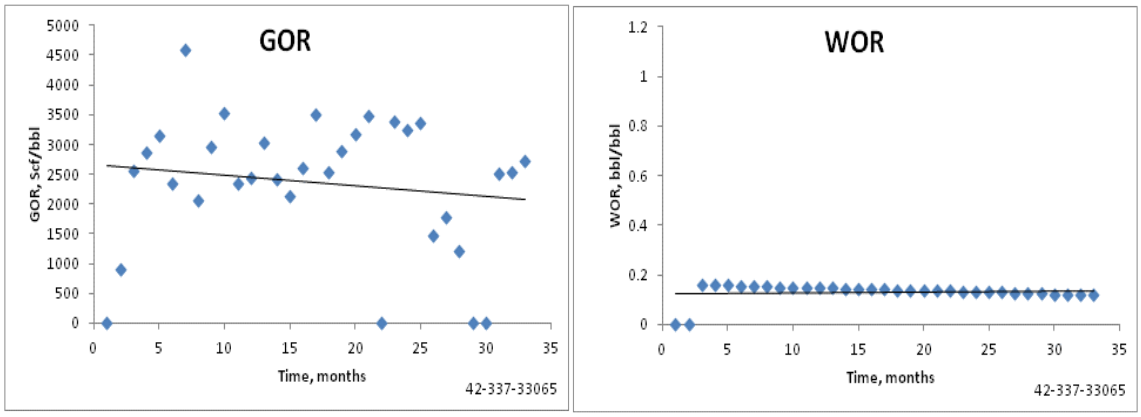

Fig. 67— GOR and WOR remain constant for oil well API# 33065 in Barnett shale, Montague County, TX

The GOR and WOR were relatively constant throughout the production history (**Fig. 67**). **Fig. 68** shows the hindcast for the well API# 33065. For the hindcast, as the well is still in linear at 8.5 years, only original Duong and SEPD and Arps/ Hyperbolic without a D_{switch} were used to compare models. SEPD was fairly conservative, while Arps was optimistic and Duong fell in between. Similar results were obtained for the 30-year production forecast.

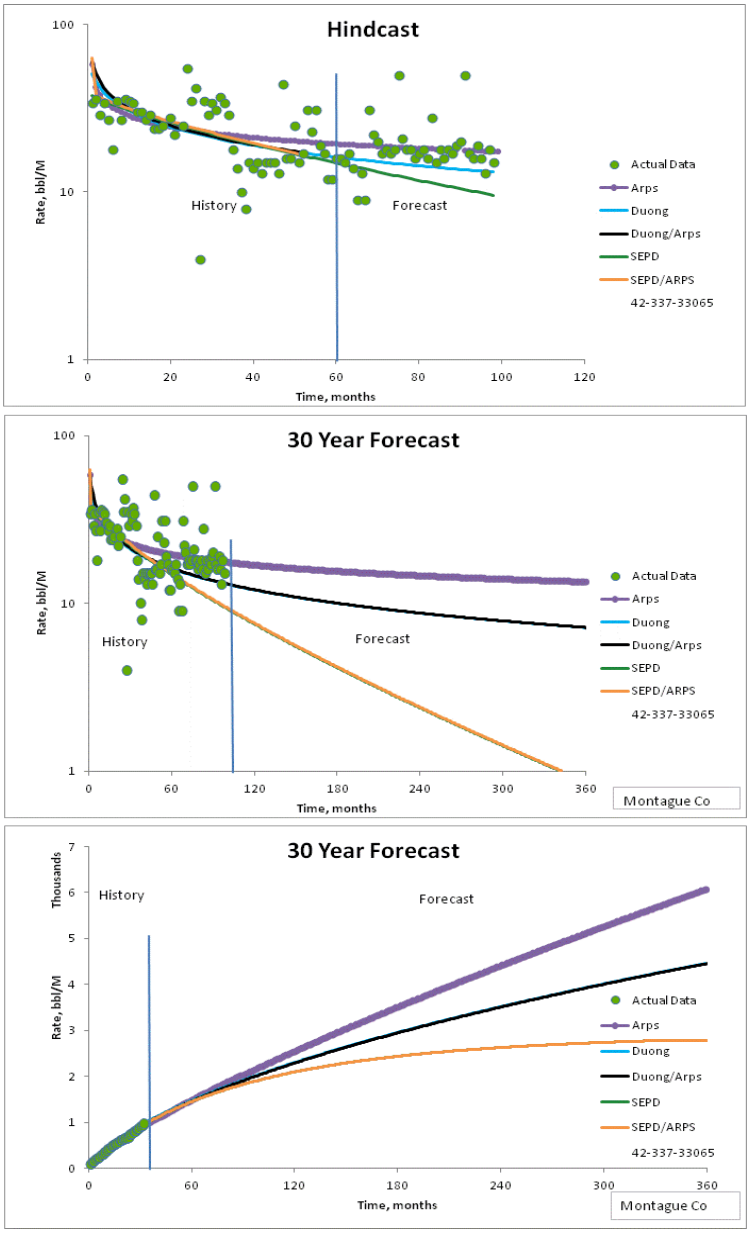

Fig. 68—Comparison of 30-year EUR from YM-SEPD model with other rate decline models

8. COMPARISON OF DECLINE TRENDS IN THE EAGLE FORD AND NORTHERN BARNETT SHALE

8.1 Study of Boundary-Dominated Flow Onset in LRS

As northern Barnett shale has oil wells with longer production history than EFS, we found 45% of the total wells studied to be in BDF while in the Eagle Ford shale only 17% of total wells studied were found to be in BDF. It can be inferred from the decline trends of northern Barnett shale that eventually more number of oil wells in EFS that are currently in LF will enter into BDF. The average expected time of end of LF in northern Barnett is 14 months, while in EFS it varies between 12 to 14 months.

A summary of number of wells and dominant flow regimes observed is given in Table 8**. Fig. 69** through **Fig. 75** gives the distribution of Di at the end of linear flow and Arps b values for various wells in LRS in BDF. Both the shale plays show variable decline parameters in each county. Thus, it was difficult to pin-point a reasonable Arps b value and decline rate at the end of linear flow for the entire play.

Table 8—Summary by county of Eagle Ford shale and northern Barnett shale analysis results

County	No. of wells	Dominant Fluid Type	Dominant Flow Regime	b
Dimmit	7	oil	3 wells in LF 4 in BDF	0.3
La Salle	348	oil	169 wells in BDF 179 in LF	0.41
McMullen	225	oil	53 wells in BDF 172 in LF	0.32
Atascosa	180	oil	7 wells in BDF 173 in LF	0.45
Karnes	833	oil	71 wells in BDF 762 in LF	0.32
Gonzales	450	oil	44 wells in BDF 406 in LF	0.29
Montague	295	oil	213 wells in BDF	0.5
Wise	20	oil	16 wells in BDF	0.4
Cooke	207	oil	131wells in BDF	0.2
Total wells analyzed	2,565			

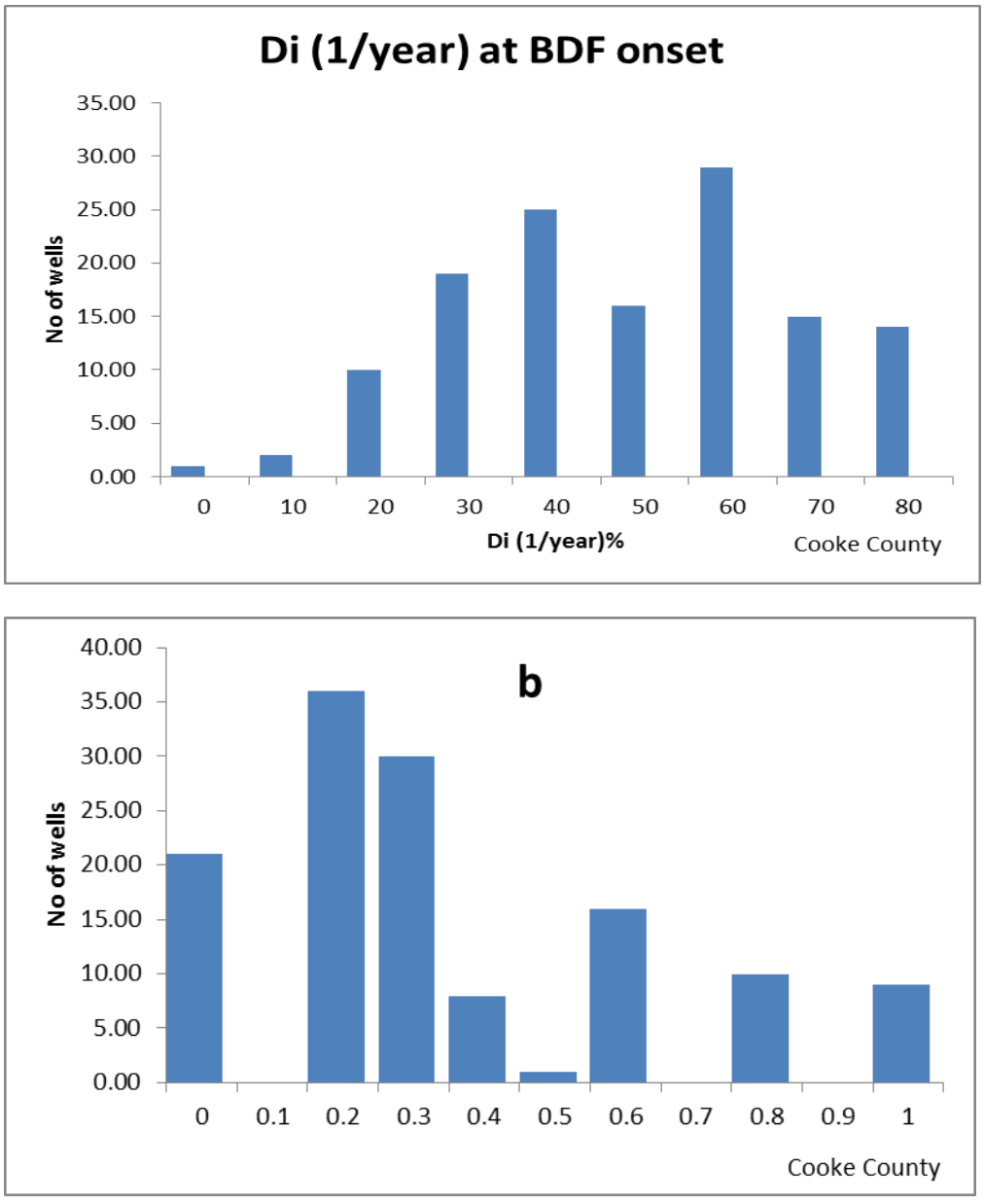

Fig. 69— Arps parameters, decline rate at the end of linear flow and Arps exponent, b, for oil wells in Barnett shale, Cooke County, TX

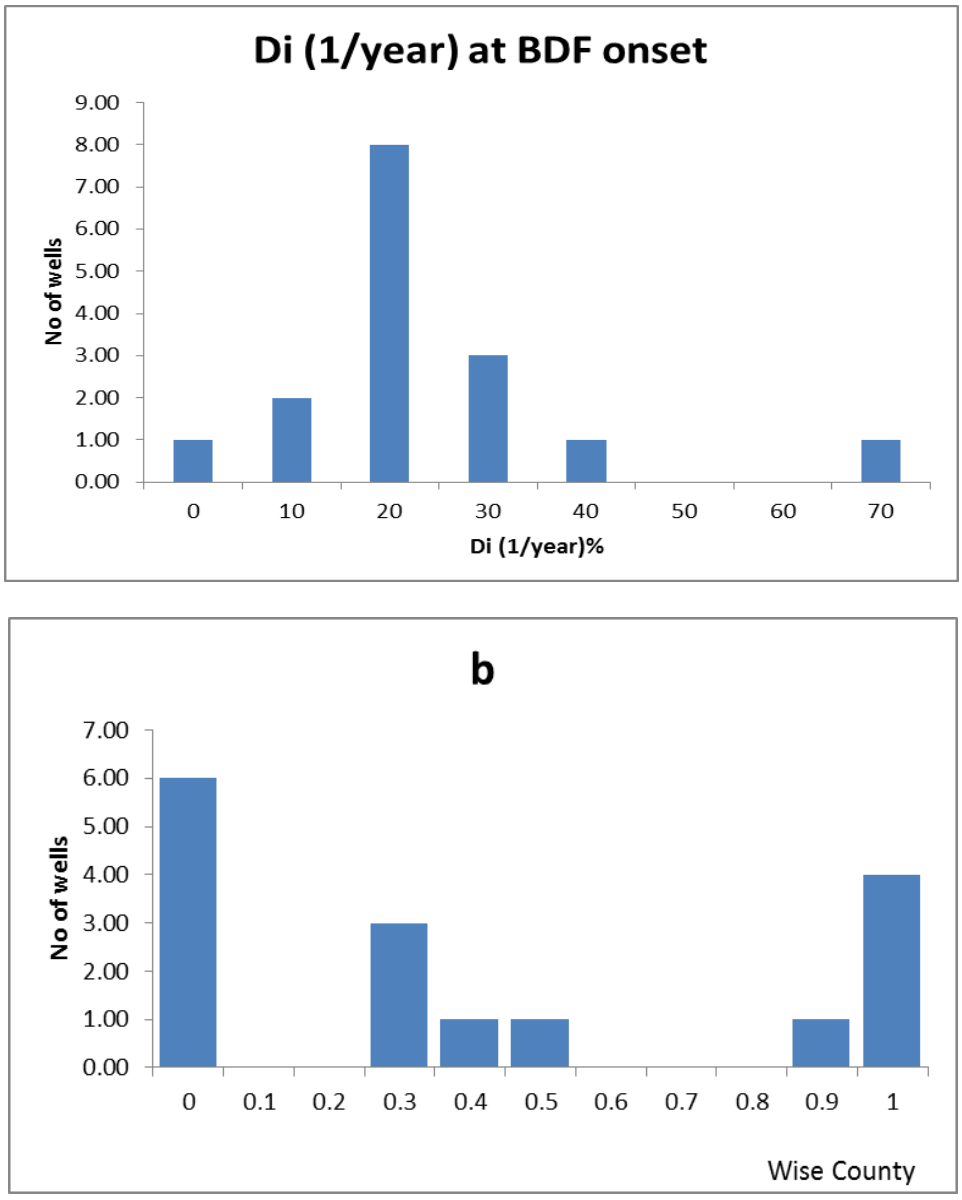

Fig. 70— Arps parameters, decline rate at the end of linear flow and Arps exponent, b, for oil wells in Barnett shale, Wise County, TX

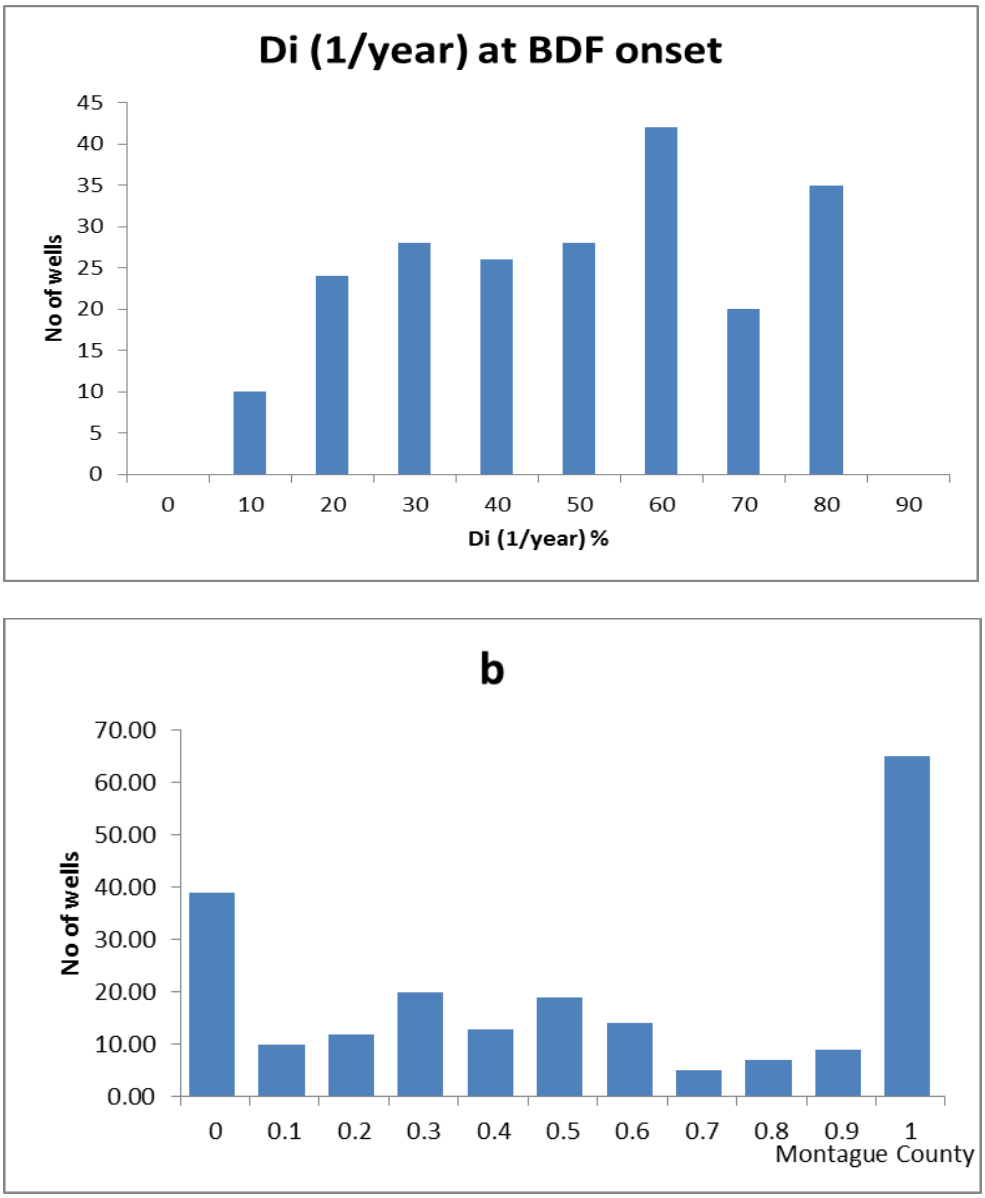

Fig. 71— Arps parameters, decline rate at the end of linear flow and Arps exponent, b, for oil wells in Barnett shale, Montague County, TX

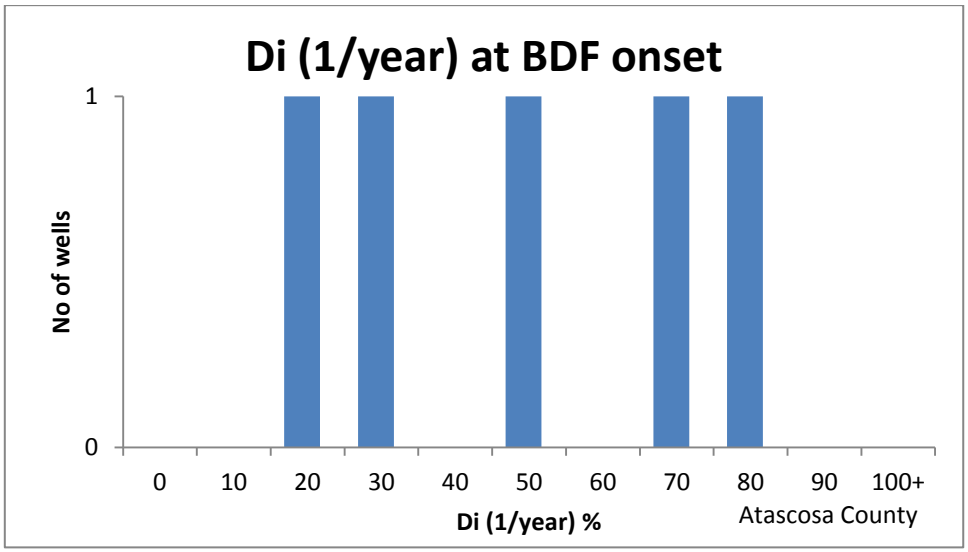

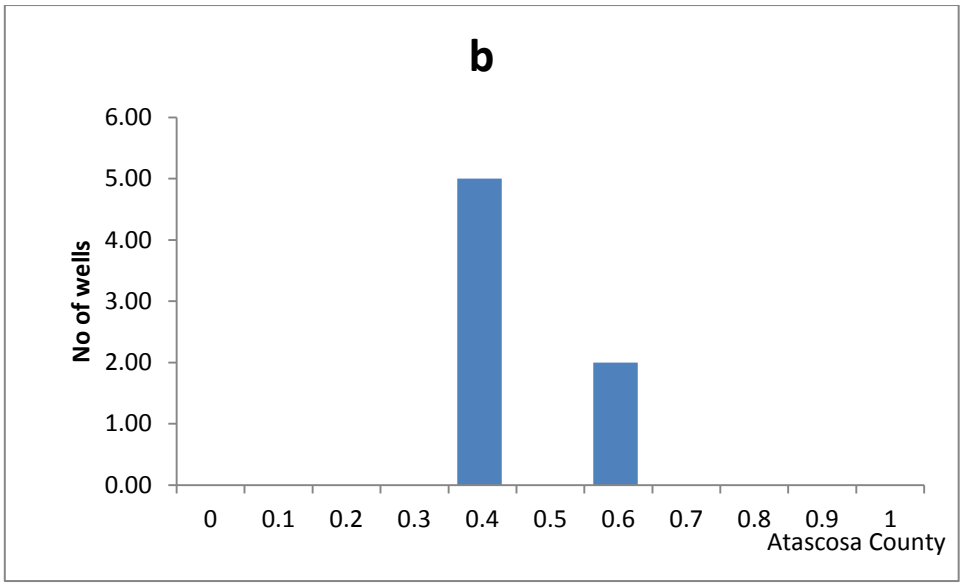

Fig. 72— Arps parameters, decline rate at the end of linear flow and Arps exponent, b, for oil wells in Eagle Ford shale, Atascosa County, TX

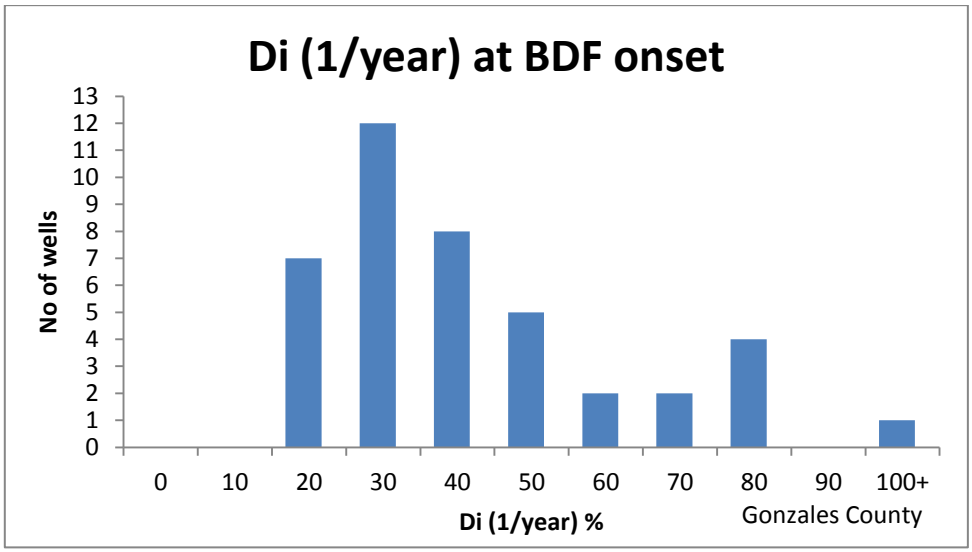

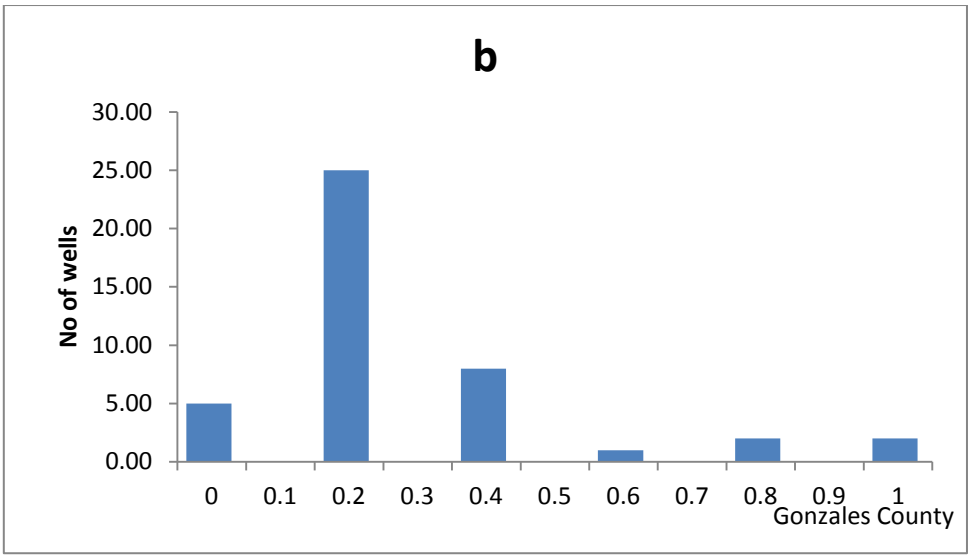

Fig. 73— Arps parameters, decline rate at the end of linear flow and Arps exponent, b, for oil wells in Eagle Ford shale, Gonzales County, TX

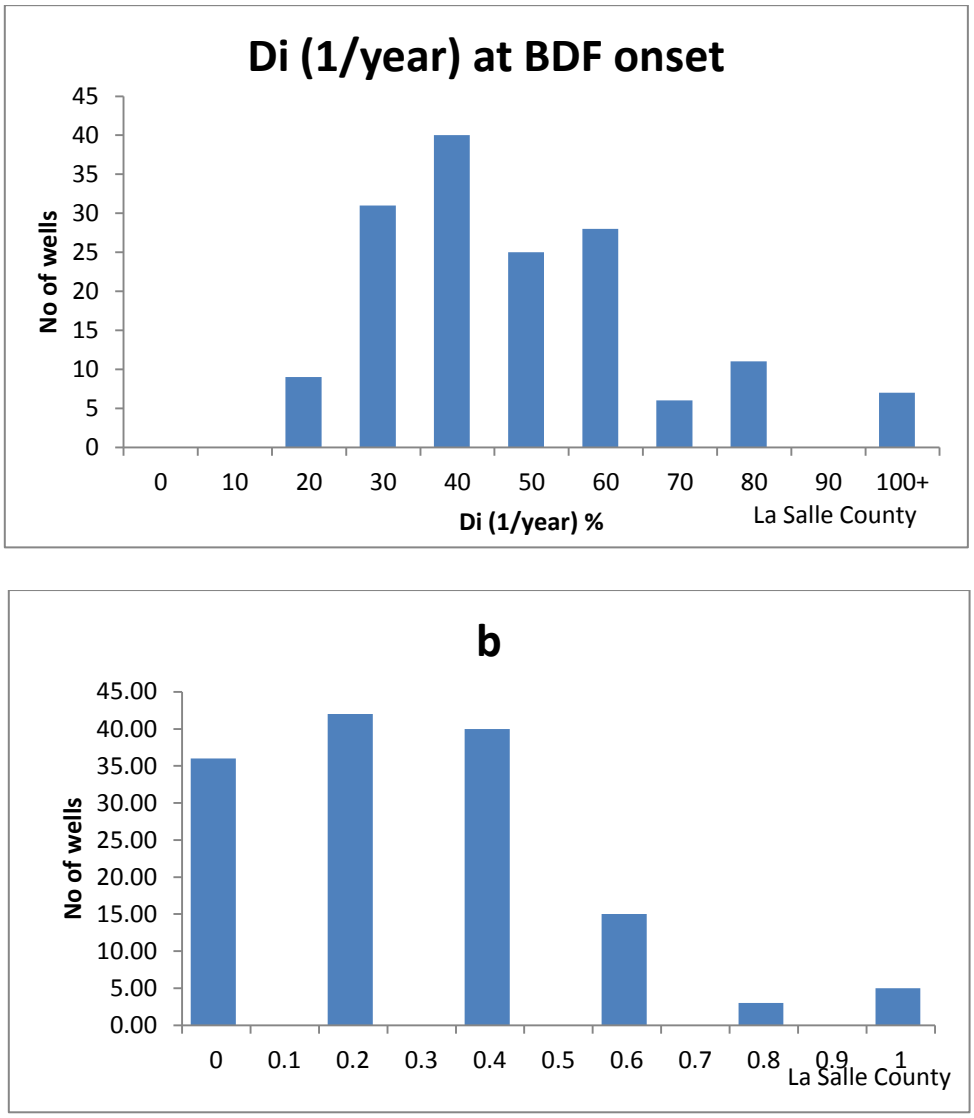

Fig. 74— Arps parameters, decline rate at the end of linear flow and Arps exponent, b, for oil wells in Eagle Ford shale, La Salle County, TX

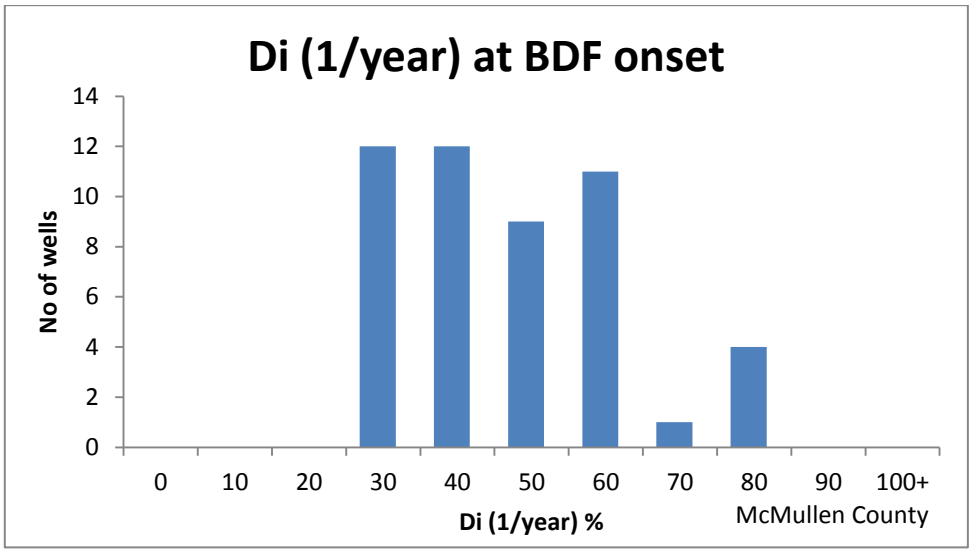

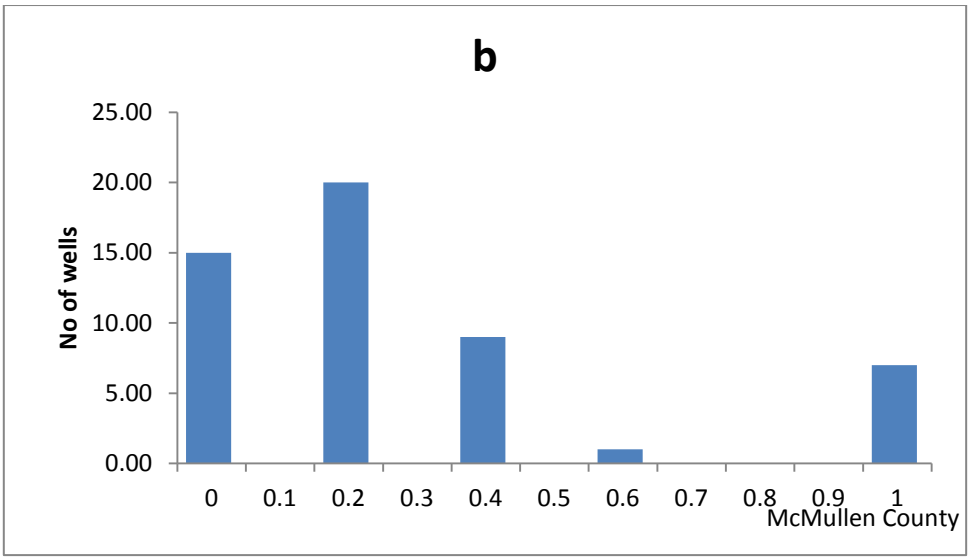

Fig. 75— Arps parameters, decline rate at the end of linear flow and Arps exponent, b, for oil wells in Eagle Ford shale, Wise County, TX

9. SUMMARY AND CONCLUSIONS

Without corrections of early data, the methods used for forecasting production in shale gas reservoirs are applicable to shale oil reservoirs. Analysis of field examples from LRS like the Eagle Ford and northern Barnett shales show that:

Oil wells in the Eagle Ford shale and northern Barnett shale provide similar decline trends by exhibiting linear flow followed by BDF in about 12-14 months of production.

The Stretched Exponential Production Decline (SEPD) model, designed for transient flow, usually produces pessimistic forecasts of future production.

The Duong method, another transient model, may be reasonable during long term transient linear flow, but it is notably optimistic after boundary-dominated flow (BDF) appears.

For wells in BDF, the Arps model provides reasonable forecasts, but the Arps model may not be accurate when applied to transient data.

A hybrid of early transient and later BDF models proves to be a reasonable solution to the forecasting problem in LRS.

In some LRS's, BDF is observed within 12 months. In any case, it is essential to identify or to estimate the time to reach BDF and to discontinue use of transient flow models after BDF appears or is expected.

Diagnostic plots (like log-log rate-time and log-log rate-material balance time plots) are useful for flow regime identification and production forecasting.

If pressure history is available, diagnostic plots (like log-log normalized rate- material balance time and log-log pressure corrected rate- time plots) add confidence in flow regimes identification from the two diagnostic plots and substantially improve the interpretation of data from unconventional oil wells flowing under unstable operating conditions.

Fetkovich (hydraulically fractured well) type curve analysis can be added to improve confidence in flow regime identification from diagnostic plots and to estimate the Arps hyperbolic exponent b from the matching b stem on the type curve, which can then be extrapolated to determine EUR.

The YM-SEPD specialized plot is useful for wells in the transient flow regime. We recommend that only the data points lying on the straight line on the specialized plot should be used for estimating the SEPD model parameters. Including early data leads to higher predicted flow rates as compared to the cases when early data is excluded for estimating the SEPD model parameters, but the EUR is essentially the same in both cases.

NOMENCLATURE

Acronyms

BDF	Boundary-dominated flow
LRS	Liquid rich shales
MBT	Material balance time, N_p/q
PVT	Pressure-volume-temperature

Variables

N_p	Cumulative oil production, STB
q	Production rate volume/time
p	Pressure, psi
t	Time
D	Decline rate, time^{-1}
q(t)	Production rate as a function of time, volume/time
q_i	Initial production rate, Arps parameter, volume/time
b	Arps exponent, degree of curvature, dimensionless
a	Arps exponential decline rate, $time^{-1}$
D_i	Initial decline rate, Arps parameter, $time^{-1}$
q_o	Initial production rate, SEPD parameter, volume/time
n	SEPD parameter, dimensionless
τ	SEPD parameter, time

REFERENCES

Anderson, David Mark, Louis Mattar. 2003. Material-Balance-Time During Linear and Radial Flow. Proc., Canadian International Petroleum Conference, Calgary, Alberta.

Anderson, David Mark et al. 2010. Analysis of Production Data From Fractured Shale Gas Wells. Proc., SPE Unconventional Gas Conference, Pittsburgh, Pennsylvania, USA.

Anderson, Samantha et al. 2012. Pressure Normalized Decline Curve Analysis for Rate-Controlled Wells. Proc., SPE Hydrocarbon Economics and Evaluation Symposium, Calgary, Alberta, Canada.

Arps, J.J. 1945. Analysis of Decline Curves. *Trans A.I.M.E.* **160**: 288-247.

Clarkson, Christopher R. 2013. Production data analysis of unconventional gas wells: Review of theory and best practices. *International Journal of Coal Geology* **109–110**: 101-146. http://www.sciencedirect.com/science/article/pii/S0166516213000050.

Drillinginfo. 2013. *http://www.drillinginfo.com/*.

Duong, Anh N. 2010. An Unconventional Rate Decline Approach for Tight and Fracture-Dominated Gas Wells. Proc., Canadian Unconventional Resources and International Petroleum Conference, Calgary, Alberta, Canada.

Duong, Anh N. 2011. Rate-Decline Analysis for Fracture-Dominated Shale Reservoirs. *SPE Reservoir Evaluation & Engineering* **14** (3): pp. 377-387. http://www.onepetro.org/mslib/app/Preview.do?paperNumber=SPE-137748-PA&societyCode=SPE.

Fekete. 2013. Rate Transient Analysis.

Gong, Xinglai et al. 2011. Integrated Reservoir and Decision Modeling To Optimize Northern Barnett Shale Development Strategies. Proc., Canadian Unconventional Resources Conference, Alberta, Canada.

Ilk, Dilhan et al. 2011. Integration of Production Analysis and Rate-Time Analysis via Parametric Correlations -- Theoretical Considerations and Practical Applications. Proc., SPE Hydraulic Fracturing Technology Conference, The Woodlands, Texas, USA.

Joshi, Krunal, W. Lee. 2013. Comparison of Various Deterministic Forecasting Techniques in Shale Gas Reservoirs. Proc., 2013 SPE Hydraulic Fracturing Technology Conference, The Woodlands, TX, USA.

Kanfar, Mohammed, Robert Wattenbarger. 2012. Comparison of Empirical Decline Curve Methods for Shale Wells. Proc., SPE Canadian Unconventional Resources Conference, Calgary, Alberta, Canada.

Liang, Peter et al. 2011. Analyzing Variable Rate/Pressure Data in Transient Linear Flow in Unconventional Gas Reservoirs. Proc., Canadian Unconventional Resources Conference, Alberta, Canada.

Mangha, Viannet Okouma et al. 2012. Practical Considerations for Decline Curve Analysis in Unconventional Reservoirs --- Application of Recently Developed Rate-Time Relations. Proc., SPE Hydrocarbon Economics and Evaluation Symposium, Calgary, Alberta, Canada.

Mayerhofer, Michael J. et al. 2008. What is Stimulated Rock Volume? Proc., SPE Shale Gas Production Conference, Fort Worth, Texas, USA.

Nobakht, Morteza, Louis Mattar. 2010. Analyzing Production Data from Unconventional Gas Reservoirs with Linear Flow and Apparent Skin. Proc., Canadian Unconventional Resources and International Petroleum Conference, Calgary, Alberta, Canada.

Reese, Dave et al. 2013. Production Analysis in the Barnett Shale - Field Example for Reservoir Characterization Using Public Data. Proc., SPE Annual Technical Conference and Exhibition, New Orleans, Louisiana, USA.

Tian, Yao et al. 2013. The Eagle Ford Shale Play, South Texas: Regional Variations in Fluid Types, Hydrocarbon Production and Reservoir Properties. Proc., 6th International Petroleum Technology Conference, Beijing, China.

Valkó, Peter P., W John Lee. 2010. A Better Way To Forecast Production From Unconventional Gas Wells. Proc., SPE Annual Technical Conference and Exhibition, Florence, Italy.

Wang, John Yilin et al. 2009. Modeling Fracture Fluid Cleanup in Tight Gas Wells. Proc., SPE Hydraulic Fracturing Technology Conference, The Woodlands, Texas.

Yu, Shaoyong, Dominic J. Miocevic. 2013. An Improved Method to Obtain Reliable Production and EUR Prediction for Wells with Short Production History in Tight/Shale Reservoirs. Proc., Unconventional Resources Technology Conference, Denver, Colorado, USA.

APPENDIX A

Additional examples of wells in BDF are presented below. These wells are representative of wells in BDF in Montague County and the decline trend observed is shown by figures below:

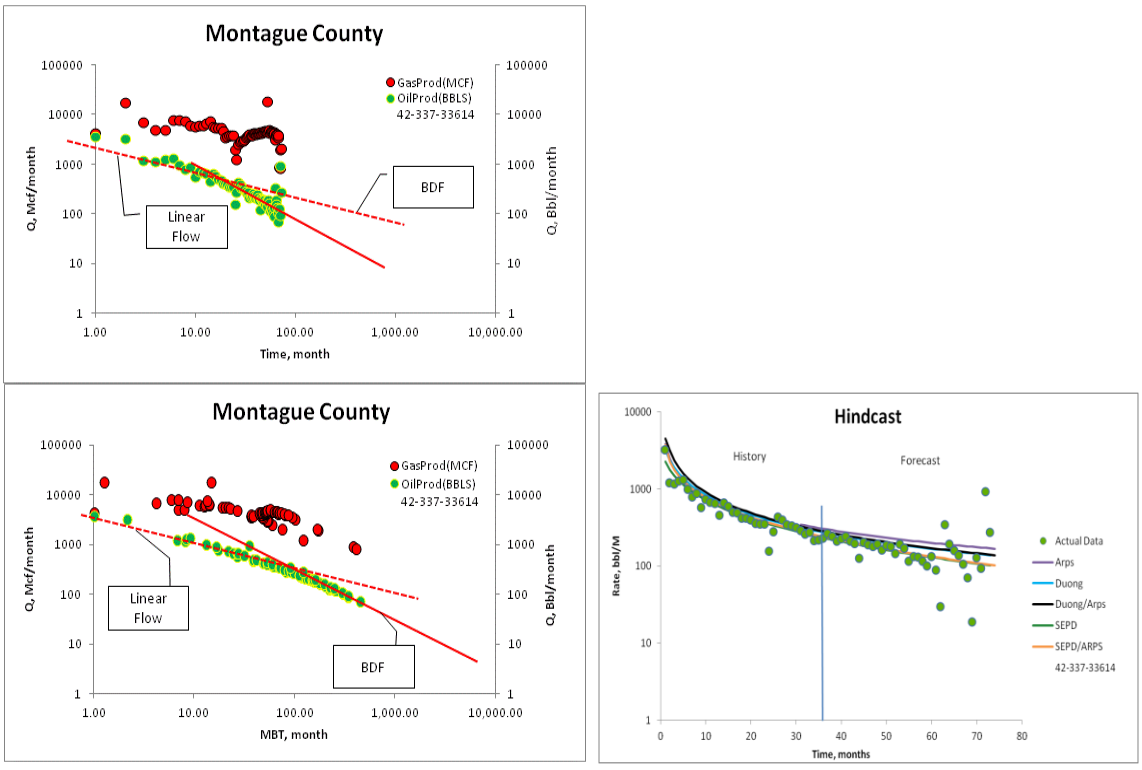

Fig. A 1—FRI and Hindcast in Barnett shale, Montague County, TX for well API# 33614

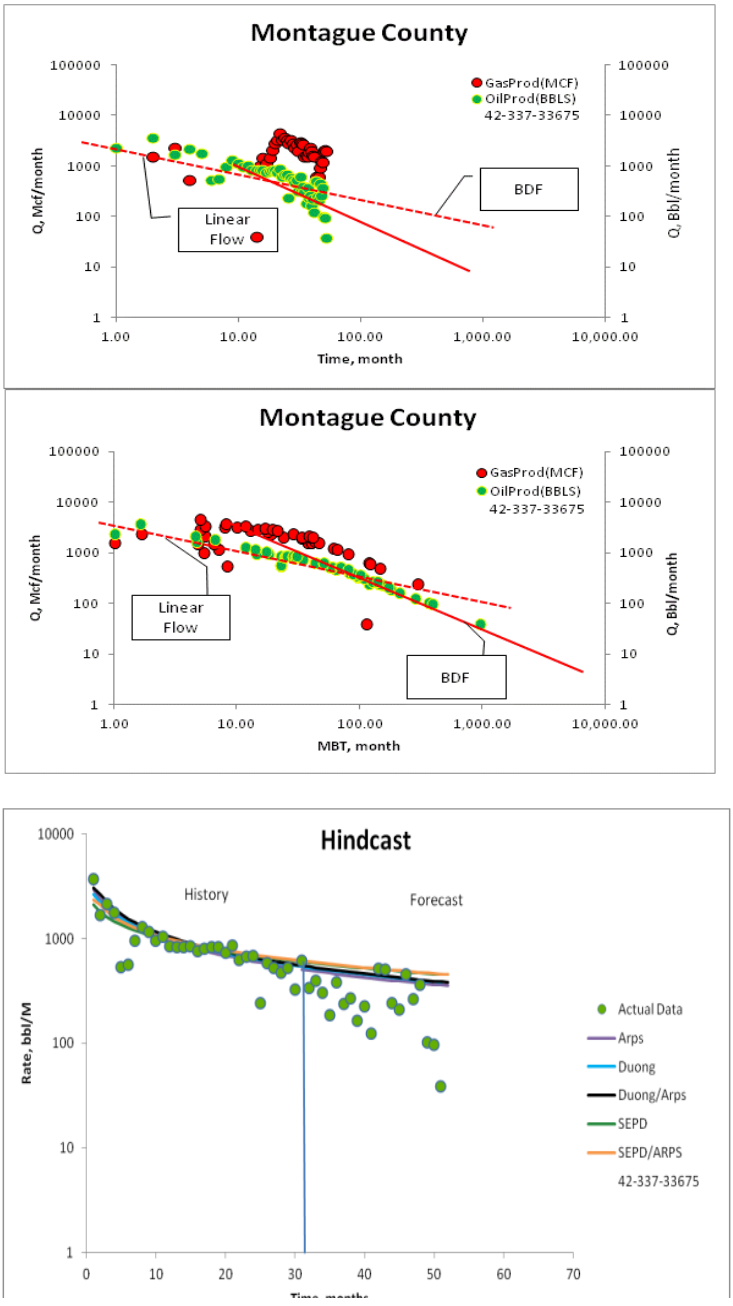

Fig. A 2—FRI and Hindcast in Barnett shale, Montague County, TX for well API# 33675

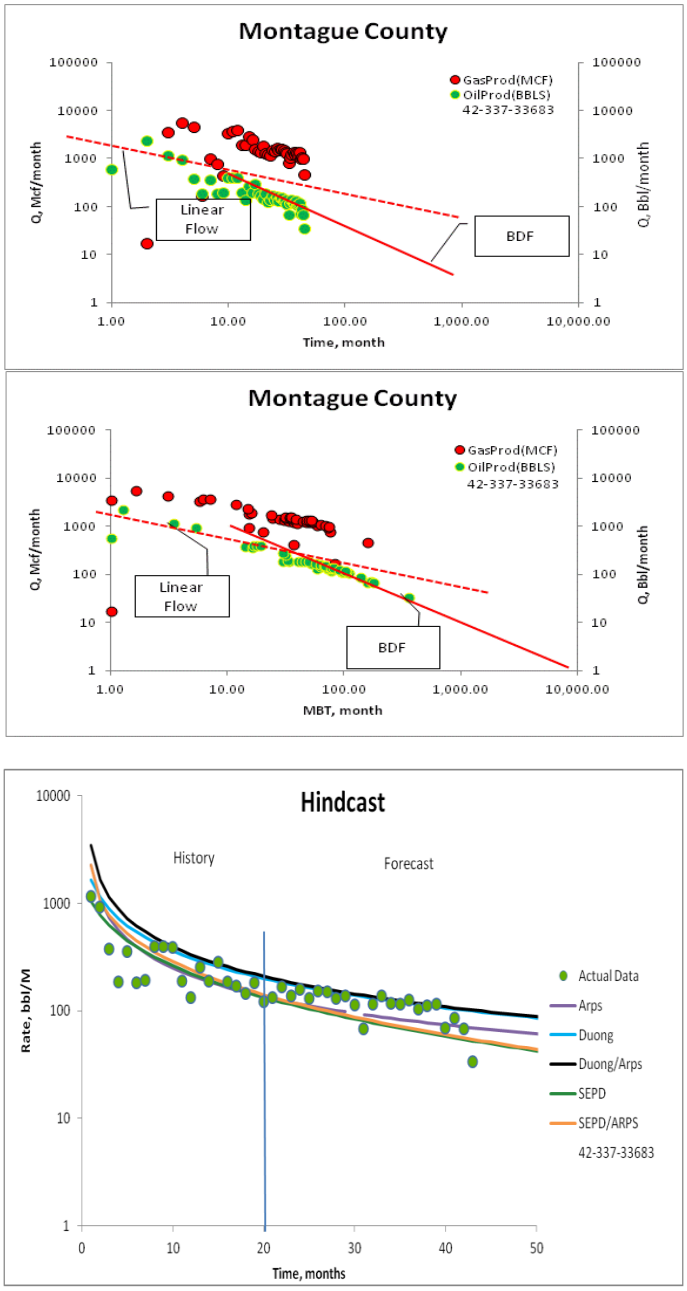

Fig. A 3—FRI and Hindcast in Barnett shale, Montague County, TX for well API# 33683

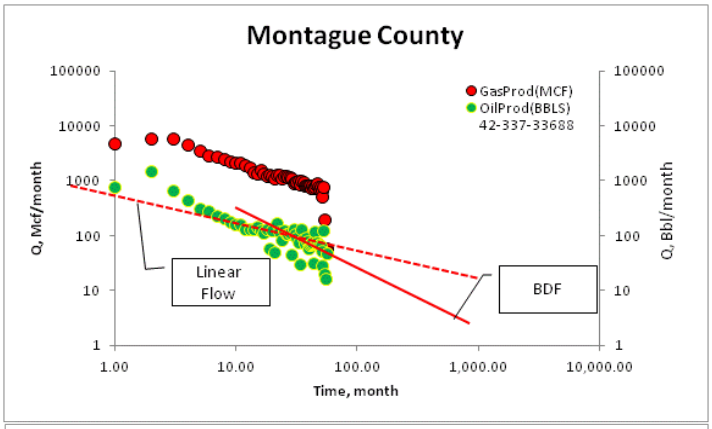

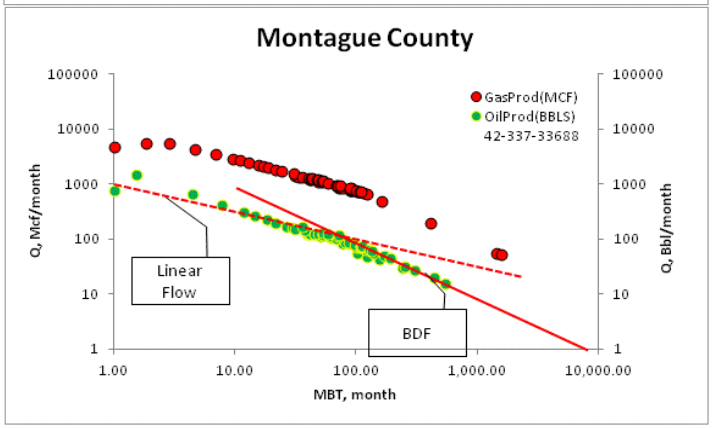

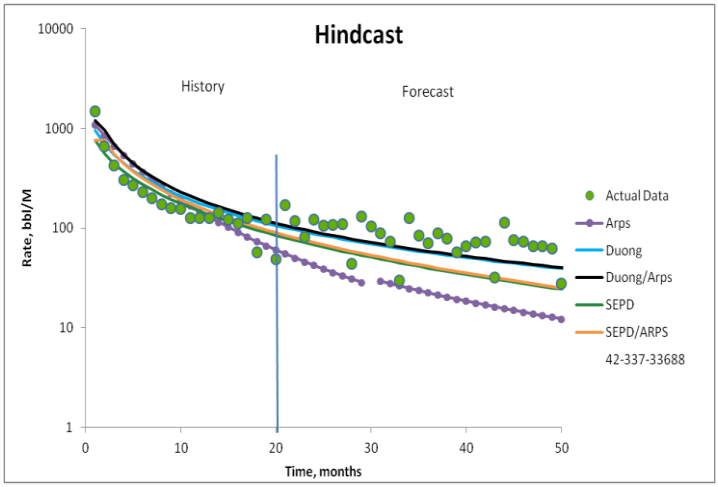

Fig. A 4—FRI and Hindcast in Barnett shale, Montague County, TX for well API# 33688

Flow Regime Identification in Gonzales County: Additional Examples

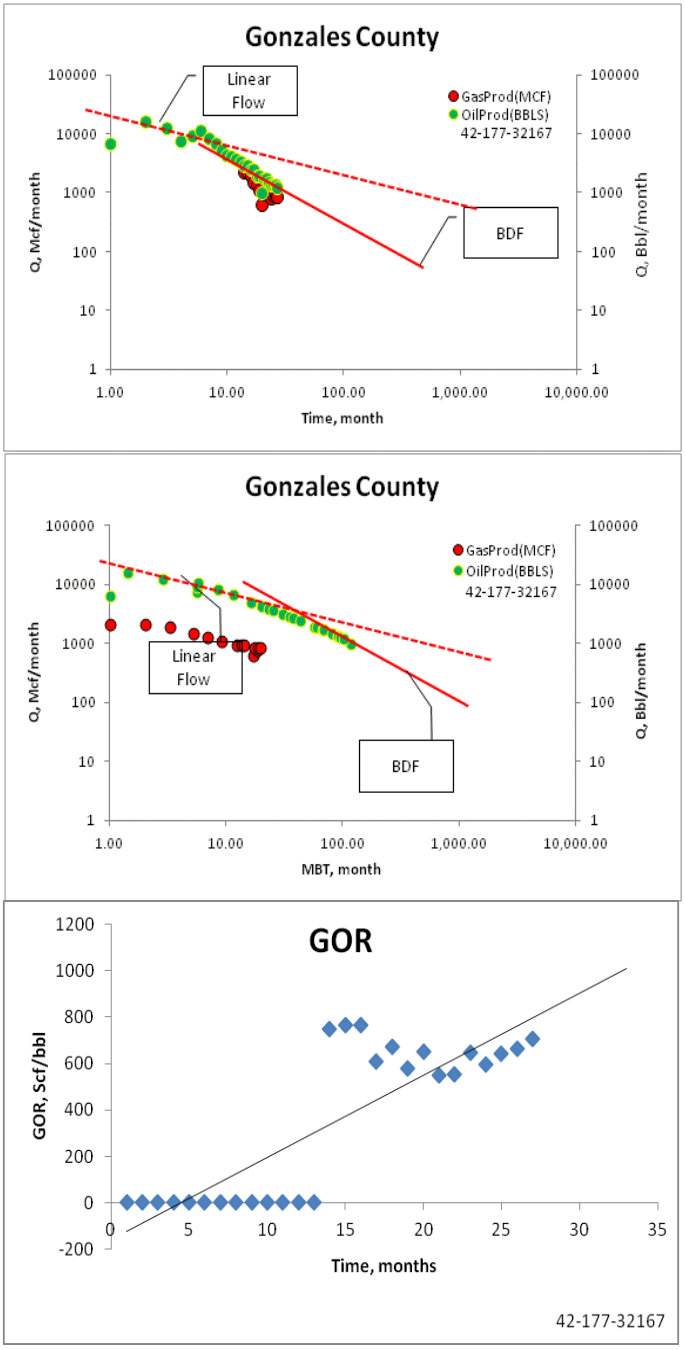

Fig. A 5—FRI and GOR for well API# 32167 in Eagle Ford shale, Gonzales County, TX

Hindcast and 30 Year forecast: Gonzales County

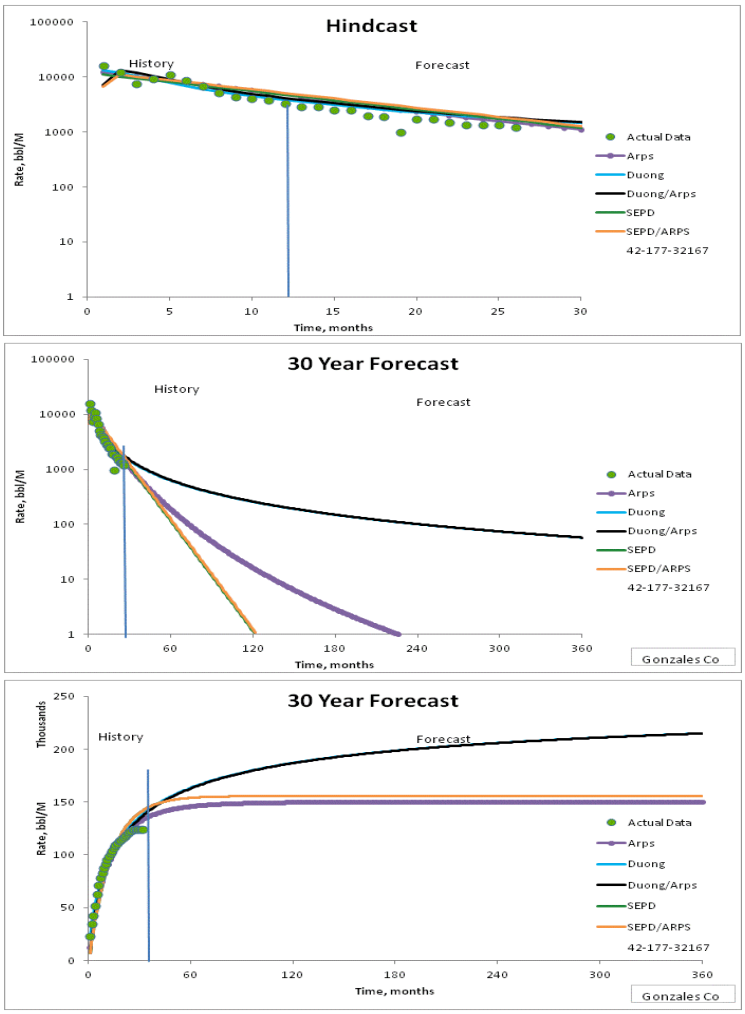

Fig. A 6—30-year forecast for well#42-177-32167 in Eagle Ford shale, Gonzales County, TX

Flow Regime Identification: Cooke County, BDF cases

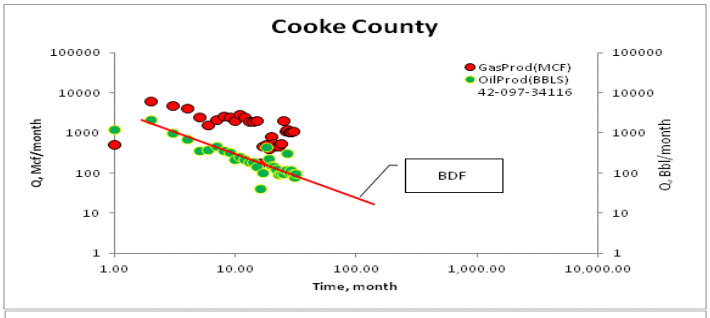

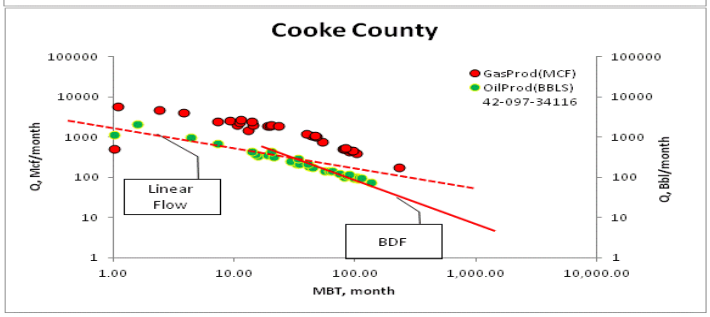

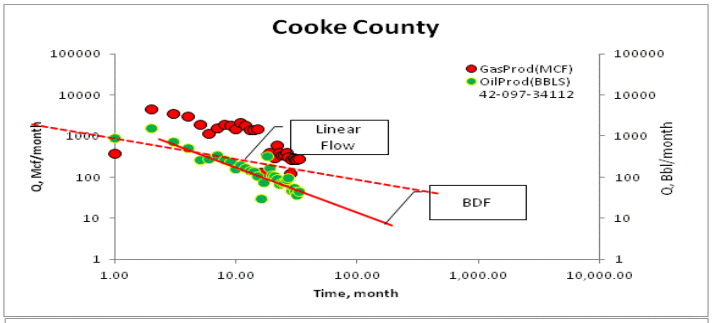

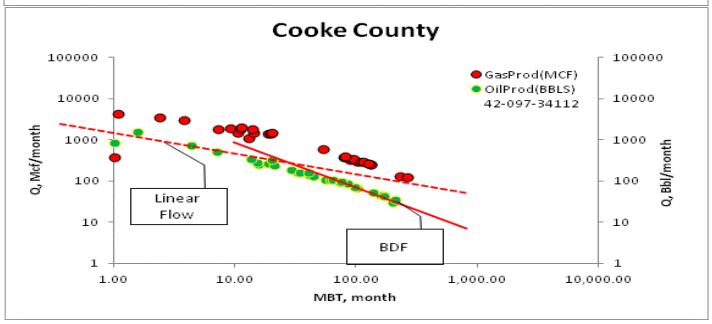

Fig. A 7—FRI for oil wells in Barnett shale, Cooke County, TX

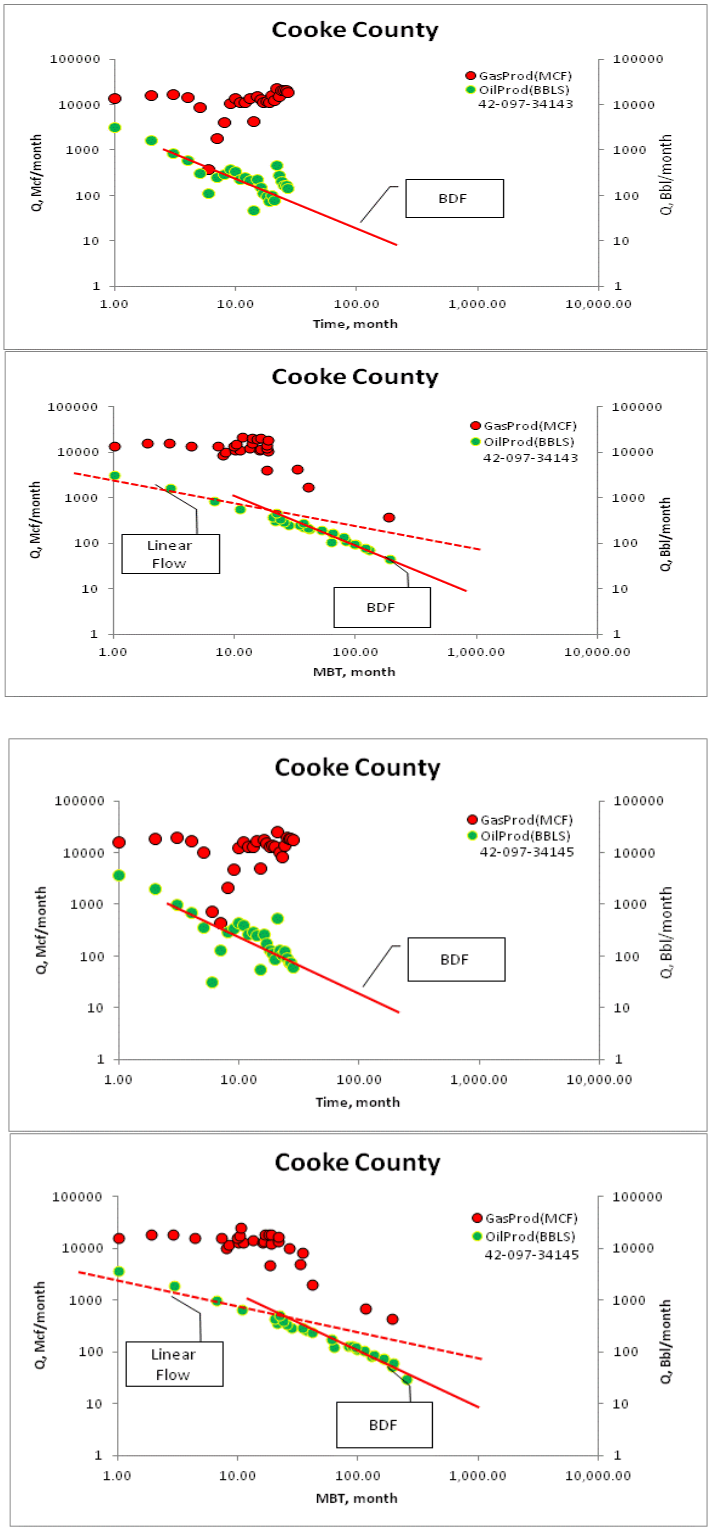

Fig. A 8—FRI for oil wells in Barnett shale, Cooke County, TX

Flow Regime Identification: Wise County, BDF cases

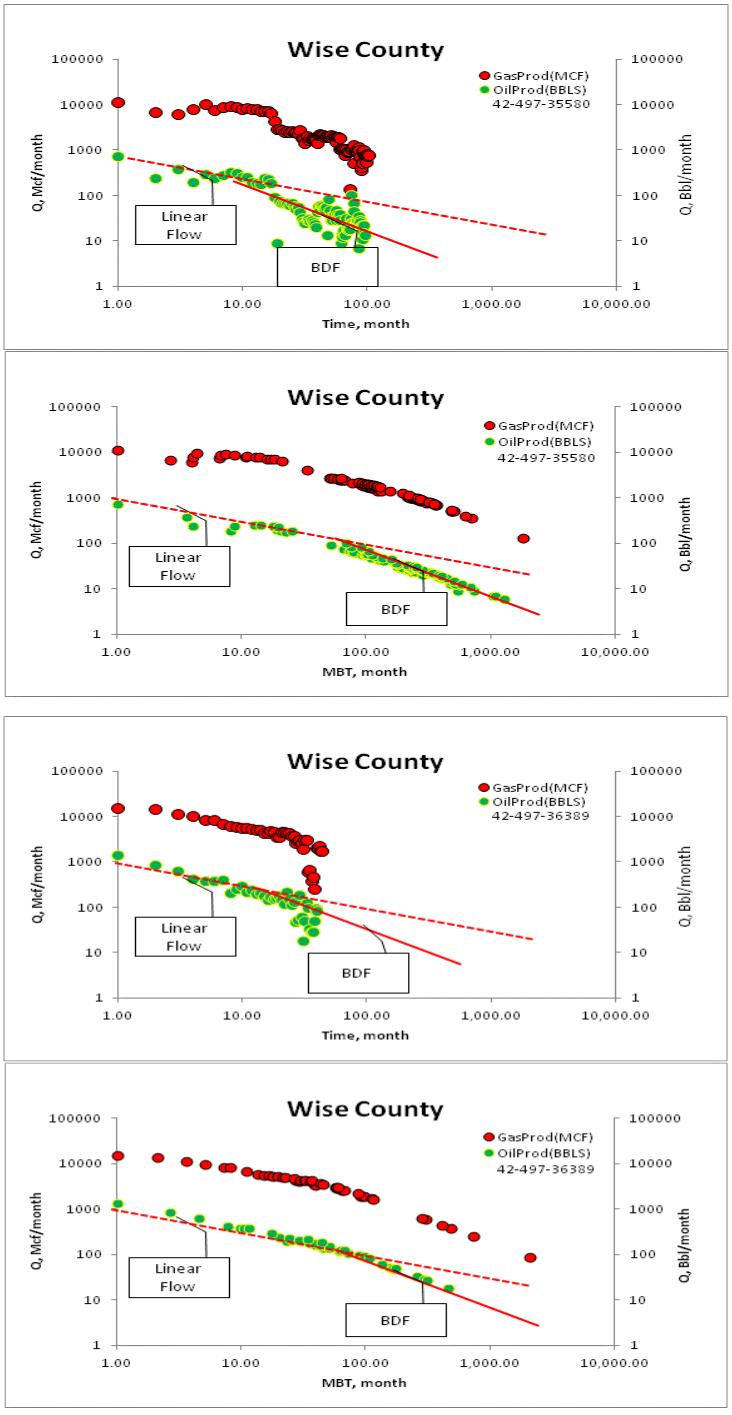

Fig. A 9—FRI for oil wells in Barnett shale, Wise County, TX